Norwegian University of Science and Technology

NTNU - Department of Structural Engineering

Title	Report No.
State-of-the-art report: Service life modelling, carbonation of concrete and corrosion in carbonated concrete	R-1-2017
	Date 11 April 2017
Authors Andres Belda Revert, Klaartje De Weerdt, Karla Hornbostel, Mette Rica Geiker	**Sign.**
	No. of pages Main report: 29 Appendices: I, II, III, IV, V
ISBN No. 82-7482-106-8	

Summary

An overview of service life models for reinforced concrete structures exposed to CO_2 is provided, including models for both the initiation period (carbonation of concrete) and propagation period (reinforcement corrosion in carbonated concrete). The applicability of selected models is illustrated by comparing with a small series of laboratory data and a series of field data. Finally, methodologies given in selected standards and guidelines are summarised.

Indexing terms	Stikkord
Concrete	*Betong*
Reinforcement	*Armering*
Carbonation	*Karbonatisering*
Service life modelling	*Levetidsmodellering*

Preface

This state-of-the-art report is prepared as part of Subproject 2B: Residual Service Life of NFR project no. 235211/O30: Development of low-carbon cement for concrete building structures with excellent durability "Lavkarbsem".

Lavkarbsem project has two main goals:

1. Development of low-carbon footprint cement but without an increased carbonation rate.
2. Enable the use of service life prediction instead of deemed-to-safety approach.

Subproject 2B focuses on the second goal.

The purpose of this state-of-the-art report is to summarize available models for prediction of the initiation and the propagation periods of carbonation-induced reinforcement corrosion.

The report is to be used as background for discussions on the limit states and the possible use of service life prediction instead of deemed-to-safety approach.

The report was prepared as part of the PhD study by Andrés Belda at Norwegian University of Science and Technology (NTNU). Supervisors were Professor Mette Geiker, Associate Professor Klaartje De Weerdt and Senior Engineer Karla Hornbostel, Norwegian Public Road Authority (Statens vegvensen). Project leaders of Lavkarbsem subproject 2B were Senior advisor Steinar Helland and Head of Concrete Technology Department Nina Plünneke Borvik, Skanska Norge.

List of symbols

The list of symbols comprises the symbols used in the main report and all Appendices.
Units are not given as they differ between models.

a: Amount of CO_2 for complete carbonation

b: Binder content

B: Binding capacity

c: Cement content

C: CaO content in hydrated cement matrix

CH: Portlandite

cm: Amount of carbonatable materials

co: Concrete cover

C-S-H: Calcium-silicate-hydrates

CO_2: Carbon dioxide concentration

D_{CO_2}: Carbon dioxide diffusion coefficient

D_{O_2}: Oxygen permeability coefficient

D_{air}: Air permeability coefficient of the cover concrete

DH: Degree of hydration of the cement clinker

FA: Fly ash content

f_c: Compressive strength

i_{corr}: Corrosion rate

k: Carbonation coefficient or carbonation rate

PC: Portland cement

P_{lim}: Corrosion allowance[*]

RH: Relative humidity

SCM: Supplementary cementitious material

t: Exposure time

T: Temperature

t_c: Duration of curing

t_{crack}: Time to cracking

t_i: Duration of initiation period

t_p: Duration of propagation period

t_{SL}: Design service life

Ty: Cement type

w: Water content

W: Amount of water to be evaporated

Wet: Wetness cycles

w/b: Water-to-binder ratio

w/c: Water-to-cement ratio

x_c: Carbonation depth

ρ: Concrete resistivity

$\emptyset$: Reinforcement diameter

[*] The amount of corrosion products required to reach a given limit state is here named "corrosion allowance".

Contents

List of Appendices

1. Introduction

Corrosion of embedded steel is a major cause of premature deterioration of reinforced concrete structures worldwide [Bamforth, 2004]. Chloride attack and carbonation are the most common causes of reinforcement corrosion.

The design service life (design working life according to EN 1990 (2002)) of structures is usually divided into the initiation and propagation period. Figure 1 presents the approach proposed by Tuutti [Tuutti, 1982].

During the initiation period, the reinforcement is covered by a passive film which limits corrosion propagation, the steel is "passivated". Depending on the exposure, aggressive substances penetrate the concrete cover from the surroundings and move gradually towards the reinforcement. In the case of carbonation, CO_2 neutralizes the concrete's alkalinity. When the pH drops to a certain level, the passive layer is no longer stable and the steel may corrode [Bertolini et al., 2013].

During the propagation period, the corrosion rate depends, among others, on the availability of water and oxygen. Carbonation-induced corrosion causes general corrosion on the steel in contact with carbonated concrete [Bertolini et al., 2013].

The design working life of a structure is according to EN 1990 (2002) defined as "*the assumed period for which a structure or part of it is to be used for its intended purpose with anticipated maintenance but without major repair being necessary*". ISO 16204 (2012) uses the term design service life with the same definition, including further description: "*the design service life is defined by the relevant limit states, number of years and level of reliability for not passing each limit state during this period*". Limit state is defined as" the *state beyond which the structure no longer satisfies the relevant design criteria*". Further description and classification of the limit states is given in ISO 2394 (2015), See section 5.

In this document the term "design service life" is applied. In addition, the term "service life" is used for the description of the life time of structures where no limit state is mentioned explicitly.
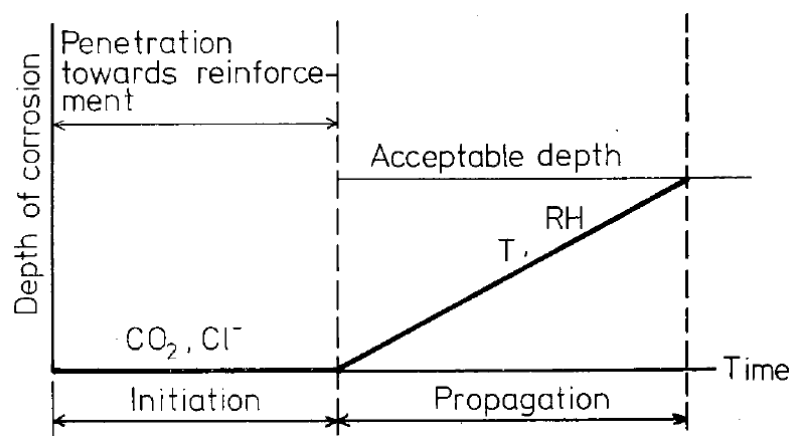

Figure 1: Schematic representation of corrosion of reinforcement in concrete. The initiation and propagation periods, and the end of the service life are indicated [Tuutti, 1982]

1.1.   Objective

The purpose of this state-of-the-art report is to summarize available models for prediction of the initiation and the propagation periods of carbonation-induced reinforcement corrosion.

The report is to be used as background for discussions on the limit states and the possible use of service life prediction instead of deemed-to-safety approach.

1.2.   Scope and limitations

This report presents an overview of models to estimate the service life of reinforced concrete structures exposed to CO_2 and potentially deteriorating due to carbonation-induced reinforcement corrosion. In addition, methodologies for service life design provided in selected standards and guidelines are summarized.

Time dependent empirical and mechanism based models for both the initiation and the propagation period are described and the applicability of selected models for the initiation period is illustrated. A brief description is given of numerical mechanism based models.

The impact of concrete discontinuities, e.g. cracks, and the structural impact of selecting different limit states for service life design are outside the scope of the report.

1.3.   Outline of report

The report is divided into six parts: the main report and five appendices.

The main report describes the key features of models for prediction of carbonation-induced reinforcement corrosion.

Section 2 provides an overview of time dependent models for carbonation development (initiation period). The models are classified in the following categories:

- Empirical models
- Analytical mechanism based models
- Numerical Mechanism based models

It should be noted that the classification used is somewhat arbitrary as some of the empirical models are fitted to equations derived from mechanism based principles, while most of the analytical models include empirical factors. Additional information is given in Appendix I, where each model is individually described. The level of detailing varies due to differences in the background information.

Section 3 provides an overview of time dependent models for corrosion propagation in carbonated concrete (propagation period). The models are classified in the following categories:

- Empirical models
- Mechanism based models

It should be noted that the classification used is somewhat arbitrary as some of the empirical models are fitted to equations derived from mechanism based principles, while most of the analytical models include empirical

factors. Additional information is given in Appendix II, where each model is individually described. The level of detailing varies due to differences in the background information.

Section 4 presents the applicability of selected time dependent models for carbonation development applied to short-term laboratory data from the Lavkarbsem project and long-term Norwegian field data. Additional information is given in Appendix III and IV.

Section 5 provides an overview of methodologies for service life design given in selected standards and guidelines. Addition information is given in Appendix V.

Section 6 presents a brief discussion on uncertainties in service life prediction.

Section 7 presents the outcome of the report.

2. Time dependent models for carbonation development

Several models which aim at estimating the depth of carbonation are available in the literature. The earliest models were proposed in the 1970s where carbonation was described by the square root law (Eq. 1)[1].

$$x_c = k\sqrt{t}$$ Eq. 1

Where

x_c Carbonation depth [mm]
k Carbonation coefficient [mm/year$^{0.5}$]
t Exposure time [years]

Several models have been proposed since then. The so-called carbonation coefficient k (mm/year$^{0.5}$) depends, among others, on the binder and water content, type of binder, casting conditions, curing, and exposure conditions. In the following, carbonation coefficient (k) is considered equal to the carbonation rate [Bertolini et al., 2013].

The models for the initiation period of carbonation-induced corrosion are classified as follows:

- Empirical models: acquired experimental data is fitted to an assumed trend which is based on a mechanism. The empirical models are either presented as a design chart or an equation.
- Analytical mechanism based models: based on diffusion including empirical factors.
- Numerical mechanism based models: several mechanism based equations combined with empirical factors. These models can neither be represented by a single equation nor be applied for hand calculations.

Table 1 presents the empirical models. The parameters considered in the models are listed and brief comments about the models are included. Additional information can be found in Appendix I.

Table 2 presents the analytical mechanism based models. All authors assume that diffusion is the mechanism which controls carbonation. The parameters considered in the models are listed and brief comments about the models are included. Additional information can be found in Appendix I. The model proposed in *fib* Model Code for Concrete Structures (2006) (in the following referred to as "*fib* model") is included in Table 2, but described in Appendix V.

Table 3 presents a summary of the numerical mechanism based models. The numerical models are composed of a set of mechanism based equations including empirical factors, which are numerically solved. Additional information can be found in Appendix I.

---

[1] Some of these models can be found in an Appendix to [Sagues, 1997]

Table 1: Empirical time dependent models for carbonation development

Reference	Concrete properties[1]						Exe.[2]	Exposure[3]					Time exponent	Comments
	b	w	w/b	Ty	f_c	D_{air}	t_c	CO_2	RH	Wet	T	Exp		
[Morinaga, 1990]			x					x	x		x	N, A	0.5	Two models depending on the w/b
[Thomas and Matthews, 1992]				x	x		x		x		x	N	-	Design chart. Focus on fly ash blends
[Parrott, 1994]	x					x			x			N	f (RH)	D_{air} governs carbonation
[Bamforth, 2004]	x			x			x		x			N	0.5	The SCMs buffer capacity governs carbonation
[engineers, 2007]]	x	x		x								N	0.5	The SCMs buffer capacity governs carbonation
[Czarnecki and Woyciechowski, 2012]	x	x		x			x					N. A	-0.5	An upper bound for x_c is given
[Silva et al., 2014]				x				x	x			N, A	0.5	$RH < 70$ %.
	x			x				x	x			N, A	0.5	70 % $< RH$
[Greve-Dierfeld and Gehlen, 2014]									x	X		N	-	Design chart for XC4 exposure (EN 1992)
[Hills et al., 2015]				x								N	-	Age has a nonlinear relation with ln(k)
				x	x							N	-	k is function of ln(parameters)

Note 1: b: Binder content; w: Water content; w/b: Water-to-binder ratio; Ty: Cement type; f_c: Concrete compressive strength; D_{air}: Air permeability coefficient of the cover concrete

Note 2: t_c: Duration of curing

Note 3: CO_2: Carbon dioxide concentration; RH: Relative humidity; Wet: Wetness cycles; T: Temperature; Exp: Exposure regarding CO2: N: Natural, A: Accelerated

Table 2: Analytical mechanism based time dependent models for carbonation

Reference	Concrete properties[1]									Exposure[2]				Comments
	b	w	C	FA	B	D_{CO_2}	D_{O_2}	DH	ρ	CO_2	RH	Wet	Exp	
[Schiessl, 1976]					x	x				x			N	An upper bound for x_c is given
[Tuutti, 1982]	x		x		x	x		x		x			N	Includes the error function
[Papadakis et al., 1991]					x	x				x			N, A	Mass-balance: CO₂, CH, C-S-H, C₂S and C₃S
[Bouquet, 2004]					x	x		x		x		x	N, A	Carbonation stops when concrete is wet
[Jiang et al., 2000]	x	x		x				x		x			A	High volume fly ash concrete
[fib, 2006]										x	x	x	N	Concrete properties are introduced by experimental tests
[Sisomphon and Lutz, 2007]					x	x				x			A	Time exponent 0.4
[Andrade and Andrea, 2010]					x				X	x			N	ρ governs carbonation
[Salvoldi et al., 2015]					x		x			x	x	x	A	D_{O_2} governs carbonation

Note 1: b: Binder content; w: Water content; C: CaO content in binder; FA: Fly ash content; B: Binding capacity; D_{CO_2}: Carbon dioxide diffusion coefficient; D_{O_2}: Oxygen permeability coefficient; DH: Degree of hydration of the cement clinker ; ρ: Concrete resistivy;

Note 2. CO_2: Carbon dioxide concentration; RH: Relative humidity; Wet: Wetness cycles; Exp: Type of exposure regarding CO₂: N: Natural, A: Accelerated.

Table 3: Numerical mechanism based time dependent models for carbonation

Reference	Comments
[Steffens et al., 2002]	Based on mass balance equations and diffusion laws. Takes into account movement and retention of heat, moisture and CO_2.
[Saetta and Vitaliani, 2004]	Based on four differential equations: moisture, heat and CO_2 flow as well as the chemical reaction rate.
[Bary and Sellier, 2004]	Based on mass balance equations: takes into account water, CO_2 and Ca^{2+} in pore solution.
[Bary and Mügler, 2006]	Updated version of [Bary and Sellier, 2004] model which includes kinetics for CH formation. Different carbonation mechanisms for each hydrate.
[Morandeau et al., 2014]	Based on mass balance equations, Fick's first law, Darcy's law, Nernst-Plank law. Allows mass interchange: CO_2 and water. Specifically formulated for blended cements (FA).

3. Time dependent models for corrosion and damage propagation in carbonated concrete

Table 4 presents a summary of the empirical time dependent models for the propagation of carbonation-induced reinforcement corrosion. The first four models estimate corrosion rate in the propagation period and the last five models the propagation period length. All authors assume that service life ends when cracks due to the expansive corrosion products appear on the surface of concrete. Additional information can be found in Appendix II.

Table 4: Empirical time dependent models for corrosion propagation in carbonated concrete

Author	T	RH	O_2	co	$\emptyset$	wetness	ρ	f_t	pH	Cl	Comment
[Alonso et al., 1988]							x				Corrosion rate
[Morinaga, 1990]	x	x	x	x	x						
[Gulikers, 2005]							x				
[Song, 2005]			x						x	x	
[Ghods et al., 2007]			x				x				Duration of propagation period
[Parrott, 1994]		x									
[Bouquet, 2004]				x		x					
[Bamforth, 2004]		x		x	x			x			
[Andrade and Andrea, 2010]							x				

T: Temperature; RH: Relative humidity; O_2: Oxygen concentration; co: Concrete cover; $\emptyset$: Reinforcement diameter; wetness: Wet cycles; ρ: Concrete resistivity; f_t: Tensile concrete strength, Cl: chloride content

Empirical models for corrosion propagation are based on limited materials and exposure data and may therefore be not generally applicable.

The potential effect of binder type on corrosion propagation is in some models indirectly included through the resistivity. Gulikers pointed that the electrical resistivity in the vicinity of the steel surface is more important rather than the resistivity of the bulk [Gulikers, 2005].

In the case of propagation models, several state-of-the-art reports are available, e.g. [Duracrete, 2000], [Markeset and Myrdal, 2008] or [Otieno et al., 2011]. These reports mainly focus on chloride-induced corrosion; but some of the models can be applied for carbonation-induced corrosion and are included in this report.

Appendix II also presents a summary of mechanism based models found in the literature for the propagation period of carbonation-induced reinforcement corrosion. No summary of these models is given in this section because of the variability of parameters and the need for detailing.

4. Application of time dependent models for carbonation development

Selected models were compared with short-term laboratory data from the Lavkarbsem project and Norwegian long-term filed data to illustrate the applicability of time dependent models for the initiation period of carbonation-induced reinforcement corrosion. Details are given in Appendix III and Appendix IV.

4.1. Comparison to short-term laboratory data

The carbonation development is predicted for two binders, CEM I and CEM II/B-V, upon 10 weeks of exposure. Mortar prisms with *w/b*=0.55 exposed to 20°, 60% RH and 1.45% CO_2 are studied. Additionally, carbonation development at 85% RH is predicted. Further description is given in Appendix III. The following models were selected based on the input data available:

- Empirical:
    - Czarnecki and Woyciechowski's model [Czarnecki, 2012]
    - Silva et al's model [Silva et al., 2014]
- Analytical mechanism based:
    - Papadakis et al's model [Papadakis et al., 1991]
    - Papadakis et al's model blended cements model [Papadakis et al., 1992]
    - Jiang et al's model [Jiang et al., 2000]
    - Bouquet's model [Bakker, 1994]; [Bouquet, 2004]
    - Sisomphon and Lutz's model [Sisomphon and Lutz, 2007]

The application of the models assumes the following:

- Carbonation resistance is a paste property. Concrete and mortar performance depends on paste carbonation resistance.
- Paste carbonation resistance depends mainly on the following parameters:
    - Amount of carbonatable material
    - Carbon dioxide diffusion coefficient
    - Moisture content

The predicted carbonation development and the measured carbonation depths are compared in Figure 2 and Figure 3. The empirical models are presented in dashed lines and analytical mechanism based models in continuous lines. All the models apart from Czarnecki's include the impact of CO_2 concentration. Czarnecki model assumes 1% CO_2, which is lower than the actual (1.45% CO_2) exposure. The predicted values ranged from 50% less to 50% more compared to the measured values.

Figure 4 and Figure 5 present the predicted carbonation development at 85% RH (no experimental data available). The modelling of the impact of relative humidity varies. In the case of Silva and Jiang's models the effect of relative humidity is explicitly included in the equation. In the other applied models, the relative humidity is implicitly included as it affects the CO_2 diffusion coefficient. The authors have used the relationship which Papadakis et al. proposed [Papadakis et al., 1991].

Figure 2: Estimated carbonation development and short-term (4, 8 and 10 weeks) experimental values (red dots) for CEM I at 20°, 60 % RH, 1.5% CO₂. Measured carbonation depth range is indicated by the error bars
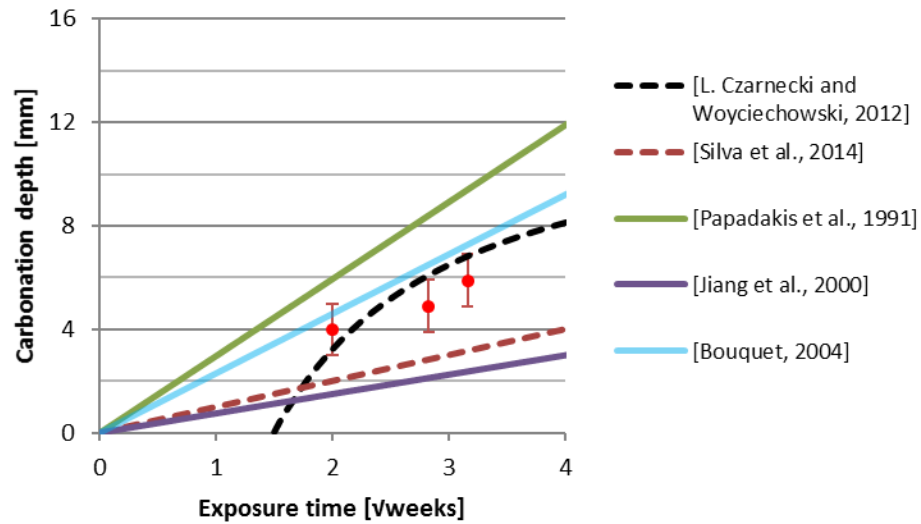

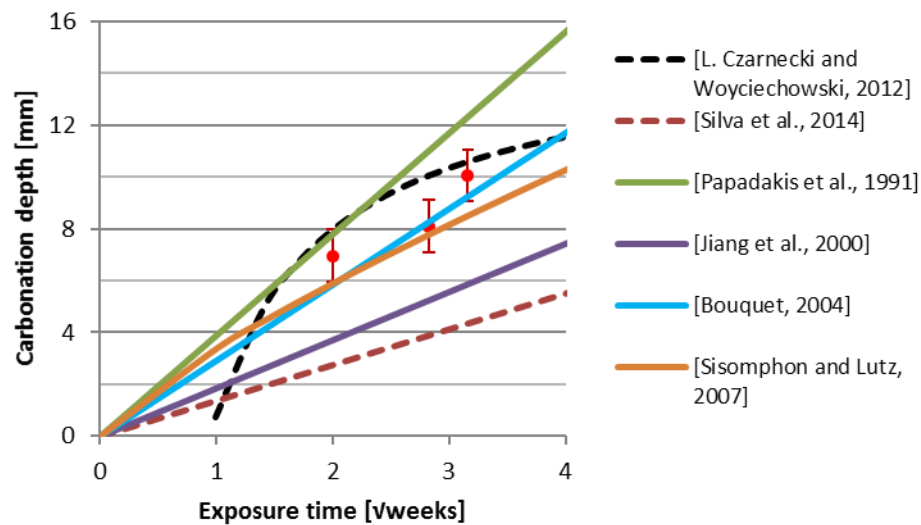
Figure 3: Estimated carbonation development and short-term (4, 8 and 10 weeks) experimental values (red dots) for CEM II/B-V at 20°, 60 % RH, 1.5% CO₂. Measured carbonation depth range is indicated by the error bars
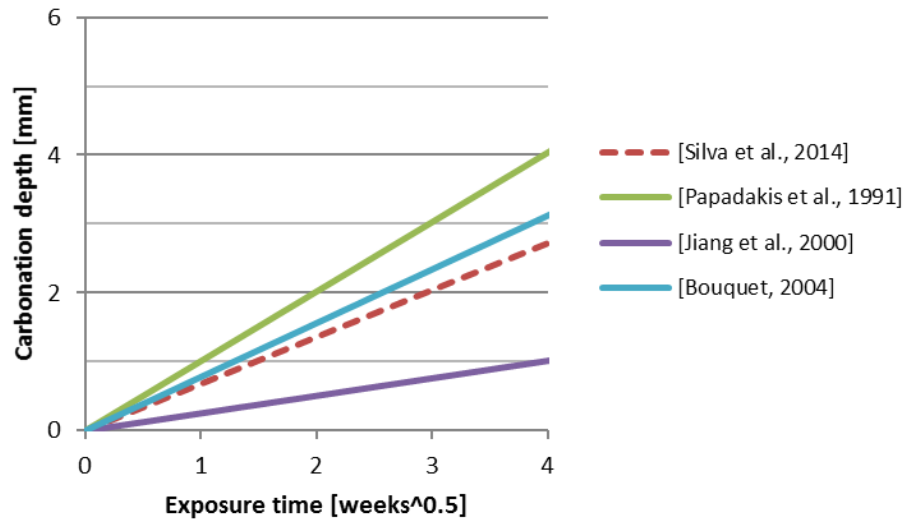
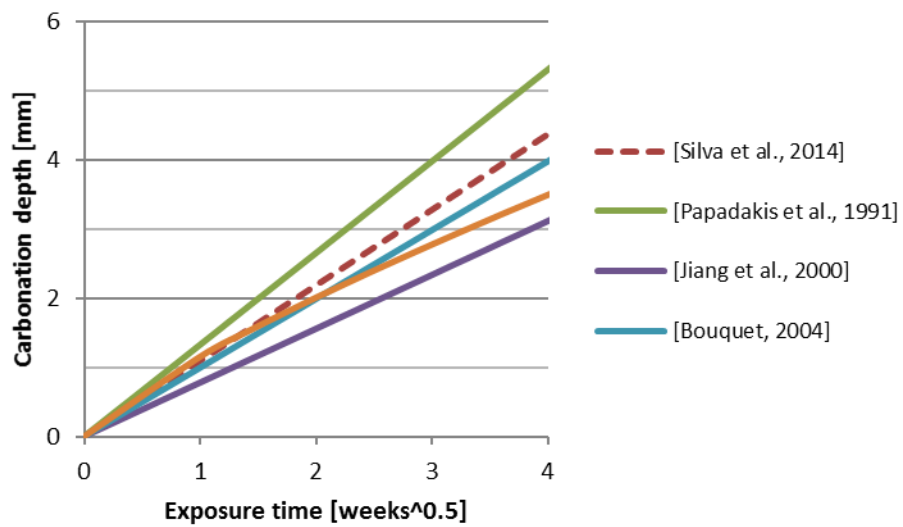**Figure 4: Estimated carbonation development: CEM I at 20°, 85 % RH, 1.5% CO_2**

Figure 5: Estimated carbonation development: CEM II/B-V at 20°, 85 % RH, 1.5% CO_2

4.2.   Comparison to long-term Norwegian field data

Selected models were compared to long-term Norwegian field data provided by Helland [Helland, 2015] to illustrate the applicability of time dependent models for carbonation. The structures, made from different concretes see Appendix IV, were classified into XC3 or XC4 exposure classes according to EN 1992 (2004). Due to limited input data, only empirical models are applied. Further description is given in Appendix IV. The following empirical models were selected based on the available input data:

- Morinaga's model [Morinaga, 1990]
- Silva et al's model [Silva et al., 2014]
- Hills et al's models [Hills et al., 2015]

Figure 6 and Figure 7 present the carbonation depth values for the structures exposed to XC3 and XC4 (dots) and the predictions using the selected models (crosses).

High scatter is observed within and between structures prepared with similar materials and in the same exposure class according to EN 1992. One potential source of the scatter is that differences in carbonation development occur within the exposure classes. Variations in concrete properties are another potential factor.

The predicted values were 300-500% higher than the measured for exposure class XC3. For exposure class XC4, the data was highly scattered, and three of four predictions were in the same range as most of the data, whereas one of the prediction models underestimated most measured carbonation depths.

Figure 6: Measured (dots) and predicted carbonation depth (crosses); structures in exposure class XC3 according to EN 1992 (2004). After [Helland, 2015]
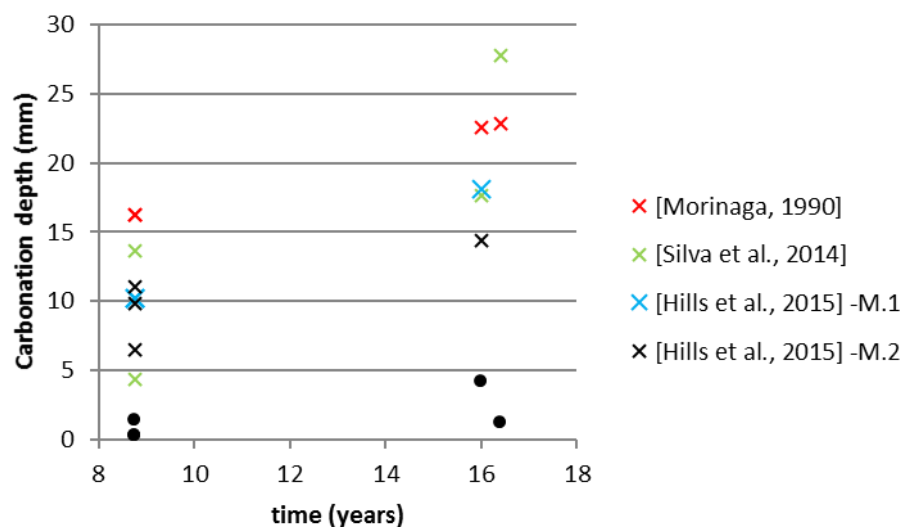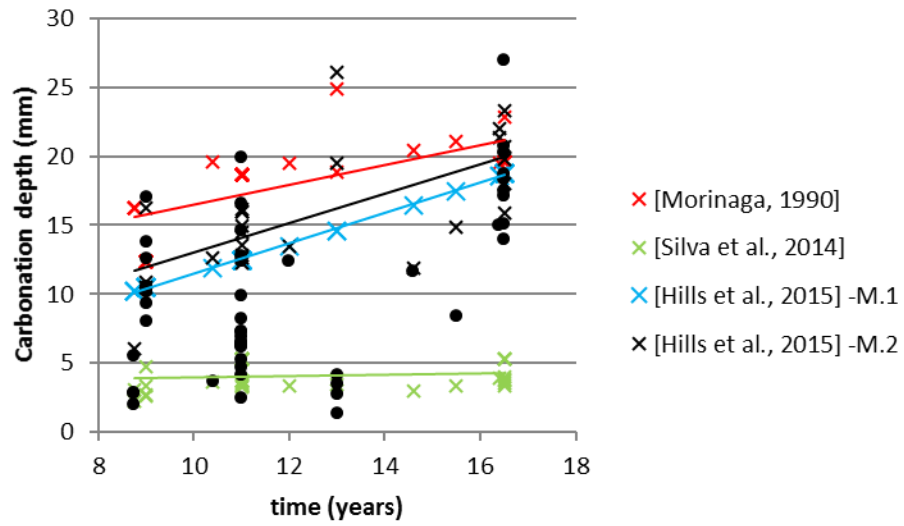
Figure 7: Measured (dots) and predicted carbonation depth (crosses); structures in exposure class XC4 according to EN 1992 (2004). After [Helland, 2015]

4.3.   Comparison of the *fib* model to long-term field data

The *fib* model (2006) is one of the most accepted models for the prediction of carbonation development. In this section literature on the applicability of the model is presented.

Gehlen and Sodeikat observed that for their study, predicted values where higher than measured values [Gehlen and Sodeikat, 2002]. They suggested that the estimation of the inverse carbonation resistance, which was not experimentally determined, and the building circular shape (the weather function in *fib* model was calibrated for rectangular buildings) were the potential reasons for the discrepancy.

Lollini et al. performed an investigation on the parameters in the *fib* model for prediction of carbonation-induced corrosion [Lollini et al., 2012]. Field data including concrete cover (normal distribution) and carbonation depth (Weibull distribution) was compared to predictions, for further description see [Bertolini et al., 2011]. Opposite to Gehlen and Sodeikat, Lollini et al. observed that the *fib* model underestimated the carbonation development.

In addition to investigating the applicability of the *fib* model, Lollini et al. performed a sensitivity analysis of the model. They investigated the impact of each parameter separately and found that there is no single parameter which controls carbonation in the *fib* model.
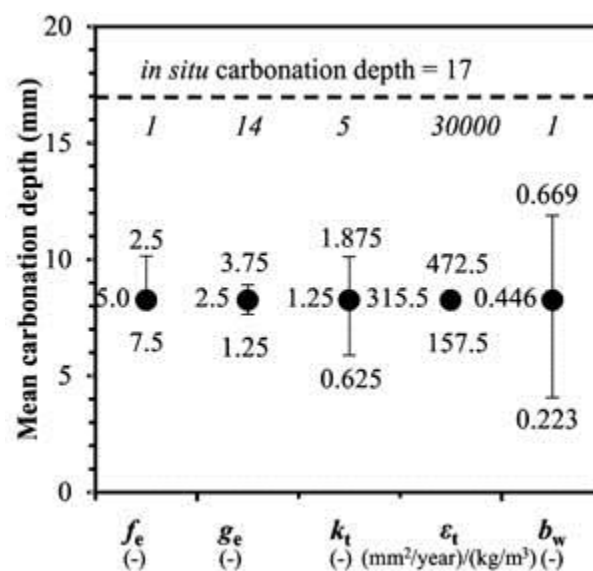

Figure 8: Sensitivity analysis of the *fib* model parameters for carbonation-induced corrosion, including field measurement carbonation depths [Lollini et al., 2012]

5. Standards and Guidelines for service life design

The initiation period covers from the exposure of the concrete to depassivation of the reinforcement, which is assumed to take place when the carbonation front reaches the reinforcement.

The propagation period starts once depassivation of the reinforcement occurs, the rate of corrosion development depends, among others, on the exposure.

Different limit states may be considered for structures affected carbonation-induced corrosion, e.g. as in [*fib*, 2006], see Figure 9:

- Depassivation: Carbonation front has reached reinforcement
- Cracking: Appearance of visible cracks due to corrosion
- Spalling: Concrete cover spalling
- Collapse: Collapse due to loss of bond or loss of cross section of the load-bearing elements
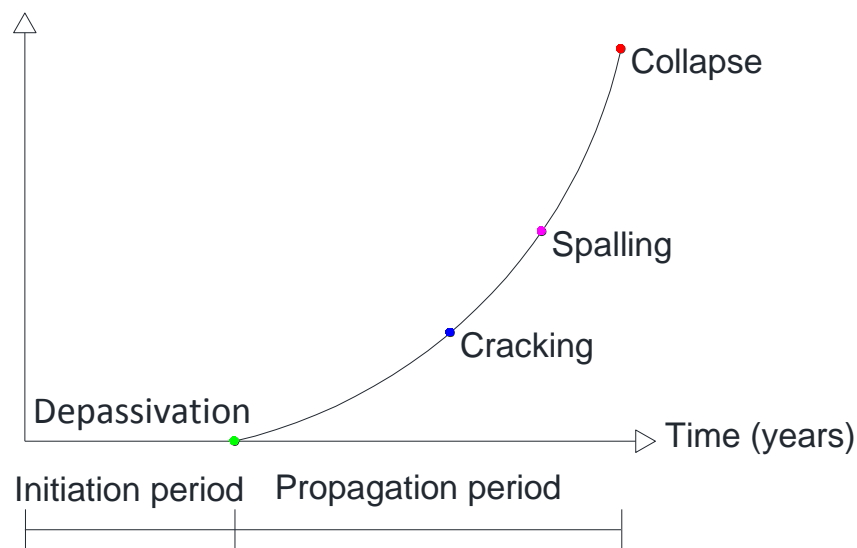
Figure 9: Service life design limit states, after [*fib*, 2006]

The design service life ends in most standards and guidelines ends when the initiation period finishes (limit state: depassivation of reinforcement), e.g. in [*fib*, 2006]. The extent of corrosion is indirectly considered through the required reliability index and the level of reliability should reflect the consequences of passing the related limit state. However, currently in the Norwegian standards, the same reliability index is used regardless the exposure class. Due to different carbonation rates, the periods of propagation will differ, as well as the corrosion rates. This will lead to different period of propagation and different rates even if same probability of failure is assumed. For example, higher cross sectional reduction will have occurred in XC4 than in XC3 at the end of the service life (corrosion initiation, P_f 10% assuming similar geometry and material. CEN TC 51 (CEN TC 104) WG 12/TG 5 is expected to propose the use of exposure class dependent reliability indexes to obtain comparable cross sectional reduction at the end of service life [Helland, 2017].

ISO 2394 (2015) classifies limit states for reinforced concrete structures, which include different reliability indexes, as follows:

- Ultimate limit state (ULS): ULS concerns the maximum load-bearing capacity. The exceedance of an ULS is almost irreversible and causes failure of the structure. The following situations are presented: loss of equilibrium of the structure considered as a rigid body, yielding, rupture or excessive deformations on the members or connections of the structure (either instantaneous or due to fatigue), instability of the structure or part of it, change on the assumed structural system (e.g. due to a large crack formation) and foundation failure.
- Serviceability limit state (SLS): SLS concerns the criteria governing the functionalities related to normal use. The following situations are presented: unacceptable deformations, excessive vibrations, local damage affecting appearance, efficacy, functional reliability of the structure, durability (e.g. cracks[2]) or structural safety.
- Conditions limit states (CLS)[3]: The following situations are presented: an approximation to the real limit state that is either not well defined or difficult to calculate (e.g. when depassivation of reinforcement is considered as a limit state for durability), local damage which can reduce durability (e.g. cracking), or additional limit state thresholds in case of continuous increasing loss function.

Classification of the limit states indicated in Figure 1 according to ISO-2394 (2015) is not straight forward. This results in ambiguity of which reliability index to be applied for e.g. cracking. The limit state "collapse" is an ULS with a reliability index from 2.3 to 4 depending on the consequences of failure ISO-13822 (2012).

Table 5 presents a summary of proposed approaches for service life design for carbonation-induced reinforcement corrosion provided in selected standards and guidelines. Further description is given in Appendix V.

---

[2] Cracking is mentioned as SLS but also is treated as CLS, e.g. ISO 13823 (2008)

3 *fib* Model Code 2010 [*fib*, 2010] and coming *fib* reports group the limit states as ULS and SLS as they are traditionally used for structural design, while the limit states relevant for service life are named "limit states associated with durability - DLS". This last group might overlap with SLS and ULS, but for instance limit state depassivation will not fit into any of these traditionally limit states [Helland, 2017].

Table 5: Service life design approaches given in selected standards and guidelines for carbonation-induced reinforcement corrosion.

| Standard / Guideline | Initiation period (limit state depassivation) | | | | Propagation period |
| | Design to resist the deterioration | | | Avoidance deterioration | |
	Full probabilistic	Partial factors	Deemed to satisfy		
[Duracrete, 2000]	x				User defined
[EN 1992, 2004]			x		
[*fib*, 2006]	x	x	x	x	
[EHE 08, 2008]			x		Limit state: cracking
[ISO 16204, 2012]	x	x	x	x	

The international standard ISO 16204 (2012) proposes two strategies for service life design. The first strategy is "design to resist the deterioration", which includes three levels of sophistication: full probabilistic method, partial factor method and deemed-to-satisfy method. The second strategy is "avoidance of the deterioration".

The standards EN 1992 (2004), NS-EN 13670 (2010) and EN 206 (2000) provide a deemed-to-satisfy approach for service life design. The national standardization bodies give environmental exposure class, structural classification, and concrete composition recommendations. Carbonation-induced corrosion is classified in four exposure classes (XC1, XC2, XC3 and XC4), depending on the water availability.

The Spanish Concrete Structural Code (EHE-08) (2008) provides a deemed-to-satisfy approach for durability service life design. However, a model for service life prediction is included in Annex 9 of the standard: "Additional considerations about durability in EHE-08".

In the report: Brite EuRam III, DuraCrete – Probabilistic Performance Based Durability Design of Concrete Structures: Final Technical Report of Duracrete project, in the following referred as [Duracrete, 2000], probabilistic models for both the initiation and the propagation period were presented. The propagation period model covers the period from steel depassivation to a user defined unacceptable level of structural deterioration.

The *fib* Model Code for service life design [*fib*, 2006] was the basis for the ISO 16204 (2012). Similar strategies are also presented in the revised version of the *fib* Model Code for concrete structures [*fib*, 2010]. A carbonation model for the full probabilistic design method for the initiation period was included in the strategy "design to resist deterioration". The limit state considered is depassivation of the steel, which also here is assumed to occur when the carbonation front reaches the reinforcement.

The *fib* Models Code for service life design [fib, 2006], and [*fib*, 2010], and ISO open for the use of all limit states and give limit states-equations for also cracking and spalling, but claims that the limit state depassivation is the most used and the only limit state with models with general international consensus [Helland, 2017].

5.1. Assessment of code requirements

Greve-Dierfeld and Gehlen [Greve-Dierfeld and Gehlen, 2016b] investigated the provisions given in the EN 1992 (2004) on a broad range of cement types and exposure conditions. They found that the level of reliability in carbonation-induced corrosion service life design varies depending on the cement type and exposure conditions due to the deemed-to-safety approach currently used. They compared "favourable" and "unfavourable" concretes which can be used in the same exposure class, e.g. according to NS-EN 1992 (2004) concrete containing CEM I and CEM III/B, for exposure class XC4 give a range of reliability indexes between 2 to 0.5 (probability of failure from 2 to 30%).

Steinar Helland [Helland, 2016a] investigated the provisions given in the Norwegian standard (NS-EN 1992 (2004)) regarding carbonation-induced corrosion, for exposure classes XC3 and XC4 based on carbonation field measurements, which are included in Appendix IV. He assumed a normal concrete cover distribution with an average value of 35 mm and a standard deviation of 6.1 mm. Figure 10 presents a comparison of normalised carbonation depths measured in Norwegian structures and the concrete cover requirements. The overlapping area between each population (exposure and cement type) and the concrete cover requirement distribution is an indication of the probability of failure. He found that for the CEM I structures, the probability of failure had an ample margin of safety compared to the requirements, P_f= 10%, whereas, the probability of failure for CEM II/A-V structures exposed to XC4 was not fulfilled for w/b=0.6 and close to the limit for w/b=0.55.

It would be relevant to perform a similar assessment for structures in exposure class XC3 containing CEM II/A-V and CEM II/B-V with w/b=0.55. Higher carbonation depths are expected in XC3 compared to XC4 exposure class, resulting in higher probabilities of failure.
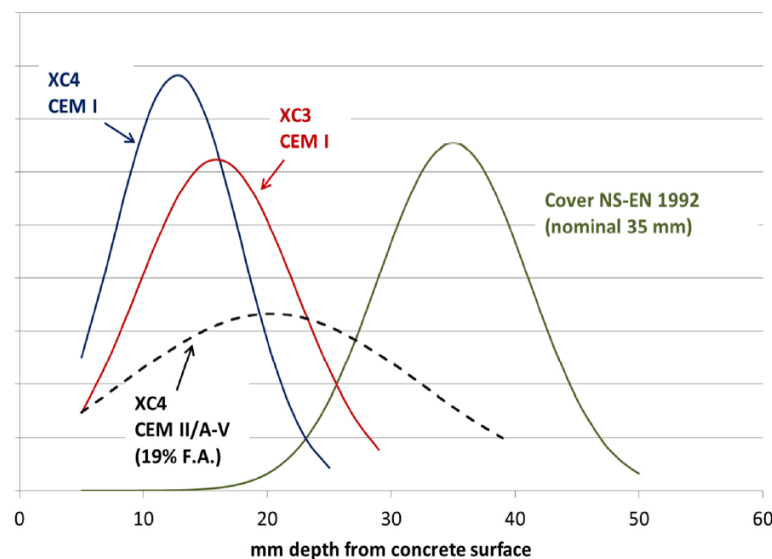

Figure 10: Distributions of normalized carbonation depth measurements and concrete cover requirement according to NS-EN 1992 (2004) [Helland, 2016a]

5.2. Future developments of the European standards

Steinar Helland [Helland, 2016b] recently discussed the performance-based service life design concept and how it will be implemented in the European framework during the coming years. Currently, the durability requirements are under national authority, which means that requirements such as minimum w/b for a given exposure class may vary between countries.

Regarding carbonation-induced corrosion, it seems that the limit state considered will be depassivation of reinforcement. The carbonation resistance of the concrete is presently suggested to be classified in three classes: RC40, RC30 and RC20. The concrete producer will have two options to document compliance with these classes. Either by testing the concrete or by applying deemed-to-satisfy provisions based on mainly binder type, water/binder ratio. The testing option is suggested to be based on "natural carbonation" ($20^{\circ}C$, 65% RH, and natural CO_2). This is a XC3 environment. The results are then extrapolated to 50 years with the square-root-of-time and should ensure a less than 10% probability of exceeding the carbonation depth of 40, 30 or 20 mm for RC40, RC30 or RC20. The needed deemed-to-satisfy provisions have to be settled by the code committee and should ensure comparable results as for the testing option (see further description in Appendix I, Section "Greve-Dierfeld and Gehlen's model description") [Helland, 2017].

"Natural carbonation" is selected because so far it is not clear to which extent accelerated carbonation mirrors the natural process.

Greve-Dierfeld and Gehlen have provided substantial background for the ongoing revision of the European standard, moving from the deemed-to-safety approach to performance-based requirements [Greve-Dierfeld and Gehlen, 2016a]. They grouped concretes depending on the carbonation performance. The classification discretises the carbonation performance depending on the carbonation rate under natural exposure (65% RH, 20° and natural CO_2) in groups of 1 $mm/year^{0.5}$ width. For example, a concrete containing CEM II/B w/b 0.55 performs similar to a concrete containing CEM I w/b 0.6, and they are both classified as RC5, which means that the natural carbonation rate is between 4 and 5 $mm/year^{0.5}$, see Table 6.

The assumed curing conditions for the cast concrete on the construction site will be given in EN 13670 (NS-EN-13670) and the minimum cover to the reinforcement in EN 1992 (2004). The application of the provisions in these standards should then ensure a certain level of reliability for keeping the reinforcement in the structure passivated during the design service life. Since the consequences of depassivation is less in exposure class XC3 than in XC4 (less moisture to support a corrosion process), it is suggested to associate XC3 with a more relaxed reliability index than for XC4. [Helland 2017]

Table 6: Top: carbonation performance classification. Bottom: Carbonation performance classified according to *w/b* and cement type. $k_{NAC,\mu}$: average natural carbonation rate at 65% RH, 20° and natural CO_2, $k_{NAC,90}$ upper 90% quantile of natural carbonation rate [Greve-Dierfeld and Gehlen, 2016a]

Natural carbonation rate	Carbonation performance class					
	RC2	RC3	RC4	RC5	RC6	RC7
$k_{NAC,\mu}$ [mm/year$^{0.5}$]	2	3	4	5	6	7
$k_{NAC,90}$ [mm/year$^{0.5}$]	3.4	4.4	5.4	6.4	7.4	8.4

Carbonation performance class	Maximum *w/b*					
	RC2	RC3	RC4	RC5	RC6	RC7
CEM I	0.45	0.5	0.55	0.6	0.65	-
CEM II/A	0.45	0.5	0.55	0.6	0.65	-
CEM II/B	0.4	0.45	0.5	0.55	0.6	0.65
CEM III/A	0.4	0.45	0.5	0.55	0.6	0.65
CEM III/B	-	0.4	0.45	0.5	0.55	0.6

6. Uncertainties in service life prediction

The uncertainties in service life prediction can be classified according to Melchers as follows [Melchers, 1996]:

- Physical (natural or fundamental) uncertainty is due to the inherent nature of the phenomena. Physical uncertainty might be reduced with more data, but is always present. [Melchers, 1996] Selected variables causing physical uncertainty are discussed below.
- Statistical uncertainty is related to differences between the observations and the real phenomena [Melchers, 1996]. In the case of carbonation-induced corrosion the statistical uncertainties come from both the load (carbonation front distribution) and the resistance (concrete cover properties and thickness), which are characterized using limited data. In Section 5.1 the impact of statistical uncertainties was discussed. Probabilities of failure were estimated for different cement types exposed to CO_2 applying EN 1992 (2004).
- Model uncertainty comes from the simplification of the actual phenomenon/phenomena investigated. It is due to the lack of knowledge or a wish to simplify. [Melchers, 1996]
- Decision uncertainty is related to the decision of whether a particular phenomenon has occurred. In terms of limit states it relates to the decision as whether a limit state violation has occurred. [Melchers, 1996] In the case of carbonation-induced corrosion the decision uncertainty will be different if e.g. limit state depassivation or cracking is considered.

The impact of uncertainties on the carbonation development is illustrated in Chapter 4, where predicted and measured short/long-term data were compared:

- Predictions using six models were compared to short term data from accelerated exposure. The predicted values ranged from 50% less to 50% more compared to the measured values. In this case, we assume that model uncertainty is the most relevant uncertainty: physical uncertainty is limited due to controlled materials and exposure, and statistical uncertainty is limited due to systematized sampling.
- Predictions of four models were compared to long-term Norwegian data from field structures. The predicted values were 300-500% higher than the measured for exposure class XC3. For exposure class XC4, the data was highly scattered, and three of four predictions were in the same range as most of the data, whereas one of the prediction models underestimated most measured carbonation depths. In this case, we assume that the physical, statistical and model uncertainties are responsible for the observed variations.

It should be noted that the current available time dependent models are based on the assumption of only one mechanism dominating the deterioration process of the structure, here carbonation or carbonation-induced corrosion. Multi-deterioration models need to be developed to cover the actual exposure of reinforced concrete structure.

In the following selected variables causing physical uncertainty in carbonation-induced corrosion service life prediction are discussed.

6.1. Variables causing physical uncertainty

In the case of carbonation-induced corrosion, the physical uncertainty is caused by the inherent nature of concrete (composite material), variations in concrete properties, possible local characteristics (e.g. cracks, spacers, concrete-steel interface defects), variable corrosion distribution and variations in exposure conditions.

6.1.1. Inherent nature of carbonation of mortar and concrete

Mortar and concrete are composite materials of aggregates embedded in a matrix of cement paste (which at a smaller scale also is a composite). Transport generally takes place through the cement paste resulting in an uneven penetration of CO_2 through the composite. In addition, carbonation is a chemical process, which among others, depends on the solids carbonating. Experimental investigations on mortars containing CEM I and CEM II B/V illustrate that for the conditions tested (w/b 0.55, 14 days sealed curing, exposure, 20°C, 60% RH, 1.5% CO_2 for 4 weeks) the carbonation front appears sharp (i.e. short reaction rate compared to CO_2 penetration rate) and the variation (range) of the carbonation front compares to the maximum aggregate size (2 mm) [Belda Revert et al., 2016]. The spatial variation of carbonation front is illustrated in Figure 11. The inherent uneven carbonation front in mortar and concrete illustrates the benefits of a probabilistic modelling approach.
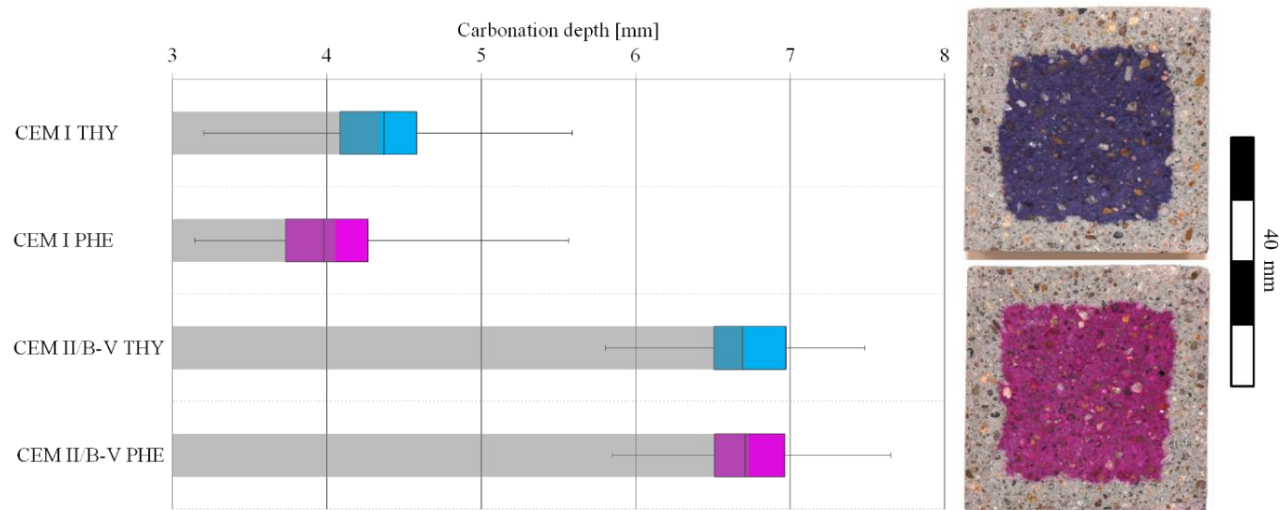

Figure 11: Left: spatial variation of carbonation depth: lateral and top sides of CEM I and CEM II/B-V mortar prisms (*w/b* 0.55) after 4 weeks at 20°C, 60% RH and 1.5% CO₂. Right: pictures of CEM II/B-V mortar sprayed with thymolphthalein (top) and phenolphthalein (bottom). After [Belda Revert et al., 2016]

6.1.2. Local characteristics

In addition to the inherent nature of concrete, possible defects and larger scale inhomogeneities, e.g. spacers, will influence the carbonation development.

Cracks

A recent PhD thesis on the influence of cracks in carbonation-induced corrosion suggests the impact of cracks in corrosion propagation is limited for static cracks in structures not affected by multiple degradation mechanism [Ghantous, 2016].

Some guidelines are given in ISO 16402 (2012) for service life designed of cracked concrete. The minimum structural reliability of cracked reinforced concrete shall be similar to un-cracked concrete exposed to similar conditions. A simplified approach was included assuming that cracks under a certain characteristic value do not influence the deterioration process, which is in line with the assumptions in most of the design codes.

Another approach is to assume a representative volume of the structure which includes defects, and estimate average properties on it, as e.g. Song proposed [Song, 2005].

Spacers

Alzyyoud et al. investigated the effect of various types of spacers on the transport properties of concrete [Alzyoud et al., 2016]. They found that the spacers in general increase the penetration of aggressive species by various mechanisms: permeation, diffusion and capillary absorption. Thus, it is expected that carbonation is influenced by the presence of spacers.

Defects around reinforcement

Ongoing investigations on reinforced mortar samples have revealed that defects in the vicinity of the reinforcement are likely to increase the carbonation rate near the reinforcement [Belda Revert et al., In preparation]. This is illustrated in Figure 12 left, which presents a cross section of a partially carbonated reinforced mortar sample w/b 0.55, after 22 weeks exposed to 20°, 60% RH, and 1.5% CO_2 sprayed with thymolphthalein.

Supporting observations were presented by Köliö [Köliö, 2016] who submitted supplementary information in continuation of a reported field investigation [Köliö et al., 2015]. Köliö observed that the embedded steel influenced the shape of the carbonation front in facades exposed to natural carbonation in Finland, see Figure 12 right.

Further investigations are ongoing in the Lavkarbsem PP 2B project.

Figure 12: Left: cross section of reinforced mortar sample (6-mm rebar) sprayed with thymolphthalein [Belda Revert et al., In preparation]. Right: reinforced concrete core sprayed with phenolphthalein (fading), uneven carbonation front indicated by blue line. Courtesy of A. Köliö

6.1.3. Variable corrosion distribution

Köliö et al. reported that the amount of corrosion products on the side of the reinforcement facing the concrete cover was 60% higher than on the opposite side of the reinforcement on facades exposed to natural carbonation [Köliö et al., 2015]. This uneven distribution of corrosion products induces additional stresses, which will cause premature cracking compared to uniformly distributed corrosion products.

Ji et al. observed that the distribution of corrosion products before cracking was uneven in reinforced mortar samples exposed to 20°, 70% RH, and 20% CO_2: the steel surface facing the concrete cover was suffering from corrosion while the other side was not corroded [Ji et al., 2011]. Unfortunately, no information about the carbonation depth is available. Ji et al. proposed that in addition to microcell corrosion, macrocell corrosion potentially also took place on the steel side facing the cover, the opposite steel surface acting as cathode, see Figure 13. The consequences would be higher corrosion rates compared to microcell corrosion, and an uneven distribution of corrosion products.
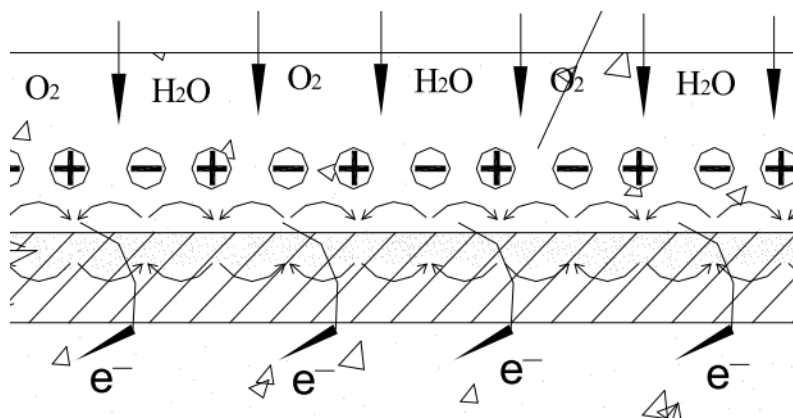

Figure 13: Uneven carbonation-induced corrosion distribution around rebar [Ji et al., 2011]

7. Summary

This report presents an overview of models to estimate the service life of reinforced concrete structures exposed to CO_2 and potentially deteriorating due to carbonation-induced reinforcement corrosion. Time dependent models for both the initiation and the propagation period were described. In addition, methodologies for service life design available in selected standards and guidelines were summarized.

General observations for the models are

- Inhomogeneities are assumed non-existent, or to be random and treated statistically. None of the models consider the impact of cracking (and several other variables) on carbonation development and corrosion propagation, except for one model where an averaging approach is used.
- Empirical models as well as analytical or numerical mechanism based models are available.
- Several of the models require input data which is not typically available.
- Several models are based on assumptions which are difficult to verify.
- All models are based on the assumption of only one mechanism dominating the deterioration process of the structure, here carbonation or carbonation-induced corrosion.

Concerning time dependent modelling of carbonation, the following can be stated:

- Predictions using six models were compared to short term data from accelerated exposure. For the actual case the predicted values ranged from 50% less to 50% more compared to the data.
- Predictions using four models were compared to long-term data from Norwegian field structures. Predicted values were 300-500% higher than measured for exposure class XC3. For exposure class XC4, the data was highly scattered, and three of four predictions were in the same range as most of the data, whereas one of the prediction models underestimated most data.

Concerning modelling of corrosion propagation, the following can be stated:

- Most empirical models are based on limited experimental investigations.
- None of the models take into account inhomogeneous distribution of corrosion products
- The potential effect of the binder type on the corrosion development is indirectly included in some of the models by considering concrete resistivity.

Standards for service life design for carbonation-induced corrosion propose either deemed-to-satisfy requirements or simplified models for the initiation period. The extent of corrosion is indirectly considered through the required reliability index. However, currently in the Norwegian standards, the same reliability index is used regardless the exposure class. Due to different carbonation rates, the periods of propagation will differ. In addition, the corrosion rates will differ. This will lead to different period of propagation and different rates even if same probability of failure is assumed. For example, higher cross sectional reduction will have occurred in XC4 than in XC3 at the end of the service life (corrosion initiation, P_f=10% assuming similar geometry and material. CEN TC 51 (CEN TC 104) WG 12/TG 5 is expected to propose the use of exposure class dependent reliability indexes to obtain comparable cross sectional reduction at the end of service life.

8. References

Alonso, C., Andrade, C., & González, J. (1988). Relation between resistivity and corrosion rate of reinforcements in carbonated mortar made with several cement types. *Cement and Concrete Research, 18*(5), 687-698. doi:10.1016/0008-8846(88)90091-9

Alzyoud, S., Wong, H. S., & Buenfeld, N. R. (2016). Influence of reinforcement spacers on mass transport properties and durability of concrete structures. *Cement and Concrete Research, 87*, 31-44. doi:http://dx.doi.org/10.1016/j.cemconres.2016.05.006

Andrade, C., & Andrea, R. (2010). *Electrical resistivity as microstructural parameter for the calculation of reinforcement service life.* Paper presented at the 2nd International Symposium on Service Life Design for Infrastructures, Delft, The Netherlands.

Bakker, R. (1994). *Predictions of service life of reinforcement in concrete under different climatic conditions at given cover.* Paper presented at the International Conference on Corrosion and corrosion protection of steel in concrete, Sheffield, UK.

Bamforth, P. (2004). *Enhancing reinforced concrete durability: Guidance on selecting measures for minimising the risk of corrosion of reinforcement in concrete.* (T. C. Society Ed. Vol. 61). Camberley, United Kingdom.

Bary, B., & Mügler, C. (2006). Simplified modelling and numerical simulations of concrete carbonation in unsaturated conditions. *Revue Européenne de Génie Civil, 10*(May 2015), 1049-1072. doi:10.1080/17747120.2006.9692905

Bary, B., & Sellier, A. (2004). Coupled moisture—carbon dioxide–calcium transfer model for carbonation of concrete. *Cement and Concrete Research, 34*(10), 1859-1872. doi:10.1016/j.cemconres.2004.01.025

Belda Revert, A., De Weerdt, K., Hornbostel, K., & Geiker, M. (2016). Carbonation Characterization of Mortar with Portland Cement and Fly Ash, Comparison of Techniques *Nordic Concrete Research*, 60-76.

Belda Revert, A., De Weerdt, K., Hornbostel, K., & Geiker, M. R. (In preparation). Carbonation-induced corrosion: investigation of the corrosion onset. *To be submitted to: Materials and Structures Journal*.

Bertolini, L., Elsener, B., Pedeferri, P., Redaelli, E., & Polder, R. (2013). Chapter 5: Carbonation-induced corrosion *Corrosion of Steel in Concrete* (pp. 79-91). Weinheim, Germany: Wiley-VCH Verlag GmbH & Co.

Bertolini, L., Lollini, F., & Redaelli, E. (2011). Durability design of reinforced concrete structures. *Proceedings of the Institution of Civil Engineers - Construction Materials, 164*(6), 273-282. doi:10.1680/coma.1000040

Bouquet, G. C. (2004). *CARBONATION INDUCED CORROSION OF REINFORCEMENT*. Paper presented at the Challenges of Concrete Construction: Volume 3, Repair, Rejuvenation and Enhancement of Concrete. http://www.icevirtuallibrary.com/doi/abs/10.1680/rraeoc.31753.0047

Czarnecki, L., & Woyciechowski, P. (2012). Concrete carbonation as a limited process and its relevance to concrete cover thickness. *Materials Journal, 109*(3), 275-282.

Duracrete. (2000). *Duracrete The European Union – Brite EuRam III, DuraCrete – Probabilistic Performance Based Durability Design of Concrete Structures. Final Technical Report of Duracrete project, Document BE95-1347/R17. CUR*. Retrieved from Gouda, the Netherlands.:

EHE 08;. (2008). Spanish Structural Concrete Code.

EN 206-1. (2000). EN 206-1 Concrete – Part 1: Specification, performance, production and conformity

EN 1990. (2002). EN 1990: Basis of structural design.

EN 1992. (2004). EN 1992: Design of concrete structures.

JSCE (2007). Standard specifications for concrete structures: Design (pp. 1-503).

fib (2006). International Federation for Structural Concrete, *fib*, Model Code for Service Life Design, Bulletin no 34. Lausanne, Switzerland.

fib (2010). International Federation for Structural Concrete, fib, Model Code for Service Life Design- bulletin no 55,56.

Gehlen, C., & Sodeikat, C. (2002). *Maintenance planning of reinforced concrete structures: redesign in A probabilistic environment inspection update and derived decision making* Paper presented at the 9th International Conference on Durability of Building Materials and Components, Brisbane, Australia.

Ghantous, R. M. (2016). *Identification desphasesd'initiationetdepropagationdelacorrosiondes armatures enrobéesdansunbétonfissuréetcarbonaté.* (PhD), University of Toulouse.

Ghods, P., Isgor, O. B., & Pour-Ghaz, M. (2007). A practical method for calculating the corrosion rate of uniformly depassivated reinforcing bars in concrete. *Materials and Corrosion, 58*(4), 265-272. doi:10.1002/maco.200604010

Greve-Dierfeld, S., & Gehlen, C. (2014). *Performance based deemed-to-satisfy rules*. Paper presented at the The Fourth International fib-Congress 2014, Mumbai.

Greve-Dierfeld, S., & Gehlen, C. (2016a). Performance-based durability design, carbonation part 2 – Classification of concrete. *Structural Concrete, 17*(4), 523-532. doi:10.1002/suco.201600066

Greve-Dierfeld, S., & Gehlen, C. (2016b). Performance based durability design, carbonation part 1 – Benchmarking of European present design rules. *Structural Concrete, 17*(3), 309-328. doi:10.1002/suco.201600066

Gulikers, J. (2005). Theoretical considerations on the supposed linear relationship between concrete resistivity and corrosion rate of steel reinforcement. *Materials and Corrosion, 56*(6), 393-403. doi:10.1002/maco.200403841

Helland, S. (2015). [Personal communication].

Helland, S. (2016a). *Assessments of carbonation ingress in-field as a tool to calibrate code requirements*. Paper presented at the *fib* Symposium, Cape Town, South Africa.

Helland, S. (2016b). *Performance-based service life design in the 2021 version of the european concrete standards- Ambitions and challenges*. Paper presented at the *fib* Symposium, Cape Town, South Africa.

Helland, S. (2017). [Personal communication].

Hills, T. P., Gordon, F., Florin, N. H., & Fennell, P. S. (2015). Statistical analysis of the carbonation rate of concrete. *Cement and Concrete Research, 72*, 98-107. doi:10.1016/j.cemconres.2015.02.007

ISO 2394. (2015). ISO 2394: General principles on reliability for structures.

ISO 13822. (2012). ISO 13822: Bases for design of structures- Assesment of existing structures.

ISO 13823. (2008). ISO 13823: General principles on the design of structures for durability

ISO 16204. (2012). ISO 16204: Durability- Service Life Design of Concrete Structures.

Ji, Y. S., Shen, J. L., Wang, L., & Xu, C. Y. (2011). Corrosion Characteristics and Corrosion Current Distribution of Steel Bar in Carbonated Concrete. *Advanced Materials Research, 239-242*, 3371-3376. doi:10.4028/www.scientific.net/AMR.239-242.3371

Jiang, L., Lin, B., & Cai, Y. (2000). A model for predicting carbonation of high-volume fly ash concrete. *Cement and Concrete Research, 30*(5), 699-702. doi:10.1016/S0008-8846(00)00227-1

Köliö, A., Honkanen, M., Lahdensivu, J., Vippola, M., & Pentti, M. (2015). Corrosion products of carbonation induced corrosion in existing reinforced concrete facades. *Cement and Concrete Research, 78, Part B*, 200-207. doi:http://dx.doi.org/10.1016/j.cemconres.2015.07.009

Lollini, F., Redaelli, E., & Bertolini, L. (2012). Analysis of the parameters affecting probabilistic predictions of initiation time for carbonation-induced corrosion of reinforced concrete structures. *Materials and Corrosion, 63*(12), 1059-1068. doi:10.1002/maco.201206720

Markeset, G., & Myrdal, R. (2008). Modelling of reinforcement corrosion in concrete - State of the art.

Melchers, R. E. (1996). *Structural reliability : analysis and prediction* (2nd ed.). Chichester Wiley

Morandeau, A., Thiéry, M., Dangla, P., & White, C. E. (2014, 2014). *Accelerated carbonation modelling of fly ash-blended cement paste*, Beijin, China.

Morinaga, S. (1990). *Prediction of service lives of reinforced concrete buildings based on the corrosion rate of reinforcing steel.* Paper presented at the Durability of building Materials and Component, London.

NS-EN 13670. (2010). NS-EN 13670: Excecution of concrete structures.

Otieno, M., Beushausen, H., & Alexander, M. (2011). Prediction of corrosion rate in RC structures - A critical review. *RILEM Bookseries, 5*(9), 15-37. doi:10.1007/978-94-007-0677-4_2

Papadakis, V. G., Fardis, M. N., & Vayenas, C. G. (1991). Fundamental modelling and experimental investigation of concrete carbonation. *Materials Journal, 88*(4), 363-373.

Papadakis, V. G., Fardis, M. N., & Vayenas, C. G. (1992). Hydration and carbonation of pozzolanic cements. *ACI Materials Journal, 89*(89), 119-130.

Parrott, L. J. (1994). A study of carbonation-induced corrosion. *Magazine of Concrete Research, 46*(166), 23-28. doi:doi:10.1680/macr.1994.46.166.23

Saetta, A. V., & Vitaliani, R. V. (2004). Experimental investigation and numerical modeling of carbonation process in reinforced concrete structures Part I: Theoretical formulation. *Cement and Concrete Research, 34*, 571-579. doi:10.1016/j.cemconres.2003.09.009

Sagues, A. (1997). *Carbonation in Concrete and Effect on Steel Corrosion*. Retrieved from

Salvoldi, B. G., Beushausen, H., & Alexander, M. G. (2015). Oxygen permeability of concrete and its relation to carbonation. *Construction and Building Materials, 85*, 30-37. doi:10.1016/j.conbuildmat.2015.02.019

Schiessl, P. (1976). *Zur Frage de zulässigen rissbreite und der erforder lichen betondeckung im stahlbetonbau-unter besonderer berücksichtigung der karbonatisierung des betongs.* Technical University of Munich, Berlin.

Silva, a., Neves, R., & De Brito, J. (2014). Statistical modelling of carbonation in reinforced concrete. *Cement and Concrete Composites, 50*, 73-81. doi:10.1016/j.cemconcomp.2013.12.001

Sisomphon, K., & Lutz, F. (2007). Carbonation rates of concretes containing high volume of pozzolanic materials. *Cement and Concrete Research, 37*(12), 1647-1653. doi:10.1016/j.cemconres.2007.08.014

Song, H. W., Kim, H. J., Kwon, S. J., Lee, C. H., Byun, K. J., Park, C. K., Ki-Bong. (2005). *Prediction of Service life in cracked Reinforced Concrete structures subjected to chloride attack and carbonation.* Paper presented at the Cement Combinations for Durable Concrete, Dundee, Scotland, U.K.

Steffens, A., Dinkler, D., & Ahrens, H. (2002). Modeling carbonation for corrosion risk prediction of concrete structures. *Cement and Concrete Research, 32*(6), 935-941. doi:10.1016/S0008-8846(02)00728-7

Thomas, M., & Matthews, J. (1992). Carbonation of fly ash concrete. *Magazine of Concrete Research, 44*(160), 217-228.

Tuutti, K. (1982). *Corrosion of steel in concrete.* Swedish Cement and Concrete Research Institute, Stockholm.

Appendix I

Time dependent models for carbonation development

Contents

1. Empirical models for the initiation period of carbonation-induced reinforcement corrosion

1.1. Model proposed by Morinaga

1.1.1. Experimental

Morinaga carried out experimental tests to investigate the service life of concrete structures affected by reinforcement corrosion [Morinaga, 1990]. The experiments included the study of carbonation rate, corrosion rate in carbonated concrete, corrosion rate in chloride contaminated concrete, and the corrosion allowance in concrete structures. The information related to the materials and exposure is limited: Concrete samples containing PC with various w/b ratios (0.4, 0.5 and 0.6) were prepared and exposed to 50-70% RH and high CO_2 concentration (not specified).

1.1.2. Model

Morinaga prosed models for the initiation and propagation period, the model for the corrosion rate in carbonated concrete is presented in Appendix II.

The time dependent model for carbonation consists of two equations, depending on the w/c.

$\frac{w}{c} < 0.6$

$$x_c = \sqrt{CO_2} \cdot (1.518 - 0.189 \cdot RH + 0.0236 \cdot T) \cdot \left(4.6 \cdot \frac{w}{c} - 1.76\right) \cdot \sqrt{t} \qquad \text{Eq. 1}$$

$\frac{w}{c} > 0.6$

$$x_c = \sqrt{CO_2} \cdot (1.518 - 0.189 \cdot RH + 0.0236 \cdot T) \cdot \frac{4.9 \cdot \left(\frac{w}{c} - 0.25\right)}{\sqrt{1.15 + 3 \cdot \frac{w}{c}}} \cdot \sqrt{t} \qquad \text{Eq. 2}$$

Where

x_c	Carbonation depth [mm]
CO_2	CO_2 concentration [%]
RH	Relative humidity [-]
T	Temperature [°C]
$\frac{w}{c}$	Water-to-cement ratio [-]
t	Exposure time [days]

1.1.3. Comments

It is not clear which experimental investigations were undertaken for the calibration of the model.

1.2. Model proposed by Thomas and Matthews

1.2.1. Experimental

Thomas and Matthews investigated carbonation development in 75x75x200 mm concrete prisms [Thomas and Matthews, 1992]. The same PC and FA were used as binders for all mixes, w/b from 0.32 to 0.57 were investigated. Various curing procedures were investigated: prisms were stored in the moulds wrapped with polyethylene at 5 or 20°C for 1 day after casting. Then prisms were stored for different periods and conditions (5 or 20°C; 40-90% RH or submerged in water). After curing, the samples were exposed to natural indoor carbonation (20°C and 65% RH) or outdoor exposure sheltered from the rain. Carbonation depth was measured by spraying phenolphthalein on a freshly broken surface after 90 days, 1 year and 2 years of exposure. Three points were measured on each side and the carbonation depth was determined as the mean value of the four sides.

1.2.2. Model

Thomas proposed a model to estimate carbonation rate on structures exposed to different environmental conditions. The model was presented as a design chart and included the following input parameters: curing period and conditions (curing time, RH and T), RH and T after demoulding, fly ash content and concrete compressive strength. Finally, the output is the carbonation coefficient (here named "carbonation rate" (mm/year$^{0.5}$).
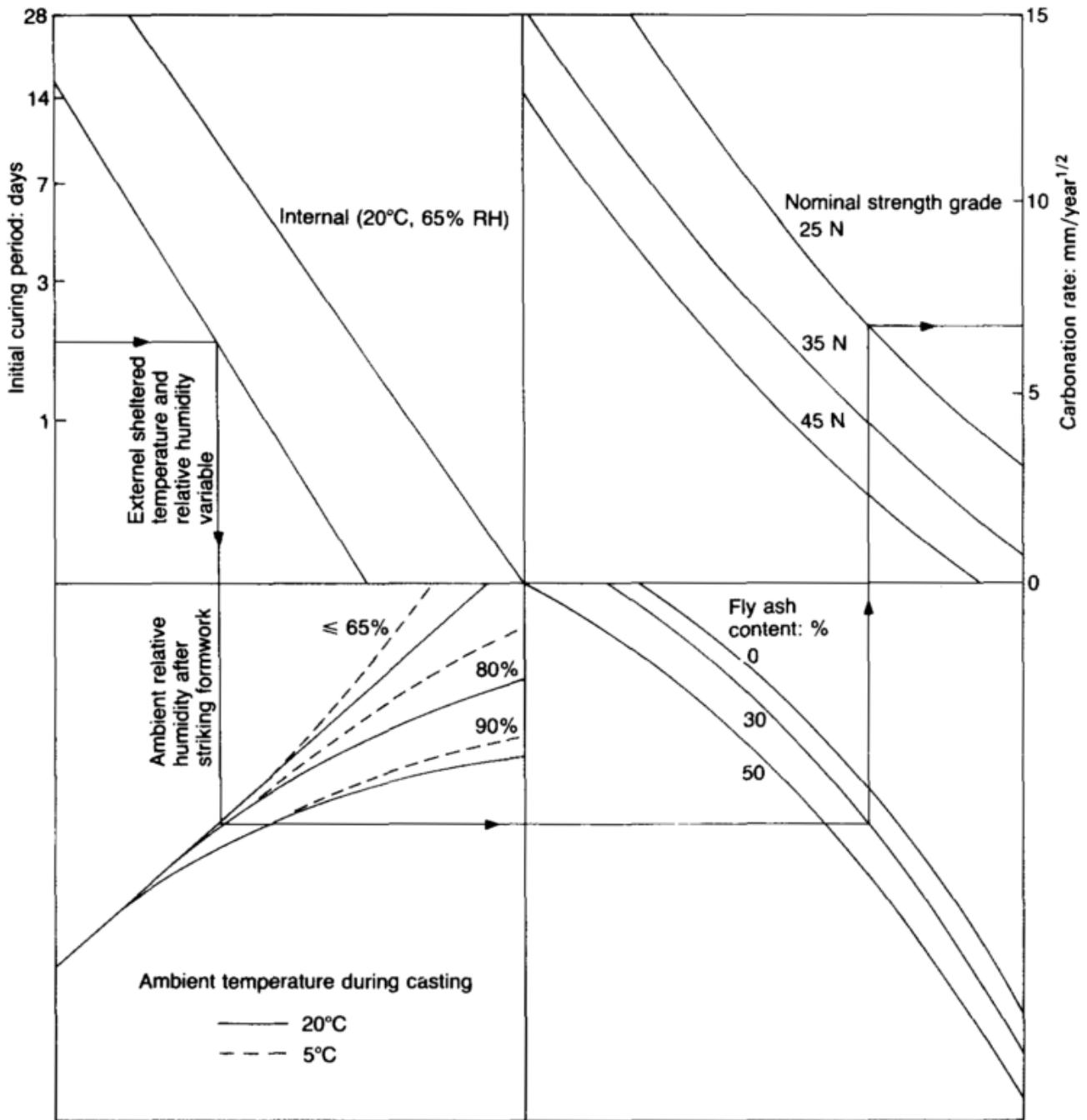
Figure 1: Chart design [Thomas and Matthews, 1992]

1.3. Model proposed by Parrott

1.3.1. Experimental

Parrot calibrated the model with published data from both laboratory and field structures, the materials and exposure conditions were not clearly specified [L. J. Parrott, 1994].

1.3.2. Model

Parrot proposed a model based on the air permeability of concrete including parameters describing the concrete quality and the exposure conditions. The model consists of two parts, the model for the propagation period is presented in Appendix II.

The time dependent carbonation depth (x_c) is given by:

$$x_c = \frac{64 \cdot D_{air}^{0.4} \cdot t^n}{C^{0.5}}$$

Eq. 3

$$n = 0.02536 + 0.01785 \cdot RH - 0.0001623 \cdot RH^2$$

Eq. 4

Where

x_c	Carbonation depth [mm]
D_{air}	Air permeability coefficient of the cover concrete [10^{-16} m²/year[1]]
n	Time exponent
RH	Relative humidity [%]
C	CaO content in hydrated cement matrix (paste) [kg/m³]
t	Exposure time [years]

1.3.3. Comments

The time exponent (n) depends on relative humidity, see Figure 2, and takes values from 0.025 (RH 0%) over 0.516 (RH 55%) to 0.187 (RH 100%). For RH from approximately 50 to 70% the model is close to the square root law. For higher or lower RH the time power exponent is lower, which means lower carbonation development compared to the square root law formulation.

---

[1] Parrot defined D_{air} in m² but this way the model presents unit incongruence.
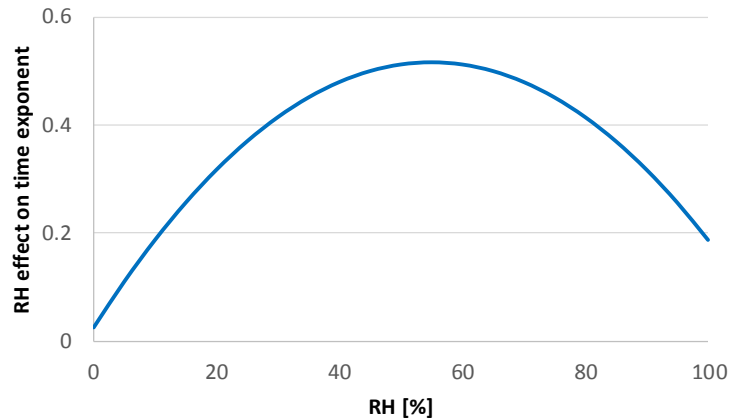
Figure 2: Time power exponent,n ,depending on RH

Parrot included some estimates of the CaO in the hydrated cement matrix for various RH and cement types (EN 197-1 (2011)), see Table 1. It is interesting to see the impact of RH on the hydration process. However, the cement types are presented in four general classes which might differ in CaO depending on the SCMs which are added.

Table 1: Cao content [kg/m³] in the hydrated cement matrix (paste) [L. J. Parrott, 1994]

RH [%]	40	50	60	70	80	90	95	98	100
CEM I	460	460	460	460	485	535	570	595	610
CEM II	360	360	360	360	380	420	445	465	480
CEM III	340	340	340	340	355	395	420	440	450
CEM IV	230	230	230	230	240	265	285	295	305

1.4. Model proposed by Bamforth

1.4.1. Experimental

Bamforth calibrated the model with experimental data published by several authors who carried out long term natural carbonation tests [Bamforth, 2004]. The data included various binder types (PC, FA, GGBFS, SF), binder contents, w/b, curing conditions and exposure conditions (external sheltered, external exposed to rain, constant temperature and relative humidity).

1.4.2. Model

Bamforth presented a model based on the buffering capacity of the binders. He assumed that the chemical buffering capacity of the cementitious materials governs carbonation. The input data are the type of cement and supplementary cementitious material (SCM), curing time, and relative humidity during exposure. The model covers both the initiation and propagation period.

The model for the propagation period is presented in Appendix II.

The carbonation coefficient (carbonation rate) is calculated as follows:

a) Buffering capacity coefficient (b_i) of binders
   For PC, b_1 is obtained from the C_3A content [% weight of cement]:

$$b_1 = 0.0019 \cdot (C_3A)^2 - 0.0056 \cdot (C_3A) + 0.7538 \qquad \text{Eq. 5}$$

   For SCMs coefficients in Table 2 are used.

Table 2: SCM: buffer capacity coefficient

SCM	b_2
Slag	0.6
Fly ash	0-0.2
Silica fume	-0.2

b) Buffering capacity, b, of blended binder:

$$b = b_1 \cdot c_1 + b_2 \cdot c_2 \qquad \text{Eq. 6}$$

   Where

   b_i Buffering capacity of binder i

   c_i Amount of binder i [kg/m^3]

c) Carbonation rate [mm/year$^{0.5}$]

$$k_n = -4.062 + 2.568 \cdot \frac{1000}{b} \qquad \text{Eq. 7}$$

d) Carbonation rate at specific curing conditions [mm/year$^{0.5}$]

$$k_{cure} = k_n(0.679 + 0.75 \cdot p^{-0.715})$$

Eq. 8

Where

p Total period of wet curing [days]

e) Carbonation rate at specific relative humidity

$$k_{cureRH} = k_{cure} \cdot (-0.000508 \cdot (RH)^2 + 0.0556 \cdot RH - 0.4472)$$

Eq. 9

1.4.3. Comments

The carbonation rate depends on RH. Carbonation will not take place either at RH below 10 % or close to 100%, while for RH 55 % carbonation takes place at the highest rate, see Figure 3.
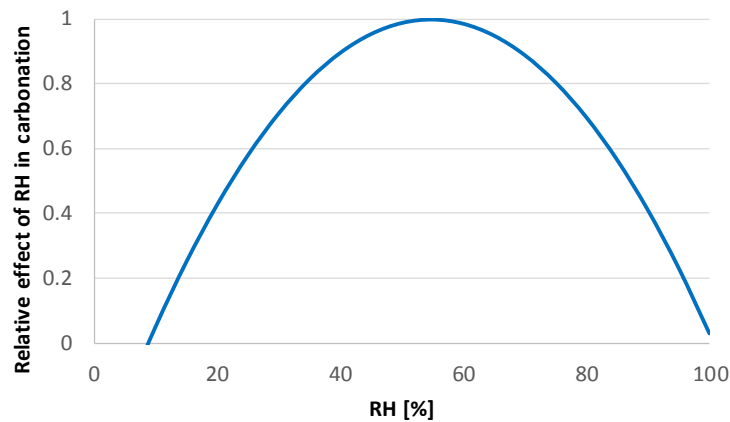
Figure 3: Carbonation rate depending on RH

Apart from w/b ratio, all the parameters tested in the experimental tests are included in the model. Bamforth observed that in the long-term natural carbonation data, w/b ratio does not seem to make a significant influence on carbonation depths. He claimed that the higher resistance against carbonation in low w/b ratio mixes could be related to the general trend of having higher cement content in these mixes.

1.5. Model proposed by the Japanese Society of Civil Engineers

1.5.1. Experimental

The experimental data was not clearly specified.

1.5.2. Model

The Japanese society of civil engineers (2007) proposed a model based on experimental data on which carbonation development follows the square root law. All parameters are related to the mixture.

$$x_c = \left(-3.57 + 9 \cdot \frac{w}{c + ad_{eff} \cdot SCM}\right) \cdot \sqrt{t} \qquad \text{Eq. 10}[2]$$

Where

x_c Carbonation depth [mm]

w Water content [kg/m³]

c Cement content [kg/m³]

ad_{eff} Suplementary cementitious material efficiency [-]

SCM Supplementary cementitious materials [kg/m³]

t Exposure time [years]

1.5.3. Comments

The fly ash efficiency factor (ad_{eff}) was assumed to be 0.

---

[2] Note that the term $\frac{w}{c+ad_{eff} \cdot SCM}$ is defined by the EN-206 (2000) as the effective water-binder ratio

1.6. Model proposed by Czarnecki and Woyciechowski

1.6.1. Experimental

Czarnecki and Woyciechowski calibrated the model with data from investigations covering both natural and accelerated exposure [Czarnecki and Woyciechowski, 2012].

Accelerated tests were carried out at 20°C, 60% RH and 1% CO_2. The impact of the cement content, w/b, aggregate content and fly ash substitution (0, 15 and 30% by mass) were studied. The carbonation depth was determined by spraying phenolphthalein indicator on a freshly broken surface of a 100x100x400 mm concrete prism.

Natural exposure tests were carried out with different binders, w/b and curing time. The carbonation depth was determined over a 6-year exposure period on concrete prisms with dimensions 300 x300x100 mm by spraying the freshly broken surfaces with thymol-phenolphthalein indicator.

1.6.2. Model

Czarnecki proposed a model on which carbonation rate follows a hyperbolic function with time.

$$x_c = A - \frac{B}{\sqrt{t}}$$

Eq. 11

Where

x_c	Carbonation depth [mm]	
A, B	Constants which depend on the material and exposure	
t	Time [days]	

1.6.3. Comments

The time exponent was chosen to be -1/2 because it had the highest correlation coefficient with the experimental data. A similar time dependency was proposed previously by [Schiessl, 1976], for which carbonation development presents an upper bound, once this value is reached carbonation front does not develop further. Schiessl's model is presented in Section **Error! Reference source not found.**.

$$h = A - Bxt^{0.5} \ (h \to \infty)$$

h_{max} = ordinate v value of asymptote

$$h = A - Bxt^{-1}$$

$$h = A - Bxt^{-0.5}$$
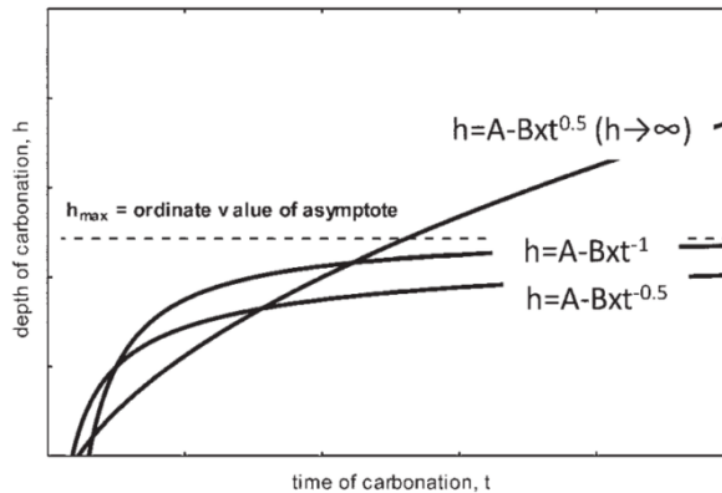
Figure 4: Comparison of parabolic and hyperbolic models for carbonation [Czarnecki and Woyciechowski, 2012]

Czarnecki and Woyciechowski faced some challenges measuring carbonation depth in concrete exposed to natural carbonation which can be relevant for the ongoing investigations in the Lavkarbsem project:

- Initially they used three pH colour indicators for determining carbonation depths: phenolphthalein (pH change 8.3 (P)), thymolphthalein (pH change 10.5(T)) and thymol-phenolphtalein (pH change 9.6 (TP)). After 2 years, the carbonation depth measured using P and TP were quite similar (±1 mm), but the average carbonation depth was much deeper for T.
- A larger carbonation depth was obtained at the bottom side of the samples. He proposed that it was due to an optimal RH for carbonation on the bottom side. It is not clear if the bottom side during exposure was the bottom side during the casting.
- The carbonation depth values presented in the paper are the ones measured on the bottom side using thymol-phenolphthalein indicator.

The applicability of pH indicators for detection of carbonation depth in mortars with PC and FA blends were tested under accelerated conditions as well as the variation in measured carbonation depths, for further description see [Belda Revert et al., 2015] and [Belda Revert et al., 2016]. Additionally, SINTEF performed a broader comparison of both pH indicators including various binders and carbonation exposures, see [Østnor et al., 2016]. Belda et al. found that for the investigated binders (CEM I and CEM II/B-V), thymolphtalein 1% solution is a proper substitute for phenolphthalein, which is classified as potentially carcinogenic. Similar to Czarnecki, Belda et al. found differences between carbonation depths depending on the side of the prisms but the potential causes seem different (inhomogenities). In the case of Belda et al. samples were exposed to accelerated conditions with constant relative humidity on all the sides.

1.7. Model proposed by Silva et al.

1.7.1. Experimental

Silva et al. calibrated the model with data from investigations covering both natural and accelerated exposure [Silva et al., 2014]. The data set included concrete containing different binders (PC, FA and GGBFS), binder contents, w/b (from 0.24 to 1), compressive strengths (from 9 to 128 MPa), curing periods (from 7 to 91 days) and exposure conditions. About half of the data set came from natural carbonation and the other half from accelerated carbonation (from 0.02 to 50% CO_2).

1.7.2. Model

Silva et al. proposed a model to estimate the carbonation coefficient (k) assuming the square root law. It consists of two equations, one for relative humidity below 70 % and other for higher relative humidity.

RH< 70 %:

$$k = 0.556 \cdot CO_2 - 3.602 \cdot X - 0.148 \cdot f_c + 18.734 \qquad \text{Eq. 12}$$

Where

k	Carbonation coefficient [mm/year$^{0.5}$]	
CO_2	CO_2 concentration [%]	
X	Exposure class according to EN-1992 (2004)	
	$XC - 1$ Dry environment or permanently wet: $X = 1$	
	$XC - 2$ Wet environment rarely dry: Not applicable (RH> 70%)	
	$XC - 3$ Environment with moderate humidity: $X = 2$	
	$XC - 4$ Environment with cyclic wet and dry: $X = 3$	
f_c	28-day compressive strength [MPa]	

RH> 70 %:

$$k = 3.355 CO_2 - 0.019 Cli - 0.042 f_c + 10.83 \qquad \text{Eq. 13}$$

Where

Cli	Clinker content in concrete [kg/m^3]

1.7.3. Comments

The model's coefficients were calibrated by linear regression. The relative humidity was introduced as function of the exposure class according to EN-1992 (2004).

The impact of the RH is included depending on the exposure class. For RH higher than 70% no effect is assumed. For the XC-3 exposure lower carbonation rates are obtained compared to XC-1.

1.8. Model proposed by Greve-Dierfeld and Gehlen

1.8.1. Experimental

Greve-Dierfeld and Gehlen calibrated the model using their own experimental data as well as data taken from the literature [Greve-Dierfeld and Gehlen, 2014].

Greve-Dierfeld and Gehlen investigated carbonation development on concretes of 48 different compositions, Table 3 presents the ranges of compositions. The carbonation depth was measured either on concrete prisms with dimensions 100x100x500 mm or mortar prisms with dimensions 40x40x160 mm. The prisms were cured for 7 days submerged in water at 20°C, and afterwards exposed to 20°C, 65% RH, 0.04% CO_2. The carbonation depth was measured at least after 140 days of exposure by spraying phenolphthalein 1 % on a freshly broken surface (5 measuring points taken per side).

Table 3: Ranges of compositions of the tested samples

Types of CEM EN 197-1 (2011)	I	II/A-S	II/A-V	II/A-LL	II/A-M	II/B-S	II/B-V	II/B-LL	II/B-M	III/A
w/b [-]	0.4-0.6	0.6-0.65	0.4-0.65	0.4-0.65	0.6-0.65	0.5-0.65	0.5-0.65	0.65	0.45-0.65	0.45-0.65
Binder content [kg/m³]	320-460	280	280-420	280-340	280	280-350	280-400	390	280-350	280-460

The data taken from the literature included the compositions given in Table 4.

Table 4: Ranges of compositions taken from the literature

Types of CEM EN 197-1 (2011)	I	II/A-S	II/A-D	II/A-V	II/A-LL	II/A-M	II/B-S	II/B-V	II/B-LL	II/B-M	III/A	III/B
w/b [-]	0.45-0.65	0.45-0.6	0.5-0.65	0.6	0.4-0.65	0.4-0.5	0.4-0.65	0.45-0.65	0.55-0.65	0.5-0.65	0.45-0.6	0.45-0.6
Binder content [kg/m³]	260-450	260-390	290-340	290-340	260-450	280-340	320-360	290-450	260-340	260-500	270-390	290-450

1.8.2. Model

Greve-Dierfeld and Gehlen proposed a design chart for exposure class XC4[3] according to EN-1992 (2004) based on experimental data and using equations from *fib (2006),* see Figure 5.

They proposed to classify the carbonation resistance in the same way as concrete compressive strength is classified: carbonation resistance classes (RCX). This approach with RCX classes is a proposal for coming CEN revisions.

Input data is the experimentally determined carbonation resistance class (RCX), relative humidity, design service life and time of wetness. The obtained output is the concrete cover.
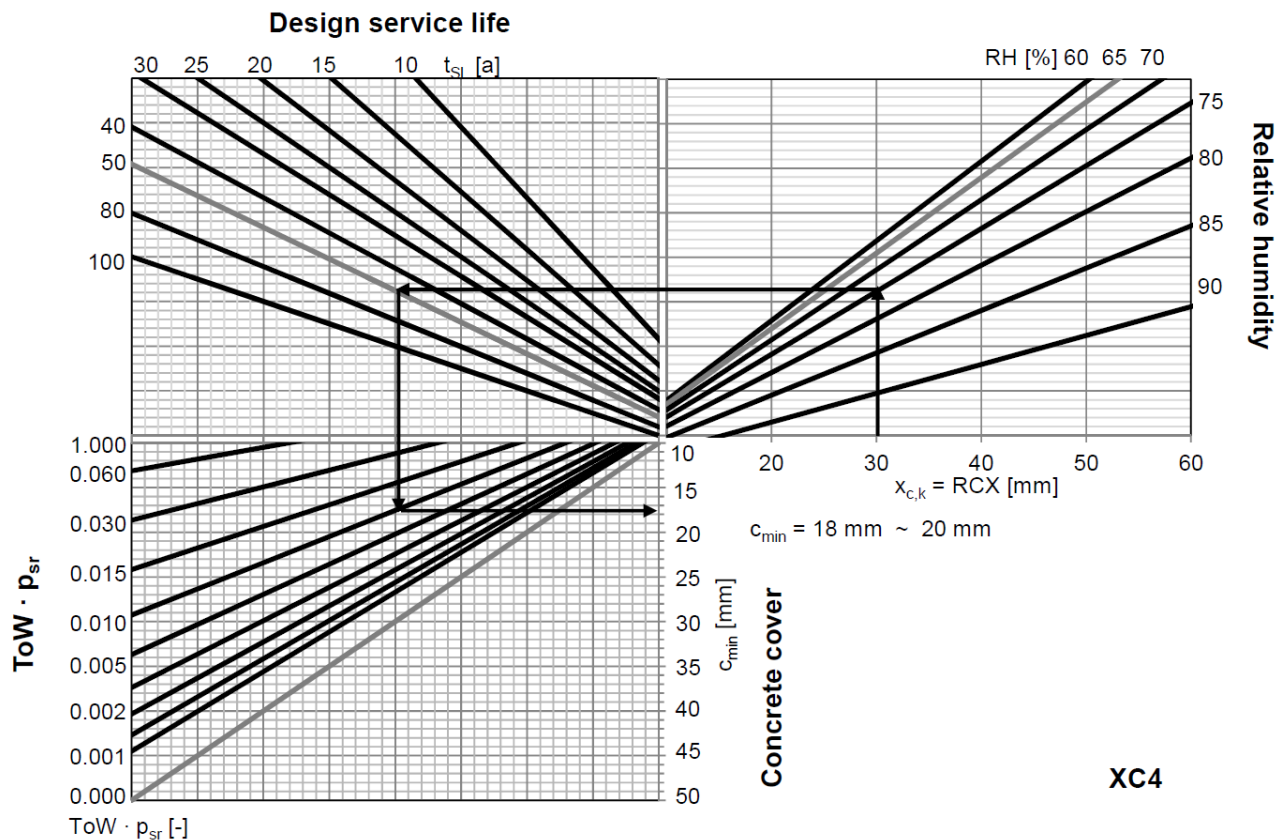
Figure 5: Proposed design chart for XC4 exposure
(RCX(or $x_{c,k}$)[4]: carbonation resistance class, $ToW \cdot p_{sr}$: Time of wetness times probability of driving rain) [Greve-Dierfeld and Gehlen, 2014]

---

[3] XC4: "Concrete surfaces subjected to water contact, not within exposure class XC2". Exposure XC2 is defined as "concrete surfaces subjected to long-term water contact" EN 1992 (2004)
4 Note that in the present report x_c is defined as the carbonation depth and it is not the same concept defined by Greve-Dierfeld with $x_{c,k}$ (RCX).

1.8.3. Comments

The carbonation resistance class of a given concrete is the carbonation depth measured in a short-term test ($x_{c,k}$), as described in section 1.8.1, which does not exceed the given quantile (*k*), see Figure 6, where the 90% quantile of the measured carbonation depths ($x_{c,90}$) is illustrated. The measured short-term data is extrapolated to a reference service life. Concretes are classified in RCX classes depending on the $x_{c,90}$, e.g. concrete in Figure 6 is classified as RC30 following Figure 7.
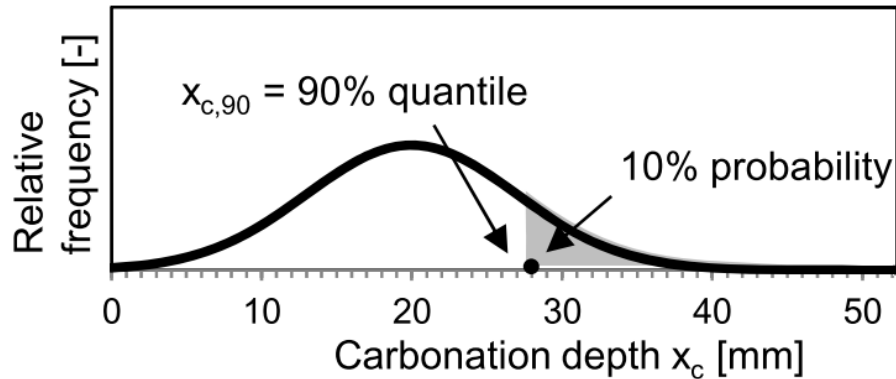
Figure 6: Measured carbonation depths relative frequency [Greve-Dierfeld and Gehlen, 2014]
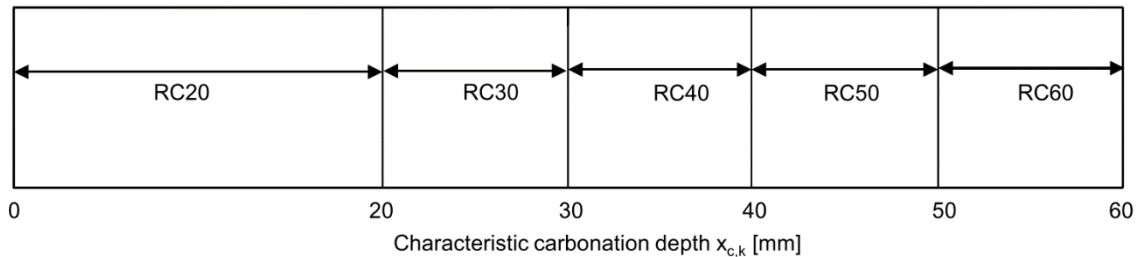
Figure 7: Carbonation resistance class based on $x_{c,k}$ [Greve-Dierfeld and Gehlen, 2014]

Time of wetness (ToW) is not defined in the publication. However, according to *fib* (2006), it is defined as the average number of days with at least 2.5 mm of precipitation per day in a year. In the case of probability of driving rain (p_{sr}) it is defined as the average distribution of the wind direction during rain events. For example, p_{sr} is 0 for elements sheltered from the rain, 1 for unsheltered horizontal elements and for vertical elements varies between 0 and 1 depending on the main wind direction when raining:

$$ToW \cdot p_{sr} = \frac{days \ with \ rain \ fall \geq 2.5 \ mm}{365} \cdot p_{sr} \qquad \text{Eq. 14}$$

1.9. Model proposed by Hills et al.

1.9.1. Experimental

Hills et al. calibrated the model using data from the literature [Hills et al., 2015]. The model estimate carbonation rate of structures exposed to natural carbonation, accelerated carbonation data was excluded.

It was assumed that field structures were exposed to the same CO_2 concentration: 350 ppm (0.035%).

1.9.2. Model

Hills et al. proposed two carbonation models to estimate the carbonation coefficient (k) assuming the square root law. A factor (I_{Exp}) was included to differentiate between field and laboratory data.

Model 1: Time dependent model which includes I_{Exp}:

$$\ln(k) = 0.567 - 0.167 \cdot I_{CEM\,I} + 0.101 \cdot I_{GGBFS} + 0.129 \cdot I_{PFA} + 0.249 \\ \cdot I_{Exposed} + 0.818 \cdot I_{Sheltered} + 0.433 \cdot I_{Indoor} \\ + \left(0.037 - 0.088 \cdot I_{Exp}\right)t + (-0.00046 + 0.0013 \cdot I_{Exp})^2 \cdot t^2$$

Eq. 15

Model 2: Compressive strength dependent model; assuming no time dependency of k:

$$\ln(k) = 1.066 + 1.761 \cdot I_{CEM\,I} + 2.062 \cdot I_{GGBFS} + 2.061 \cdot I_{PFA} - 0.639 \\ \cdot I_{Exposed} - 0.182 \cdot I_{Sheltered} - 0.648 \cdot I_{Indoor} \\ + (0.025 - 0.053 \cdot I_{CEM\,I} - 0.052 \cdot I_{GGBFS} - 0.05 \cdot I_{PFA}) \cdot f_c$$

Eq. 16

Where

k	Carbonation coefficient [mm/year$^{0.5}$]
I	Factor which takes value 1 if the subscript applies or 0 in case it does not:
	Type of cement: CEM I, blends of GGBFS or PFA
	Exposure conditions: Exposed, Sheltered or Indoor
	Origin of the data: Exp (in case data comes from laboratory tests)
f_c	Compressive concrete strength [MPa]
t	Exposure time [years]

1.9.3. Comments

Hills et al. found that the distribution of the carbonation rate constant of structures exposed to natural carbonation is not normally distributed: values far from the average value of the distribution were found.

The models present a logarithmic relation between the carbonation rate constant and the parameters affecting carbonation.

It is not clear for which conditions Model 1 or Model 2 should be used. It is stated that Model 1 focuses on the origin of concrete and age while Model 2 on the concrete strength.

2. Mechanism based models for the initiation period of carbonation-induced reinforcement corrosion

2.1. Model proposed by Schiessl

2.1.1. Experimental

Schiessl investigated concrete containing PC with three w/b: 0.45, 0.6 and 0.8, with the following respective binder contents: 420, 300 and 240 kg/m^3 [Schiessl, 1976]. The curing conditions and exposure were not clearly specified (3% CO_2).

2.1.2. Model

Schiessl proposed a diffusion based model with an upper carbonation depth bound (x_∞). The carbonation depth (x_c) is determined using the following equations:

$$t = -\frac{B}{\bar{b}}\left[\left(x_c + x_\infty ln\left(1 - \frac{x_c}{x_\infty}\right)\right)\right]$$

Eq. 17

$$x_\infty = \frac{D_{CO2} \cdot CO_2}{f \cdot D_{CO2}.CO_2 + A}$$

Eq. 18

Where:

t	Exposure time [years]
B	Binding capacity [kg /m^3]
$\bar{b}$	Retardation factor due to carbonation [kg/m^3]
x_c	Carbonation depth at time "t" [m]
x_∞	Upper carbonation depth bound [m]
D_{CO2}	Surface CO_2 diffusion coefficient [m^2/s]
CO_2	CO_2 concentration [%]
f	Decrease of diffusion coefficient factor [-]
A	CO_2 necessary for complete carbonation [kg /m^3]

2.1.3. Comments

The model includes a retardation factor ($\bar{b}$) and assumes a decrease in the diffusion coefficient due to carbonation.

Tuutti [Tuutti, 1982] argued that Schiessl's model assumes that concrete becomes impermeable against CO_2 at a certain stage, which cannot be fully correct. He claimed that the actual carbonation rate would be between the square root law approximation and Schiessl approximation (Eq. 17 and Eq. 18). Figure 8 presents the comparison of both approaches: Equ. (1) represents the square root law while Equ. (2) represents Schiessl's model.
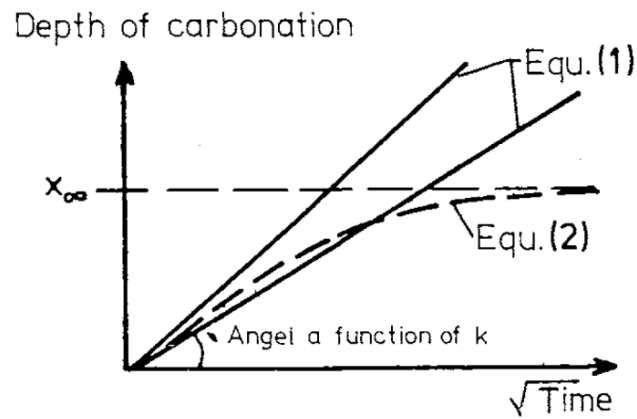
Figure 8: Schiessl's model (Equ. 2) versus the square root law model (Equ. 1) [Tuutti, 1982]

Other authors have also proposed equations with an upper carbonation front bound. A similar approach was presented by Houst suggesting a high and a low rate stage in carbonation development [Houst et al., 1983].

2.2. Model proposed by Tuutti

2.2.1. Experimental

Tuutti calibrated the model with data presented in German publications from 1965 and 1967 including long term tests on concrete exposed to natural carbonation [Tuutti, 1982]. However, this data was not found.

2.2.2. Model

Tuutti presented a diffusion based model including the error function:

$$\frac{\Delta C_s}{a} = \sqrt{\pi} \cdot \left(\frac{x/\sqrt{t}}{2 \cdot \sqrt{D_{CO_2}}} \right) \cdot e^{\left(\frac{\left(x/\sqrt{t} \right)^2}{4 \cdot D_{CO_2}} \right)} \cdot erf \left(\frac{x/\sqrt{t}}{2 \cdot \sqrt{D_{CO_2}}} \right) \qquad \text{Eq. 19}$$

Where

ΔC_s	Difference in CO_2 concentration between air and concrete [kg/m^3]
a	Amount of CO_2 necessary for complete carbonation [kg/m^3]
x	Carbonation depth [m]
t	Exposure time [s]
D_{CO_2}	CO_2 diffusion coefficient [m^2/s]
erf	Error function [-]

2.2.3. Comments

Tuutti assumed a discontinuous pH profile due to carbonation: a thin layer is completely carbonated on one side and sound on the other side. This process can be described mathematically as a moving boundary.

He assumed that carbonation development follows the square root law with time.

Carbonation rate is dependent on the CO_2 concentration, absorption of CO_2 in concrete and permeability, x_c can be determined if these three parameters are known.

2.3. Model proposed by Papadakis et al: PC

2.3.1. Experimental

Papadakis et al calibrated the model with experimental tests [Papadakis et al., 1991]. Concrete prisms containing PC with different w/b, aggregate content and type with dimensions 100x100x300 mm were cast in Plexiglas moulds. After 24 hours, samples were demoulded and cured submerged in saturated $Ca(OH)_2$ solution at 30°C for 90 days to ensure complete hydration. After curing, samples were oven-dried and all sides except two opposite lateral sides were covered with a gas-tight paint. Then samples were exposed to various constant accelerated conditions: temperature (22, 30 or 42°C), relative humidity (35, 45, 55, 65, 70, or 85%) and about 50% CO_2. The carbonation depth was measured after 1, 3, 5, 10, 15, and 20 days of exposure by spraying phenolphthalein on a freshly broken surface of a 20-mm thick slice.

2.3.2. Model

Papadakis et al. proposed an analytical model for the time dependent carbonation based on diffusion:

$$x_c = \sqrt{\frac{2 \cdot D_{CO_2} \cdot CO_2}{[CH]^0 + 3 \cdot [CSH]^0 + 3 \cdot [C_3S]^0 + 2 \cdot [C_2S]^0} \cdot t} \qquad \text{Eq. 20[5]}$$

Where

D_{CO_2}	Carbon dioxide diffusion coefficient [m^2/s]
CO_2	Carbon dioxide concentration [mol/m^3]
$[Ca(OH)_2]^0$ …	Denominator: carbonatable material [mol / m^3]
t	Exposure time [years]

2.3.3. Comments

Papadakis et al described the physicochemical processes involved in carbonation including CO_2 diffusion through concrete pores and its dissolution in the aqueous film of the pores, calcium hydroxide (CH) dissolution, diffusion of dissolved CH in pore water, and finally reaction with CO_2.

They considered that carbonatable phases were CH, C-S-H and the unhydrated phases: C$_3$S and C$_2$S.

The changes in carbonatable materials during hydration and the reduction of concrete porosity due to carbonation and hydration were included in complementary models, see Section 2.4.

---

[5] Note that the super indexes in the denominator refer to the molar concentration of each component after the moist curing, when carbonation starts (t=0)

2.4. Model proposed by Papadakis et al: blended cements

2.4.1. Experimental

Papadakis et al. calibrated the model with experimental tests [Papadakis et al., 1992]. The set up and parameters of the accelerated conditions were the same as for the previous investigation. In this case, additional binders were tested to study the influence of various pozzolanic materials on carbonation: natural pozzolana and two artificial pozzolans (one with high and other with low pozzolanic activity).

2.4.2. Model

Papadakis et al. presented an updated model for blended cements:

$$x_c = \sqrt{\frac{2 \cdot D_{CO_2} \cdot CO_2}{[CH] + 3 \cdot [CSH]} \cdot t}$$

Eq. 21

2.4.3. Comments

The Ca/Si ratio of the C-S-H was considered constant (3-1) and not to have an influence in carbonation development.

Papadakis et al. proposed an equation to estimate the carbon dioxide diffusion coefficient which needs as input the porosity and RH. They also proposed an equation for the porosity development.

$$\varepsilon_p = (\varepsilon_0 - \Delta\varepsilon_H - \Delta\varepsilon_c)\left(1 + \frac{\frac{a}{b}\frac{\rho_c}{\rho_a}}{1 + \frac{w}{b}\frac{\rho_c}{\rho_w}}\right)$$

Eq. 22

Where

ε_p	Hardened paste porosity [-]
ε_0	Fresh concrete porosity [-]
$\Delta\varepsilon_H$	Porosity reduction due to hydration [-]
$\Delta\varepsilon_c$	Porosity reduction due to carbonation [-]
a	Aggregate content [kg/m³]
b	Binder content [kg/m³]
w	Water content [kg/m³]
ρ_a	Sand density [kg/m³]
ρ_c	Binder density [kg/m³]
ρ_w	Water density [kg/m³]

$$D_{CO_2} = 1.64 \cdot 10^{-6} \varepsilon_p^{1.8} \left(1 - \frac{RH}{100}\right)^{2.2}$$

Eq. 23

Where

D_{CO_2}	Carbon dioxide diffusion coefficient [m²/s]

2.5. Model proposed by Bouquet based on Bakker's previous work

2.5.1. Experimental

Bouquet [Bouquet, 2004] took the model Bakker [Bakker, 1994] proposed and verified it applying his own data set. Additionally, Bouquet included a propagation period model which is described in Appendix II.

Bouquet investigated carbonation on concrete samples with dimensions 500x100x100 mm containing slag cement [Bouquet, 2004]. Samples were kept in the moulds wrapped with plastic for three days after casting. Then they were placed in different natural exposures and carbonation depth was measured after 4, 23, 24, 52 105, 208 and 345 weeks of exposure.

2.5.2. Model

Bouquet verified the model previously presented by Bakker:

$$x_c = \sqrt{\frac{2 \cdot D_{CO_2} \cdot CO_2}{CaO} \cdot t_{eff,n}}$$

Eq. 24

Where

D_{CO_2} CO₂ diffusion coefficient of dry concrete [m²/s]

CO_2 CO₂ concentration [kg/m³]

CaO CaO content in the binder [kg/m³]

$t_{eff,n}$ Effective time of exposure after n cycles of drying and wetting [s]

The effective time of exposure takes into account wetting and drying cycles. The effective time of exposure after n cycles of drying and wetting is presented as follows:

$$t_{eff,n} = t_{d,1} + \sum_n \left(t_{d,n} - \left(\frac{\sqrt{\frac{D_{CO_2} \cdot CO_2}{Alkalis} \cdot t_{eff,n-1}}}{\sqrt{\frac{D_v \cdot (C_3 - C_4)}{W}}} \right)^2 \right)$$

Eq. 25

Where

D_v Water vapour diffusion coefficient [m²/s]

$C_3 - C_4$ Moisture difference between air and the evaporation front [kg/m³]

D_{CO_2} Carbon diffusion coefficient of dry concrete [m²/s]

W Amount of water to be evaporated [kg/m³]

t_d Length of dry periods [s]

2.5.3. Comments

The model considers the effect of moisture in the carbonation process. When concrete is wet, carbonation stops because CO_2 diffusion through water is about 10^4 smaller compared to air. Carbonation only occurs when the concrete is dry. When there is a wet cycle, carbonation stops and starts again once the dry depth is equal to the actual carbonated depth. Figure 9 gives a schematic representation of the drying and wetting depths and the time required for each cycle.
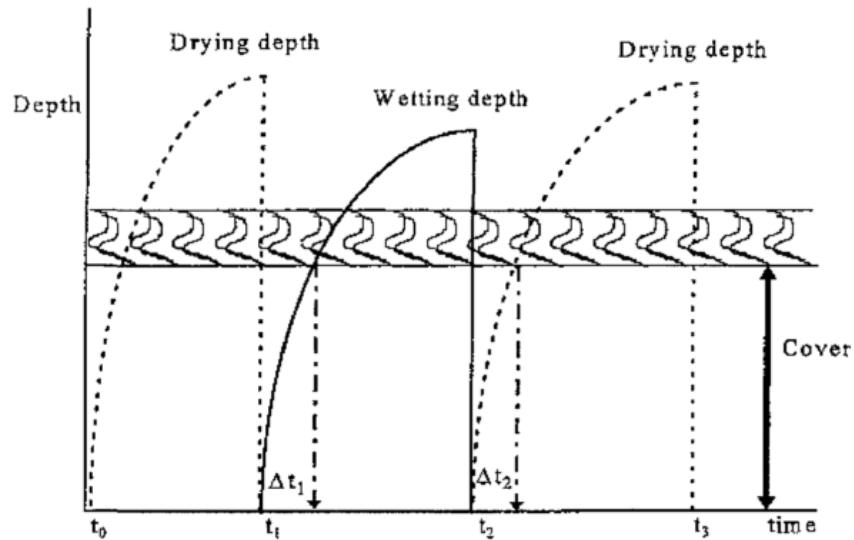
Figure 9: Schematic representation of wetting and drying depths [Bouquet, 2004]

2.6. Model presented by Jiang et al.

2.6.1. Experimental

Jiang et al. calibrated the model with experimental accelerated tests on concrete prisms with dimensions 100x100x200 mm [Jiang et al., 2000]. Portland cement was used as binder with different amounts of fly ash replacement and water-to-binder ratios. Accelerated conditions were: 20°C, 70% RH and 20% CO_2. Carbonation depth was assessed by spraying phenolphthalein indicator on a freshly broken surface of a 50-mm thick slice. Eight points were taken per side.

2.6.2. Model

Jiang et al. proposed a model for carbonation of concrete containing PC including minor amounts of SCMs:

$$x_c = 839 \cdot (1 - RH)^{1.1} \cdot \sqrt{\frac{\frac{W}{r_c \cdot c} - 0.34}{DH \cdot c}} \cdot CO_2 \cdot \sqrt{t} \qquad \text{Eq. 26}$$

Where

RH	Relative humidity [-]
W	Water content [kg/m³]
r_c	Coefficient for the cement type [-]
c	Cement content [kg/m³]
DH	Degree of hydration of the cement clinker [-]
CO_2	Carbon dioxide concentration [%]
t	Exposure time [days]

This model did not fit the results for concrete with high fly ash content They presented a modified model for fly ash blended concrete:

$$x_c = 839 \cdot (1 - RH)^{1.1} \cdot \sqrt{\frac{\frac{W}{c+F} \cdot \frac{1-M}{1-FA} - 0.34}{DH \cdot k' \cdot c}} \cdot CO_2 \sqrt[n]{t} \qquad \text{Eq. 27}$$

$$k' = \frac{M}{1-M} \cdot m_{fa} \cdot \frac{1}{0.82} \qquad \text{Eq. 28}$$

Where

FA	Fly ash content [%]
k'	Factor related to hydrated fly ash [-]
M	Maximum fly ash content which can react [%]
m_{fa}	Al₂O₃ content in the fly ash [%]
n	Factor related to the pore structure $[2 \leq n \leq 2.1]$[6]
t	Exposure time [days]

---

[6] Jiang, Lin et al. did not specify how to estimate the parameter "n"

2.6.3. Comments

The authors did not define what meant "concrete with high fly ash content".

Fly ash replacement higher than 30 % could be considered high.

2.7. Model proposed by Sisomphon and Lutz

2.7.1. Experimental

Sisomphon and Lutz calibrated the model with experimental tests which included constant binder content with various fly ash replacement (from 0 to 50%), water binder ratios and curing conditions [Sisomphon and Lutz, 2007]. Cylindrical concrete samples were prepared, demoulded one day after casting and water cured. Samples were preconditioned at 20°C and 50% RH. Accelerated carbonation tests started when samples were 5 months old. The exposure conditions were 65% RH (it was controlled by NH_4NO_3 solution) and 3% CO_2. Carbonation depth was measured by spraying phenolphthalein indicator on both halves of the freshly broken surfaces of the cylinder, taking three measuring points per half. The carbonation depth value was the average value of these six points.

2.7.2. Model

Sisomphon and Lutz proposed a carbonation model for high fly ash content blended cement.

$$x_c = \sqrt{\frac{2 \cdot D_{CO_2} \cdot CO_2}{a}} \cdot t^{0.4}$$

Eq. 29

Where:

D_{CO_2}	Carbon diffusion coefficient of dry concrete [m^2/s]
CO_2	Carbon dioxide concentration [g/m^3]
a	Amount of CO_2 necessary for complete carbonation [g/m^3]
t	Exposure time [days]

2.7.3. Comments

Sisomphon and Lutz proposedthe time exponent of 0.4 based on the experimental results. Following Fick's first law, time exponent should be 0.5, however he justified the proposed time exponent because carbonation products block the pores in concrete reducing the diffusivity. Thus, to consider a constant *k*, it is necessary to change the time exponent to obtain lower carbonation depth development over the time.

The author did not define what meant "high fly ash content blended cement".

2.8. Model proposed by Andrade and Andrea

2.8.1. Experimental

Andrade and Andrea proposed the model was as a new approach on service life modelling [Andrade and Andrea, 2010]. However, no experimental tests to verify the results nor numerical simulations to check the values were found.

2.8.2. Model

Andrade and Andrea proposed a model including both initiation and propagation period based on the concrete resistivity. For the initiation period the penetration of CO_2 as well of chlorides is described applying Einstein's equation for a random walk of an ion in an electrolyte, which is a diffusion equation.

The model for the propagation period is described in Appendix II.

The equation for carbonation development is the following:

$$x_c = \sqrt{\frac{k_{CO_2}}{\rho_{ef} \left(\frac{t}{t_0}\right)^q \cdot r_{CO_2}} t}$$

Eq. 30

Where

k_{CO_2} Environmental factor, depends on the exposure. Some values for given exposure classes according to EN 1992 (2004) were included:

         X0: 200 [cm^3·Ω/year]

         XC1: 1000 [cm^3·Ω/year]

         XC3: 3000 [cm^3·Ω/year]

ρ_{ef} Concrete resistivity in saturated conditions [cm^3·Ω/year]

t Exposure time [years]

t_0 Time where ρ_{ef} is measured [years]

q Concrete resistivity ageing factor, depends on the cement type (EN 197-1 (2011)) [-]:

         CEM I: 0.22

         CEM II/A-P: 0.37

         CEM II/A-V: 0.57

r_{CO_2} Binding factor for the aggressive agent [-][7]

2.8.3. Comments

The parameters to apply the model are only tabulated for some specific exposure and materials.

---

[7] Values were presented for chloride attack, not for carbonation. It was estated that r_{CO_2} can be estimated from direct measurements, by relating effective and apparent diffusion coefficient or by calculation from the cement composition.

2.9. Model proposed by Salvoldi et al.

2.9.1. Experimental

Salvoldi et al. performed experimental tests to study the relationship between carbonation and oxygen permeability [Salvoldi et al., 2015]. PC including various SCMs (FA, GGBFS and SF) were used. Various w/b (0.4, 0.5 and 0.55) were investigated. Concrete beams with dimensions 500x100x100 mm were casted. Cylindrical samples for oxygen permeability test (ϕ 68 and thickness 30) and prisms for carbonation tests (100 x 85 x 90 mm) were extracted from the concrete beams. Samples were demoulded one day after casting and cured submerged in water at 23°C for 28 days. After the curing, a 5 mm slice was removed from the exposed sides of the carbonation prisms to avoid the wall effect from the surface skin. The other sides were sealed with epoxy to allow one-dimensional carbonation ingress from the two opposite sides. Subsequently, the samples were preconditioned by storing them for 60 days at 45% RH, 20°C and then for 14 days at 65% RH, 20°C. Finally, samples were exposed to accelerated conditions: 20± 2°C, 65±5% RH and 2±0.1% CO_2. Carbonation depth was measured after 3, 6, 9 and 12 weeks of exposure: 15-mm thick slices were split and phenolphthalein was sprayed on the freshly broken surface.

2.9.2. Model

Salvoldi et al. proposed a model based on the oxygen permeability of concrete.

$$D_{dry} = \left(1.4 \cdot \left(\frac{k}{10^{-11}} \right)^{2.2} \right) \cdot 10^{-11} \qquad \text{Eq. 31}$$

Where

D_{dry} Effective dry diffusion coefficient (10^{-11} m²/s)

k Oxygen permeability coefficient (10^{-11} m/s)

$$x_c = \sqrt{ \frac{2 \cdot D_{dry} \cdot CO_2 \cdot (23.32 \cdot (1 - RH)^2 \cdot (RH)^{2.6})}{a} \left(1 - \frac{ToW}{365} \right) \cdot t } \qquad \text{Eq. 32}$$

Where

CO_2 Carbon dioxide concentration [mol/m³]

RH Relative humidity [-]

a Amount of necessary CO_2 for complete carbonation [mol/m³]

ToW Number of days in a year with rainfall > 2.5 mm [days]

t Time of exposure [s]

2.9.3. Comments

The effective dry diffusion coefficient is calculated based on the experimentally determined oxygen permeability. The relationship was empirically found. A mistake was found in the equation. The author was contacted and further information is awaited before implementing the model.

3. Numerical mechanism based models for the initiation period of carbonation-induced reinforcement corrosion

3.1. Model proposed by Steffens et al.

3.1.1. Experimental

Steffens et al. [Steffens et al., 2002] calibrated the model using the experimental data published by Thomas and Matthews [Thomas and Matthews, 1992].

3.1.2. Model

Steffens et al. proposed a carbonation model which takes into account the movement and retention of heat, moisture and CO_2. The CO_2 diffusion was described by Fick's first law, carbonation rate by Arrhenius' function and mass balance equations. They only considered carbonation of calcium hydroxide arguing that the content is substantially larger than the content of other carbonatable alkaline hydrated products which they considered: sodium and potassium hydroxide. They assumed that soluble CH governs the alkalinity of the pore liquid, neglecting C-S-H carbonation.

3.1.3. Comments

Figure 10 left represents the bound CO_2 concentration (κ_r) and the degree of carbonation (k)[8]. It was assumed that carbonation front is related to a 90% degree of carbonation.

Figure 10 right presents the relation between the relative changes in the CO_2 diffusion coefficient and relative humidity, for relative humidity higher than 60 % diffusion coefficient drops abruptly.
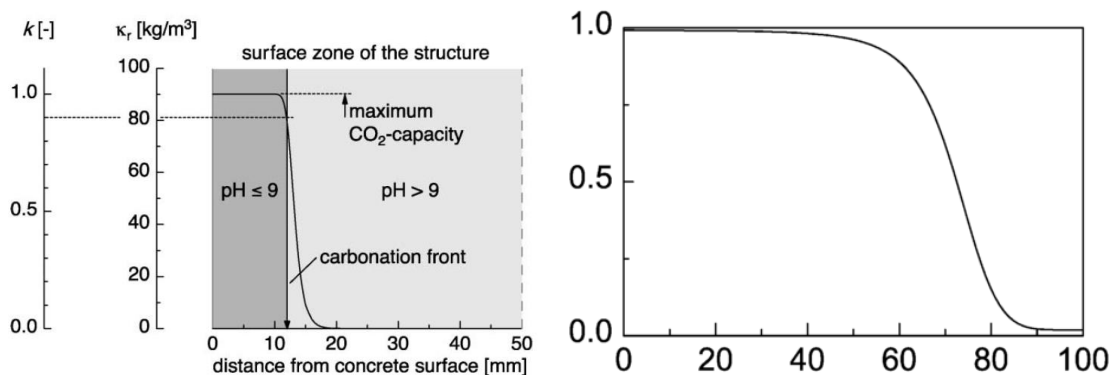
Figure 10: Left: Bound CO_2 concentration and degree of carbonation. Right: Relative changes in CO_2 diffusion coefficient as function of RH. [Steffens et al., 2002]

---

[8] k in Figure 10 means degree of carbonation

3.2. Model proposed by Saetta and Vitaliani

3.2.1. Experimental

Saetta and Vitaliani calibrated the model with experimental accelerated tests and data from field structures [Saetta and Vitaliani, 2004].

The accelerated tests were carried out on concrete containing PC with various w/b (0.45, 0.5 and 0.55) cured for three days. The accelerated conditions were not clearly stated.

Data from real structures consisted of cores from two sheds. The sheds were made of precast elements supplied by the same manufacturer. Concrete dosage, age and exposure were known. Carbonation depth was measured by spraying 1 % phenolphthalein indicator on drilled cores.

3.2.2. Model

Saetta et al. proposed a numerical carbonation model based on four differential equations which were solved numerically including experimentally determined empirical factors. The four differential equations describe:

- Moisture flow
- Heat flow
- Pollutant flow (CO_2)
- Rate of chemical reaction

These differential equations are influenced by factors which take into account the relation between:

- Carbonation and humidity
- Carbonation and CO_2 concentration
- Ideal carbonation rate

3.2.3. Comments

Only carbonation of CH was considered.

3.3. Model proposed by Bary and Sellier, and Bary and Mügler

3.3.1. Experimental

Bary and Sellier [Bary and Sellier, 2004] calibrated the model using experimental data from concrete containing CEM I (EN 197-1 (2011)), water-to-binder ratio 0.44. Later, Bary and Mügler [Bary and Mügler, 2006] presented an updated version.

3.3.2. Model

Bary and Sellier proposed a model based on macroscopic mass balance equations. The model was composed of three balance equations:

- Water
- CO_2 contained in the gaseous phase
- Calcium contained in the pore solution

This model describes Portland cement concrete carbonation and takes into account the formation of these four phases in the cement hydration:

- CH
- C-S-H (Ca/Si=1.65)
- Monosulphate
- Ettringite

Bary and Mügler published an updated model including kinetics for the CC formation due to CH carbonation. The CH was considered to have a higher initial reactivity, which decreases due to the CC layer development surrounding the CH crystal. CC constitutes a diffusive barrier for ion migration.

3.3.3. Comments

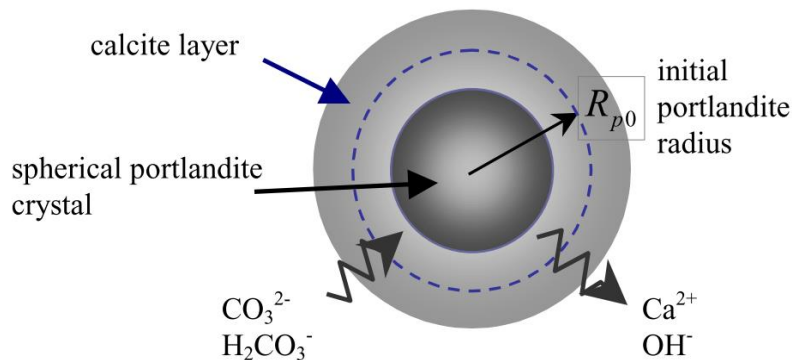Figure 11 presents the CC diffusive barrier for ion migration.

Figure 11: Calcite layer coating portlandite crystal, [Bary and Mügler, 2006]

3.4. Model presented by Morandeau et al.

3.4.1. Experimental

Morandeau et al. calibrated the model using experimental data [Morandeau et al., 2014]. Cement paste samples with CEM I (EN 197-1 (2011)) and CEM I containing 30% fly ash addition, w/b 0.45 were cast. The samples were sealed cured for six months. Then all the sides were wrapped in aluminium foil except one, which was exposed to accelerated conditions. Before exposure the samples were dried at 63% RH for three months. Accelerated conditions were 63% RH and 10% CO_2.

3.4.2. Model

Morandeau et al. proposed a numerical carbonation model based on a previous model prepared by Thiery et al. [Thiery et al., 2007]. The previous model described the carbonation of CEM I paste. Morandeau, Thiéry et al. adapted the model for blended cements.

The chemical reactions which the model includes are the following:

- Dissolution of gaseous CO_2 in the pore water and the formation of aqueous CO_2
- Formation of H_2CO_3 from water and aqueous CO_2
- Dissociation of H_2CO_3 to HCO^-_3 and CO^{2-}_3
- Dissolution of CH and C-S-H
- Formation of calcium carbonate

The molar flux of CO_2 was described using Fick's first law: the flux is proportional to the CO_2 gradient. The flux of liquid through the pores was described using Darcy's law for partially-saturated porous materials: the flux is proportional to the liquid water pressure gradient. The transport of the species present in the pore solution was described using the extended Nernst-Plank equation. The diffusion coefficient is proportional to the porosity and liquid water saturation. A global mass balance equation was added to allow mass exchange with the environment: water and CO_2.

3.4.3. Comments

Figure 12 presents the output of the model for one week of accelerated exposure of a cement paste sample (70% CEM I + 30% fly ash). The results include pH, C/S ratio of the C-S-H (1.7 for non-carbonated and 0 for C-S-H fully carbonated (silica gel)) and the volumetric distribution of phases.
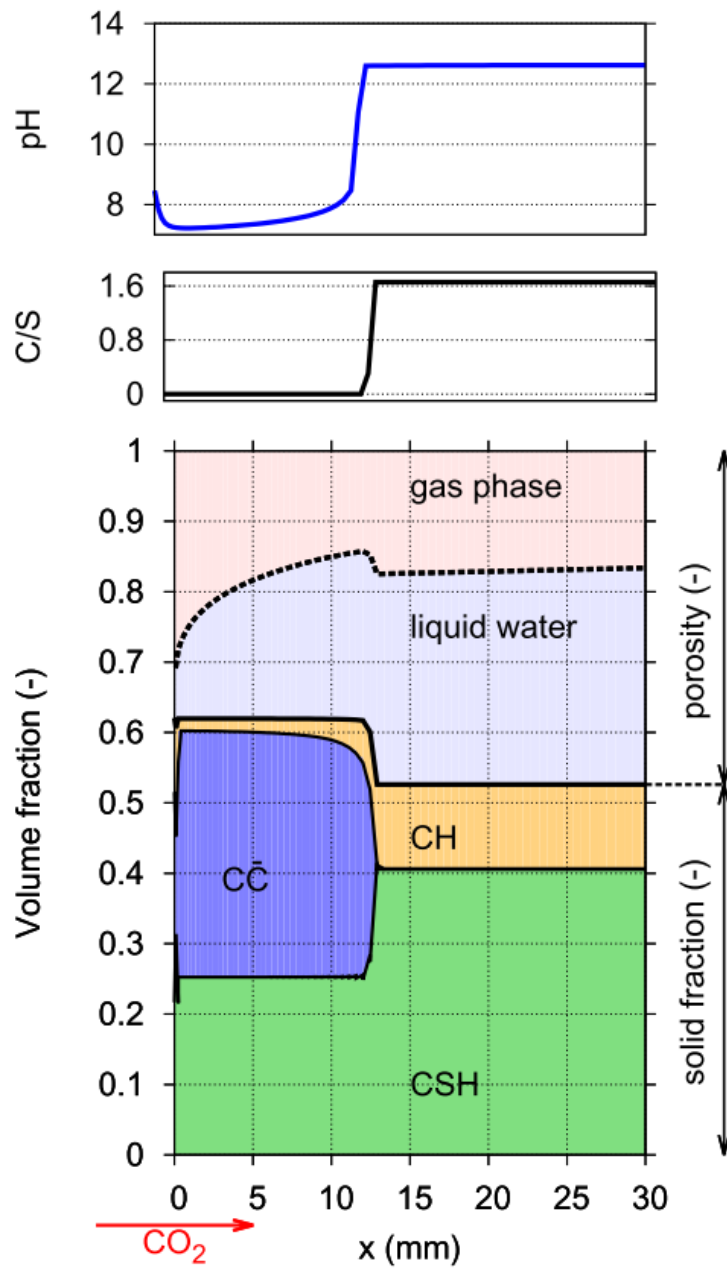
Figure 12: Numerical results for carbonation of a cement paste sample exposed for 1 week to accelerated carbonation (25 °C, 65% RH and 10% CO2) [Morandeau et al., 2014]

4. References

Andrade, C., & Andrea, R. (2010). *Electrical resistivity as microstructural parameter for the calculation of reinforcement service life.* Paper presented at the 2nd International Symposium on Service Life Design for Infrastructures, Delft, The Netherlands.

Bakker, R. (1994). *Predictions of service life of reinforcement in concrete under different climatic conditions at given cover.* Paper presented at the International Conference on Corrosion and corrosion protection of steel in concrete, Sheffield, UK.

Bamforth, P. (2004). *Enhancing reinforced concrete durability: Guidance on selecting measures for minimising the risk of corrosion of reinforcement in concrete.* (T. C. Society Ed. Vol. 61). Camberley, United Kingdom.

Bary, B., & Mügler, C. (2006). Simplified modelling and numerical simulations of concrete carbonation in unsaturated conditions. *Revue Européenne de Génie Civil, 10*(May 2015), 1049-1072. doi:10.1080/17747120.2006.9692905

Bary, B., & Sellier, A. (2004). Coupled moisture—carbon dioxide–calcium transfer model for carbonation of concrete. *Cement and Concrete Research, 34*(10), 1859-1872. doi:10.1016/j.cemconres.2004.01.025

Belda Revert, A., De Weerdt, K., & Geiker, M. (2015). *Carbonation front characterization pH color indicators*. Paper presented at the 35th Cement and Concrete Science Conference, Aberdeen, Scotland.

Belda Revert, A., De Weerdt, K., Hornbostel, K., & Geiker, M. (2016). Carbonation Characterization of Mortar with Portland Cement and Fly Ash, Comparison of Techniques *Nordic Concrete Research*.

Bouquet, G. C. (2004). *CARBONATION INDUCED CORROSION OF REINFORCEMENT*. Paper presented at the Challenges of Concrete Construction: Volume 3, Repair, Rejuvenation and Enhancement of Concrete. http://www.icevirtuallibrary.com/doi/abs/10.1680/rraeoc.31753.0047

Czarnecki, L., & Woyciechowski, P. (2012). Concrete carbonation as a limited process and its relevance to concrete cover thickness. *Materials Journal, 109*(3), 275-282.

EN 197-1. (2011). EN 197-1 Cement - Part 1: Composition, specifications and conformity criteria for common cements.

EN 206-1. (2000). EN 206-1 Concrete – Part 1: Specification, performance, production and conformity

EN 1992. (2004). EN 1992: Design of concrete structures.

fib. (2006). International Federation for Structural Concrete, *fib*, Model Code for Service Life Design, Bulletin no 34. Lausanne, Switzerland.

Greve-Dierfeld, S., & Gehlen, C. (2014). *Performance based deemed-to-satisfy rules*. Paper presented at the The Fourth International fib-Congress 2014, Mumbai.

Hills, T. P., Gordon, F., Florin, N. H., & Fennell, P. S. (2015). Statistical analysis of the carbonation rate of concrete. *Cement and Concrete Research, 72*, 98-107. doi:10.1016/j.cemconres.2015.02.007

Houst, F., Roelfstra, P., & Wittmann, F. (1983, 1983). *A model to predict service life of concrete structures*.

JSCE. (2007). Standard specifications for concrete structures: Design (pp. 1-503).

Jiang, L., Lin, B., & Cai, Y. (2000). A model for predicting carbonation of high-volume fly ash concrete. *Cement and Concrete Research, 30*(5), 699-702. doi:10.1016/S0008-8846(00)00227-1

Morandeau, A., Thiéry, M., Dangla, P., & White, C. E. (2014, 2014). *Accelerated carbonation modelling of fly ash-blended cement paste*, Beijin, China.

Morinaga, S. (1990). *Prediction of service lives of reinforced concrete buildings based on the corrosion rate of reinforcing steel.* Paper presented at the Durability of building Materials and Component, London.

Papadakis, V. G., Fardis, M. N., & Vayenas, C. G. (1991). Fundamental modelling and experimental investigation of concrete carbonation. *Materials Journal, 88*(4), 363-373.

Papadakis, V. G., Fardis, M. N., & Vayenas, C. G. (1992). Hydration and carbonation of pozzolanic cements. *ACI Materials Journal, 89*(89), 119-130.

Parrott, L. J. (1994). *Design for avoiding damage due to carbonation-induced corrosion.* Paper presented at the 3rd International Conference on Durability of Concrete, Nice, France.

Parrott, L. J. (1994). A study of carbonation-induced corrosion. *Magazine of Concrete Research, 46*(166), 23-28. doi:doi:10.1680/macr.1994.46.166.23

Saetta, A. V., & Vitaliani, R. V. (2004). Experimental investigation and numerical modeling of carbonation process in reinforced concrete structures Part I: Theoretical formulation. *Cement and Concrete Research, 34*, 571-579. doi:10.1016/j.cemconres.2003.09.009

Salvoldi, B. G., Beushausen, H., & Alexander, M. G. (2015). Oxygen permeability of concrete and its relation to carbonation. *Construction and Building Materials, 85*, 30-37. doi:10.1016/j.conbuildmat.2015.02.019

Schiessl, P. (1976). *Zur Frage de zulässigen rissbreite und der erforder lichen betondeckung im stahlbetonbau- unter besonderer berücksichtigung der karbonatisierung des betongs.* Technical University of Munich, Berlin.

Silva, a., Neves, R., & De Brito, J. (2014). Statistical modelling of carbonation in reinforced concrete. *Cement and Concrete Composites, 50*, 73-81. doi:10.1016/j.cemconcomp.2013.12.001

Sisomphon, K., & Lutz, F. (2007). Carbonation rates of concretes containing high volume of pozzolanic materials. *Cement and Concrete Research, 37*(12), 1647-1653. doi:10.1016/j.cemconres.2007.08.014

Steffens, A., Dinkler, D., & Ahrens, H. (2002). Modeling carbonation for corrosion risk prediction of concrete structures. *Cement and Concrete Research, 32*(6), 935-941. doi:10.1016/S0008-8846(02)00728-7

Thiery, M., Villain, G., Dangla, P., & Platret, G. (2007). Investigation of the carbonation front shape on cementitious materials: Effects of the chemical kinetics. *Cement and Concrete Research, 37*, 1047-1058. doi:10.1016/j.cemconres.2007.04.002

Thomas, M., & Matthews, J. (1992). Carbonation of fly ash concrete. *Magazine of Concrete Research, 44*(160), 217-228.

Tuutti, K. (1982). *Corrosion of steel in concrete.* Swedish Cement and Concrete Research Institute, Stockholm.

Østnor, T., Skjølsvold, O., & Belda Revert, A. (2016). *Phenolphthalein and thymolphthalein for carbonation measurements*.

Appendix II

Time dependent models for corrosion and damage propagation in carbonated concrete

Contents

1. Empirical models for the propagation period of carbonation-induced reinforcement corrosion: corrosion rate estimation

1.1. Model proposed by Alonso et al.

1.1.1. Experimental

Alonso et al. performed experimental tests on reinforced mortar samples including two steel bars and one carbon bar [Alonso et al., 1988]. Various cement types were tested, see Table 1. After curing, samples were exposed to 50-70% RH in a chamber filled with CO_2. Once specimens were completely carbonated, they were exposed to humidity periods at 100%, 50% RH and partial immersion. Corrosion potential and polarization resistance were measured.

Table 1: Description of the experimental tests

Material	w/b	Binder	SCM	Sample size [mm]	Curing conditions	Carbonation exposure	Corrosion exposure
Mortar	0.5	PC, SR-PC[1]	Slag, FA	20x55x80	28 days: 100% RH	50-70% RH High CO_2[2]	Cycles of 50, 100% RH and water immersion

1.1.2. Model

Alonso et al. proposed the model based on the experimental results obtained from the carbonated mortar samples. The corrosion rate is estimated from the mortar resistivity.

$$i_{corr} = \frac{30000}{\rho_{es}}$$

Eq. 1

Where

i_{corr} Corrosion rate [$\mu A/cm^2$]

ρ_{es} Concrete resistivity [Ω]

1.1.3. Comments

Even though there is a relationship between corrosion rate and concrete resistivity the scatter is high, additional parameters should be considered [Hornbostel et al., 2013].

---

[1] Sulphate resistant PC

[2] Not specified

1.2. Model proposed by Morinaga

1.2.1. Experimental

Morinaga calibrated the model using experimental data from reinforced concrete prisms [Morinaga, 1990]. The materials and exposure tested were not clearly specified, Table 2 presents the available information. The prisms were first carbonated and then exposed to various conditions. Corrosion rate was estimated by gravimetric analysis.

Table 2: Description of the experimental tests

Material	w/b	Binder	SCM	Sample size	Curing conditions	Carbonation exposure	Corrosion exposure
Concrete	0.4 0.5 0.6	PC	-	-	-	50-70% RH High CO_2[3]	20 and 40^{0}C 0, 51, 62 and 100% RH 0,10 and 20% O_2

1.2.2. Model

Morinaga proposed a model to the estimate corrosion rate in carbonated concrete considering the interaction between the parameters affecting corrosion: T, RH and O_2 concentration.

$$i_{corr} = 21.84 - 1.35T - 35.43RH - 234.76O_2 + 2.33X_4 + 4.42X_5 + 250.55X_6 \qquad \text{Eq. 2}$$

Where

i_{corr}	Corrosion rate [10^{-4} g/cm^2/year]
T	Temperature [^{o}C]
RH	Relative humidity [-]
O_2	Oxygen concentration [-]
X_4	T and RH interaction [T·RH]
X_5	T and O_2 interaction [T·O_2]
X_6	RH an O_2 interaction [RH O_2]

1.2.3. Comments

The model for the corrosion rate estimation assumes that the higher the RH or T the lower the corrosion rate, which is the opposite that one would expect.

---

[3] Not specified

1.3. Model proposed by Gulikers

1.3.1. Experimental

Gulikers tried to prove the theoretical basis of the empirical model proposed by Alonso et al. [Alonso et al., 1988] on which concrete resistivity governs corrosion process [Gulikers, 2005]. It is a theoretical formulation based on experimental data from the literature.

1.3.2. Model

Gulikers assumed the following:

- Corrosion process of steel embedded in concrete can be described using an equivalent circuit which considers: concrete resistance, anodic and cathodic polarization resistance
- Tafel behaviour was assumed: linear relationship between log (i_{corr}) and E
- Anodic and cathodic reaction are activation polarization
- Standard anodic and cathodic corrosion potential, anodic and cathodic tafel slopes and anodic and cathodic exchange current densities are constant
- Concrete resistivity geometry factor is constant
- The proposed model is obtained fitting concrete resistance and current density data
- The model is presented as an analogy of Alonso et al.'s model

The model Gulikers proposed was the following

$$i_{corr} = \frac{F_G^{-0.8125} \cdot 0.098696}{\rho^{0.8125}}$$

Eq. 3

Where

i_{corr} Corrosion rate [A/m^2]
F_G Geometrical factor [m^{-1}]
ρ Concrete resistivity [$\Omega \cdot$m]

1.3.3. Comments

A theoretical elucidation is presented on the linear relationship between concrete resistance and current density. However, the model Gulikers proposed is the fitting of experimental data on which the materials and exposure are not clearly specified.

Gulikers pointed that the model assumes that the bulk resistivity controls corrosion rate. However, the bulk resistivity could differ from the resistivity of the concrete-steel interface, where the corrosion process occurs.

1.4. Model proposed by Song et al.

1.4.1. Experimental

Song et al. presented a model for the propagation period on which the experimental data used for the calibration is not clearly specified [Song et al., 2005].

1.4.2. Model

Song et al. developed a model for chloride and carbonation-induced corrosion. The model included the following assumptions:

- A hydration model was developed to estimate heat and moisture distribution
- Crack model: the properties of the bulk concrete are related to a representative elementary volume:
    - Diffusivity coefficients
    - Permeability coefficients
- Free and bound Cl were considered, but only free Cl affect corrosion rate
- Influence of pH in corrosion rate was included
- The corrosion rate is estimated depending on the total chloride content
    - Passive: Chloride content < 1.2 kg/m³, see Eq. 5
    - Becoming active: Chloride content is between 1.2 and 2.4 kg/m³, see Eq. 6
    - Active: Chloride content > 2.4 kg/m³, see Eq. 7

The model includes three equations depending on the state of the steel:

$$i_{corr} = i_{Fe} \qquad \text{Eq. 4}$$

$$\log(i_{corr}) = \frac{0.998 - 0.06 \cdot pH - 0.059 \cdot \log(i_{O_2}) + \beta \cdot \log(i_{Fe})}{\beta + 0.059} \qquad \text{Eq. 5}$$

$$\log(i_{corr}) = 8.458 - 0.508 \cdot pH + 0.05 \cdot \log(i_{O_2}) + 0.5 \cdot \log(i_{Fe}) \qquad \text{Eq. 6}$$

$$\beta = \frac{0.059 \cdot \left([Cl^-]_p - [Cl^-]_i\right)}{[Cl^-] - [Cl^-]_i} \qquad \text{Eq. 7}$$

Where

i_{corr}	Corrosion rate [A/m²]
i_{O_2}	Oxygen current density [A/m²]
i_{Fe}	Iron current density [A/m²]
β	Anodic tafel slope [V]
$[Cl^-]$	Free chloride content by cement weight [%]

$[Cl^-]_i$ Free chloride content by cement weight at corrosion initiation [%]

$[Cl^-]_p$ Free chloride content by cement weight at corrosion propagation [%]

1.4.3. Model

The model includes carbonation-induced corrosion, but it is not specified how corrosion develops in carbonated concrete.

The corrosion rate depends on the free chloride content but it was not specified how to differentiate between bound and free. Additionally, carbonation will cause a change in the free chloride content which was not considered

1.5. Model proposed by Ghods et al.

1.5.1. Experimental

Ghods et al.presented a model which is a regression analysis performed on a numerical model [Ghods et al., 2007]. First, the numerical model was developed and then a regression analysis was performed to obtain the proposed equation. Finally, data from literature was taken to validate the model. The model is conceived for uniformly depassivated reinforcement embedded in concrete, Gods et al. pointed that is the case of carbonation-induced corrosion or concrete containing high content of chlorides.

Initially a first model which includes concrete resistivity and oxygen concentration was presented, the data taken for the validation of the model is presented in Table 3.

Then an updated model which included as input the concrete resistivity, oxygen diffusion coefficient and concentration, and concrete cover was presented. The validation of this model included three steps: validation on different binders based [Alonso et al., 1988] work. Validation on different corrosion measurement techniques based on [Luping, 2002] work, see Table 3. Finally they investigated the effect of the concrete resistivity on corrosion rate based on [Enevoldsen et al., 1994] work, see Table 4.

Table 3: Description of the experimental tests taken from the literature [Luping, 2002]

Material	w/b	Binder	SCM	Sample size [mm]	Curing conditions	Cl [% in cement mass]	Corrosion exposure
Concrete	0.5	PC	-	250x70x250	21 days, high RH	0, 1.5, 3 and 6%	Saturated KCl solution (RH≈ 85%)

Table 4: Description of the experimental tests taken from the literature [Enevoldsen et al., 1994]

Material	w/b	Binder	SCM	Sample size [mm]	Curing conditions	Cl [% in cement mass]	Corrosion exposure
Mortar Concrete	0.5	PC	-	Not clear	-	0, 1 and 2	Various RH 80-98%

1.5.2. Model

Ghods et al. took the following assumptions for the numerical model:

- The anodic reaction is under activation polarization
- The cathodic reaction is under concentration polarization
- The anode-to-cathode ratio is an input
- Standard anodic and cathodic corrosion potential, anodic and cathodic tafel slopes and anodic and cathodic exchange current densities are constant
- Concrete resistivity geometry factor is constant

Ghods et al. proposed a model for estimating the corrosion rate of uniformly depassivated steel in concrete. The equation is a regression analysis of the numerical model. The data was taken for the anode-to-cathode ratios which gave the highest corrosion rates. These points were defined as the equilibrium points on which the total energy of the system is minimized. To obtained the current density the corrosion current was normalized with the surface of the steel.

$$i_{corr} = -0.00133 + \frac{3}{\rho} - 0.000383 ln(O_2) + 0.333 \frac{ln(O_2{}^R)}{\rho} \qquad \text{Eq. 8}$$

Where

i_{corr} Corrosion rate [A/m^2]

ρ Concrete resistivity [$\Omega \cdot$m]

$O_2{}^R$ Oxygen concentration at the steel surface [Kg/m^3]

Ghods et al. [Ghods et al., 2008] presented an updated equation of the previous model [Ghods et al., 2007]. The formulation is the same but the input data was modified.

$$i_{corr} = -0.0037 + \frac{5.06}{\rho} + \left(\frac{0.333}{\rho} - 0.000383\right) \cdot ln\left(\frac{D_{O_2} \cdot C_{O_2}{}^s}{co}\right) \qquad \text{Eq. 9}$$

Where

D_{O_2} Oxygen diffusion coefficient [m^2/s]

$C_{O_2}{}^s$ Oxygen concentration on pore solution [kg/m^3]

co Concrete cover [mm]

1.5.3. Comments

In the first model, the oxygen concentration and concrete resistivity were the inputs. However, the data used for the validation did not include the oxygen concentration, it was assumed based on the exposure. The model is conceived for uniformly depassivated steel. However, the data used for the validation shows that the corrosion induced by the chlorides was not uniform.

The second model was conceived to be more practical, the authors claimed that the input data can be easily measured or estimated. They proposed that the D_{O_2} can be estimated from [Papadakis et al., 1991], who proposed a hydration model including porosity development and allowed to estimate the D_{O_2}. The $C_{O_2}{}^s$ can be assumed 0.005 kg/m^3 and the concrete cover can be measured easily.

There is an interesting comment on which the corrosion rate in mortar and concrete is discussed. They claimed that concrete presents more tortuosity for the oxygen to reach the reinforcement, even if mortar samples are prepared containing the same w/b, the corrosion rate on the concrete samples will be lower, as long as oxygen is a limiting factor, e.g. concentration control.

Ghods et al. claimed that the effect of the binder in corrosion development can be addressed by the concrete resistivity and the oxygen diffusion coefficient.

2. Empirical models for the propagation period of carbonation-induced reinforcement corrosion: duration of propagation period estimation

2.1. Model proposed by Alonso et al.

2.1.1. Experimental

Alonso et al. presented this model based on the data presented in Section 1.1 [Alonso et al., 1988].

2.1.2. Model

Alonso et al. proposed the following model for service life prediction. Propagation period ends when the structure suffers from a certain amount of corrosion penetration which should be defined.

$$t_p = \frac{P_{lim} \cdot \rho_{ef}}{30000^4}$$

Eq. 10

Where:

P_{lim} Corrosion allowance [μm]

ρ_{ef} Concrete resistivity: can be estimated from $\rho_{standard}$. Depends on cement type and exposure conditions

---

[4] This regression value was originally presented by the authors. Other values are found in the literature

2.2. Model proposed by Morinaga

2.2.1. Experimental

Morinaga presented this model based on the data presented in Section 1.2 [Morinaga, 1990].

2.2.2. Model

Morinaga proposed the following model for service life prediction which considers that service life ends when cracks appear due to corrosion expansion products.

$$t_{crack} = \frac{P_{lim}}{i_{corr}} = \frac{0.602\left(1 + \frac{2co}{\emptyset}\right)^{0.85}}{i_{corr}} \qquad \text{Eq. 11}$$

Where

co Concrete cover [mm]

$\emptyset$ Reinforcement diameter [mm]

i_{corr} Corrosion rate [10^{-4} g/cm²/year]

2.2.3. Comments

Morinaga claimed that once corrosion develops in carbonated concrete, the corrosion rate is so high that the duration of the propagation period is negligible.

2.3. Model proposed by Parrott

2.3.1. Experimental

Parrott presented a model for the propagation period on which the experimental data used for the calibration was not clearly specified [L. J. Parrott, 1994].

2.3.2. Model

Parrot defined the propagation period as the time in years from corrosion initiation to cracking cover without spalling. Propagation equation is a relation between corrosion allowance and corrosion rate. The corrosion allowance was taken from others studies (100 μm) [Tuutti, 1982]. Corrosion rate depends on RH, see Table 5.

$$t_{crack} = \frac{P_{lim}}{i_{corr}} = \frac{100}{i_{corr}}$$

Eq. 12

Where

P_{lim}	Corrosion allowance [μm]
i_{corr}	Corrosion rate [μm/year]

Table 5: Values of corrosion rate for selected RH (after [L. J. Parrott, 1994])

RH [%]	40	50	60	70	80	90	95	98	100
i_{corr} [μm/year]	0.3	0.3	0.3	2	5	10	20	50	10

2.3.3. Comments

It is interesting to see the relationship between RH and i_{corr}, the maximum corrosion rate occurs at 98% and even at 100% RH the i_{corr} is relatively high (same as 90% RH).

Currently, there is still a lack of knowledge on the i_{corr} in the range of 95 to 100% RH.

2.4. Model proposed by Bouquet

2.4.1. Experimental

Bouquet presented a model for the propagation period on which the experimental data used for the calibration is not clearly specified [Bouquet, 2004].

2.4.2. Model

Bouquet defined the propagation period as the time in years from corrosion initiation to cracking along the reinforcement. Propagation equation is a relation between corrosion allowance and corrosion rate including a moisture factor. The numerical values Bouquet presented in a practical application are included.

$$t_p = \frac{P_{lim}}{W \cdot i_{corr}} = \frac{100}{W \cdot 50}$$

Eq. 13

Where:

P_{lim} Corrosion allowance [μm]

W Period on which reinforcement depth is wet (RH > 80%) [-]

i_{corr} Corrosion in the wet period [μm/year]

2.4.3. Comments

Bouquet differed between dry and wet periods of exposure for the propagation period: corrosion takes place when humidity is higher than 80 %. Additionally, he also considered the time delay after wetting and drying where the reinforcement is still wet or dry.

When steel corrodes in carbonated concrete a constant corrosion rate of 50 μm/year is assumed.

2.5. Model proposed by Bamforth

2.5.1. Experimental

Bamforth presented a model for the propagation period on which the experimental data used for the calibration is not clearly specified [Bamforth, 2004].

2.5.2. Model

Bamforth defined the propagation period as the time in years from corrosion initiation to cracking cover. Propagation equation is a relation between the corrosion allowance, which was taken from Duracrete (2000) , and corrosion rate, which depends on the relative humidity and was taken from Andrade and Alonso, see Table 6.

$$t_p = \frac{83.3 + 7.4\frac{Co}{\emptyset} - 22.6 \cdot f_t}{i_{corr}}$$

Eq. 14

Where

Co Concrete cover [mm]

$\emptyset$ Reinforcement diameter [mm]

f_t Concrete tensile streght [MPa]

i_{corr} Corrosion rate [μm/year]

Table 6: Relative humidity and corrosion rate in carbonated concrete after [Andrade and Alonso, 1996]

RH [%]	< 50	50-60	60-70	70-80	80-90	90-98	>98
i_{corr}[μm/year]	0.1	0.2	0.3	0.5	1	2	0.1

2.5.3. Comments

Corrosion allowance equation was taken from Duracrete (2000) but using different fitting parameters. The bigger the cover to reinforcement diameter ratio the longer the propagation period, which seems logical. However, the higher the f_t the shorter the propagation period. According to Bamforth, it is because the resistance of concrete to cracking is a strain-limited problem rather than strength-limited. Furthermore, f_t gives an indirect measurement of the porosity, thus a high-porous concrete will allow the corrosion products to diffuse much more compared to a high-quality concrete, which will induce less strain [Bamforth, 2004].

Corrosion rates taken by Bamforth are up to 25 times smaller compared to the ones Parrott assumed.

3. Mechanism based models for the propagation period of carbonation-induced reinforcement corrosion

Corrosion rate is modelled by solving theoretical equations including empirical factors and boundary conditions. These models focus on the corrosion process without paying attention to concrete deterioration, they aim at estimating the corrosion rate. Due to their complexity in the following sections is given a brief description of the models and some of the strong/weak points. These models can be found at Otieno's review [Otieno et al., 2011].

3.1. Model proposed by Kranc and Sagüés

3.1.1. Experimental

Kranc and Sagüés developed a theoretical formulation on which a concrete cylinder containing one rebar was simulated [Kranc and Sagüés, 1997]. The rebar was assumed to be in the passive state apart from an annular region in the middle of the bar, which was in the active state. An external non-polarizable counter electrode was simulated wrapping the concrete cylinder surface. Finally, a reference electrode was included in the system at various positions between the active steel and the counter electrode.

3.1.2. Model

Kranc and Sagüés developed a model which describes the response of corrosion microcell on a steel bar exposed to a potential-step excitation. Various situations were investigated: quasi-steady-state free corrosion condition of the reinforcement, effect of placing the counter electrode, quasi-steady-state after polarization and quasi-steady-state after removing external polarization. The model included the following assumptions:

- Electrolyte behaves as a pure resistor
- Metal-electrolyte interface behaves as a pure capacitive charge storage
- Tafel behaviour is assumed: linear relationship between log (i_{corr}) and E
- Anodic reaction
  - ○ Active steel: Activation polarization
  - ○ Passive steel: Constant rate, not potential dependent
- Cathodic reaction is under mixed polarization (concentration and activation)
- OH$^-$ concentration and concrete resistivity are constant
- Oxygen transport occurs by diffusion

3.1.3. Comments

The model describes the response of reinforcement exposed to a potential-step excitation but the applicability to the estimation of corrosion rates was missing.

3.2. Model proposed by Isgor and Razaqpur

3.2.1. Experimental

Isgor and Razaqpur developed a theoretical model and took data from the literature for the validation [Isgor and Razaqpur, 2006]. Qing [Qing, 2001] tested reinforced concrete elements exposed to chloride-induced corrosion containing various cement types, crack size and exposure conditions. Isgor and Razaqpur selected some of the elements for the validation of the model, see Table 7.

Table 7: Description of the experimental tests taken from the literature, [Qing, 2001]

Material	w/b	Binder	SCM	Sample size [mm]	Curing conditions	Cl [%]	Corrosion exposure
Concrete	0.45 0.6	PC	-	Beams 2000 in lenght and prims 360x62x62	21 days, high RH	3.5 NaCl solution was regulargly sprayed	Wetting-drying cycles

3.2.2. Model

Isgor and Razaqpur developed a model for chloride and carbonation-induced corrosion. The potential distribution of the embedded steel can be known by solving Laplace equation. Then the corrosion current can be estimated once the potential distribution is known. They assumed that $Fe(OH)_3$ was the formed corrosion product for the rust production estimation. The following assumptions were taken:

- Cathodic reaction is under mixed polarization (concentration and activation)
- Anodic reaction is activation polarization
- The polarization characteristics of the steel vary depending on the following parameters
  - Heat
  - Moisture
  - Chloride, CO_2 and O_2 content
  - pH pore solution
- Concrete resistivity was obtained by Hincrichson-Rash law: the resistivity at any temperature can be calculated based on resistivity changes due to temperature
- Laplace's equation for electrical potential was numerically solved
- Cracks can be included
  - Treated as free surface elements
  - Crack width does not affect chloride/CO_2 penetration

3.2.3. Comments

The model includes the initiation and propagation period and simulates chloride and carbonation-induced corrosion. There is a paper on the applicability of the carbonation initiation period [Isgor and Razaqpur, 2004]. However, there is not a validation for the carbonation-induced corrosion propagation period.

The active and passive areas can be defined by threshold values, e.g. for carbonation a pH value can be stablished on which steel will become active. However, in some cases the user must include the anode-to-cathode areas/ratio as input, e.g. when a sharp carbonation front depassivates the steel uniformly.

The model includes a drop in the pH of the pore solution due to the comsumption of OH^- in the anodic reaction. However, to keep the neutral charge in the system the OH^- should be taken from the cathodic reaction (oxygen reduction) rather than from the electrolyte.

4. References

Alonso, C., Andrade, C., & González, J. (1988). Relation between resistivity and corrosion rate of reinforcements in carbonated mortar made with several cement types. *Cement and Concrete Research, 18*(5), 687-698. doi:10.1016/0008-8846(88)90091-9

Andrade, C., & Alonso, C. (1996). Corrosion rate monitoring in the laboratory and on-site. *Construction and Building Materials, 10*(5), 315-328. doi:http://dx.doi.org/10.1016/0950-0618(95)00044-5

Bamforth, P. (2004). *Enhancing reinforced concrete durability: Guidance on selecting measures for minimising the risk of corrosion of reinforcement in concrete.* (T. C. Society Ed. Vol. 61). Camberley, United Kingdom.

Bouquet, G. C. (2004). *CARBONATION INDUCED CORROSION OF REINFORCEMENT*. Paper presented at the Challenges of Concrete Construction: Volume 3, Repair, Rejuvenation and Enhancement of Concrete. http://www.icevirtuallibrary.com/doi/abs/10.1680/rraeoc.31753.0047

Duracrete. (2000). *Duracrete The European Union – Brite EuRam III, DuraCrete – Probabilistic Performance Based Durability Design of Concrete Structures. Final Technical Report of Duracrete project, Document BE95-1347/R17. CUR*. Retrieved from Gouda, the Netherlands.:

Enevoldsen, J. N., Hansson, C. M., & Hope, B. B. (1994). The influence of internal relative humidity on the rate of corrosion of steel embedded in concrete and mortar. *Cement and Concrete Research, 24*(7), 1373-1382. doi:http://dx.doi.org/10.1016/0008-8846(94)90122-8

Ghods, P., Isgor, O. B., & Pour-Ghaz, M. (2007). A practical method for calculating the corrosion rate of uniformly depassivated reinforcing bars in concrete. *Materials and Corrosion, 58*(4), 265-272. doi:10.1002/maco.200604010

Ghods, P., Isgor, O. B., & Pour-Ghaz, M. (2008). Experimental verification and application of a practical corrosion model for uniformly depassivated steel in concrete. *Materials and Structures, 41*(7), 1211-1223. doi:10.1617/s11527-007-9320-3

Gulikers, J. (2005). Theoretical considerations on the supposed linear relationship between concrete resistivity and corrosion rate of steel reinforcement. *Materials and Corrosion, 56*(6), 393-403. doi:10.1002/maco.200403841

Hornbostel, K., Larsen, C. K., & Geiker, M. R. (2013). Relationship between concrete resistivity and corrosion rate – A literature review. *Cement and Concrete Composites, 39*, 60-72. doi:http://dx.doi.org/10.1016/j.cemconcomp.2013.03.019

Isgor, O. B., & Razaqpur, A. G. (2004). Finite element modeling of coupled heat transfer, moisture transport and carbonation processes in concrete structures. *Cement and Concrete Composites, 26*(1), 57-73. doi:http://dx.doi.org/10.1016/S0958-9465(02)00125-7

Isgor, O. B., & Razaqpur, A. G. (2006). Modelling steel corrosion in concrete structures. *Materials and Structures/Materiaux et Constructions, 39*(287), 291-302. doi:10.1617/s11527-005-9022-7

Kranc, S. C., & Sagüés, A. A. (1997). Modeling the Time-Dependent Response to External Polarization of a Corrosion Macrocell on Steel in Concrete. *Journal of The Electrochemical Society, 144*(8), 2643-2652. doi:10.1149/1.1837877

Luping, T. (2002). *Calibration of the electrochemical methods for the corrosion rate measurement of steel in concrete*. Retrieved from

Morinaga, S. (1990). *Prediction of service lives of reinforced concrete buildings based on the corrosion rate of reinforcing steel.* Paper presented at the Durability of building Materials and Component, London.

Otieno, M., Beushausen, H., & Alexander, M. (2011). Prediction of corrosion rate in RC structures - A critical review. *RILEM Bookseries, 5*(9), 15-37. doi:10.1007/978-94-007-0677-4_2

Papadakis, V. G., Fardis, M. N., & Vayenas, C. G. (1991). Fundamental modelling and experimental investigation of concrete carbonation. *Materials Journal, 88*(4), 363-373.

Parrott, L. J. (1994). *Design for avoiding damage due to carbonation-induced corrosion.* Paper presented at the 3rd International Conference on Durability of Concrete, Nice, France.

Parrott, L. J. (1994). A study of carbonation-induced corrosion. *Magazine of Concrete Research, 46*(166), 23-28. doi:doi:10.1680/macr.1994.46.166.23

Qing, L. C. (2001). Initiation of Chloride-Induced Reinforcement Corrosion in Concrete Structural Members—Experimentation. *Structural Journal, 98*(4). doi:10.14359/10293

Song, H. W., Kim, H. J., Kwon, S. J., Lee, C. H., Byun, K. J., Park, C. K., & Ki-Bong. (2005). Prediction of Service life in cracked Reinforced Concrete structures subjected to chloride attack and carbonation *Cement Combinations for Durable Concrete* (pp. 767-775).

Tuutti, K. (1982). *Corrosion of steel in concrete.* Swedish Cement and Concrete Research Institute, Stockholm.

Appendix III

Application of time dependent models for carbonation development to short-term laboratory data

Contents

1. Short-term laboratory data

The short-term laboratory data is obtained from experimental tests performed within the Lavkarbsem project. The carbonation depth is measured on mortar prisms exposed to accelerated carbonation. Selected models are applied to predict carbonation development.

Mortar was mixed following the EN 196-1 (2005) with a water-to-binder ratio 0.55 and binder-sand ratio 1:3. Mortar prisms with dimensions 40x40x160 mm were cast, demoulded one day after casting and cured for 13 days at 20°C T sealed at high RH. The accelerated exposure conditions were 20°C, 60% RH and 1.45%[1] CO_2. The carbonation depth was determined by image analysis (30 points per side) on freshly split mortar surfaces sprayed with thymolphthalein 1%, for further details see [Belda Revert et al., 2016a].

Carbonation development is predicted by applying selected models and compared to the experimental values. Additionally, carbonation development at 85% RH is predicted.

The following two binders supplied by Norcem AS are studied, Table 1 presents the chemical composition.

- CEM I: 96 % Portland cement+ 4 % limestone
- CEM II/B-V (Lavkarbsem): 66 % Portland cement+ 30 % Fly ash + 4 % limestone

Table 1: Oxides composition of cements and fly ash determined by XRF [%]

	CEM I	CEM II/B-V	Fly ash
SiO_2	20.4	29.5	56.8
Al_2O_3	4.8	10.8	24.3
Fe_2O_3	3.4	4.5	6.9
CaO	61.7	44.6	4.9
MgO	2.2	2	1.7
SO_3	3.5	3.2	0.6
P_2O_5	0.2	0.4	0.8
K_2O	0.9	1.1	1.7
Na_2O	0.5	0.5	0.6

---

[1] CO_2 concentration was set to 1% but due to technical problems was 1.45%

The following input is needed depending on the model:

- Degree of hydration of the cement clinker
- Cement phases content
- Compressive strength
- Amount of binder
- Amount of CO_2 for complete carbonation

1.1. Degree of hydration of the cement clinker

The Degree of hydration of the cement clinker is required in some of the models.

Based on [De Weerdt et al., 2011], the degree of hydration of the cement clinker after 14 days of curing is approximately 77% for the CEM I sample.

Based on [Belda Revert et al., 2016b], the degree of hydration of the cement clinker after 14 days of curing is higher for the CEM II/B-V sample, a value of 95% is assumed.

1.2. Cement phases content

De Weerdt et al. used similar materials as the ones used in the Lavkarbsem project. Therefore the necessary input data for the model could be retrieved from [De Weerdt et al., 2011]. The chemical composition of the binders OPC-L and OPC-FA-L determined by XRF from [De Weerdt et al., 2011] are presented in Table 2. Their composition is very similar to respectively the CEM I and CEM II/B-V used in the Lavkarbsem investigation, see Table 1.

Table 2: Oxide composition of cements determined by XRF from [De Weerdt et al., 2011]

	OPC-L	OPC-FA-L
SiO_2	19.7	28.7
Al_2O_3	5.3	10.8
Fe_2O_3	3.1	3.9
CaO	59.7	43.4
MgO	2.9	2.6
SO_3	1.4	1.1
P_2O_5	0.1	0.4
K_2O	1.2	1.2
Na_2O	0.5	0.5

Figure 1 presents the degree of reaction of cement phases of CEM I over time retrieved from [De Weerdt et al., 2011]. The molar concentrations of the major constituents after 14 days of hydration for the OPC-L

related to the volume of mortar have been estimated from Figure 1, applying Papadakis et al's model [Papadakis et al., 1991]. Papadakis et al. proposed a hydration model on which the input data are the initial molar concentration and the molar concentration at the given time of C_3S, C_2S, C_3A and C_4AF, and parameters related to the mortar recipe. The CSH is assumed to have a fixed Ca/Si ratio of 1.5. Table 3 presents the results. The molar concentration of the considered cement phases after 14 days of hydration are given in Table 3.
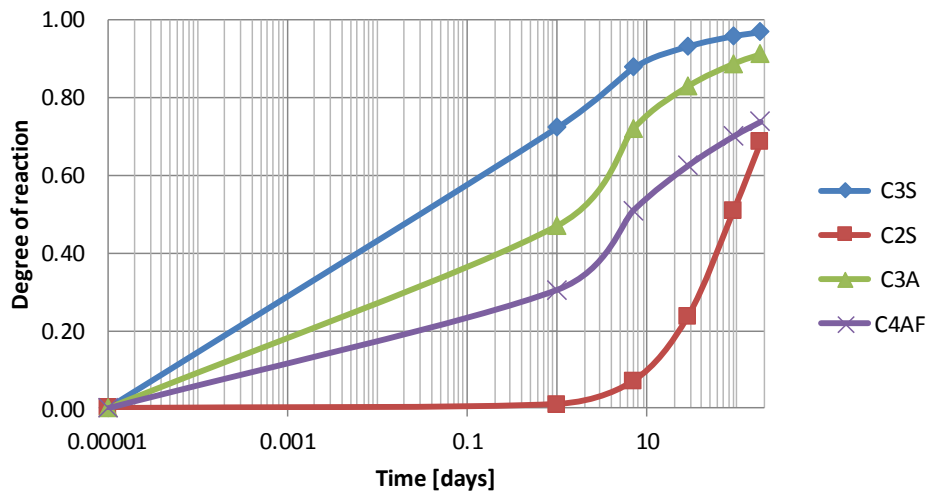
Figure 1: Degree of reaction of cement phases of CEM I over time, after [De Weerdt et al., 2011]

Table 3: Molar concentration of the major constituents after 14 days of hydration for CEM I

Molar concentration	CH	C-S-H	C_3S	C_2S
[10^{-3} mol/m^3]	1.31	0.53	0.1	0.43

1.3. Compressive strength

The 28-day-compressive strength of the mortar prisms with a water-to-cement ratio 0.5 and cement-to-sand ratio 1:3, cured submerged in saturated Ca(OH)$_2$ solution at 20 ^{o}C are shown in Table 4.

Table 4: Mortar compressive strength [De Weerdt et al., 2011]

Sample	f_c (MPa)
OPC-L	43.9
OPC-FA-L	39.8

1.4. Amount of binder

Some models include the amount of binder per unit of mortar/concrete volume as input. Based on the mortar recipe, the amount of binder is 490 kg per cubic meter of mortar, see Table 5. This value is taken for the models which require this parameter. Even if the value of 490 kg/m^3 seems a bit for concrete, it is applied for the comparison of the models.

Table 5: Amount of binder per volume of mortar[2]

Material	ρ [g/cm^3]	mass/batch [g]	vol/batch [cm^3]
Binder	2.91	450	154.6
Water	1	247.5	247.5
Sand	2.6	1350	519.2
Binder [kg/m^3]			490

1.5. Amount of CO2 for complete carbonation

The following equation is used to estimate amount of CO$_2$ for complete carbonation [Lagerblad, 2006]:

$$a = c \cdot \frac{C}{100} \cdot DH \cdot \frac{M_{CO_2}}{M_{CaO}} \cdot DC \qquad \text{Eq. 1}$$

Where

a	Amount of CO$_2$ for complete carbonation [kg/m^3]
c	Cement content [kg/m^3]
C	CaO content in the binder [-]
DH	Degree of hydration of the cement clinker [%]
M_{CO_2}	CO$_2$ molar mass [44 kg/mol]
M_{CaO}	CaO molar mass [56 kg/mol]
DC	Degree of carbonation [%]

Table 6 presents the application of Eq. 1 to the tested fly ash blend. The degree of carbonation has been assumed 100%, based on [Belda Revert et al., 2016a], who observed using thermogravimetric analysis a plateau on the CC content on the carbonated area with a complete depletion of the CH, indicating a high degree of carbonation in the same materials investigated in this report.

Table 6: Amount of CO$_2$ to complete carbonation

	c [Kg/m^3]	C [-]	DH [-]	a [kg/m^3]
CEM II/B-V	490	0.45	0.95	164

---

[2] Densities given by the supplier (binder: NORCEM AS, sand: NORMENSAND)

2. Predicted carbonation depths

This section describes how each model is applied. If additional assumptions are made, they are specified in each subsection. The results from each model are presented as the predicted carbonation depth after 10 weeks of exposure for the following conditions: T 20°C, RH 60% and CO_2 1.45% (apart from Czarnecki and Woyciechowski's model which was calibrated against 1% CO_2). The predicted carbonations depths are compared with the experimental data. Additionally, predictions for 85% RH are performed.

A summary of the results after 10 weeks of exposure is presented in Figure 2 and Figure 3. The experimental values include an error bar showing the range of measured values.

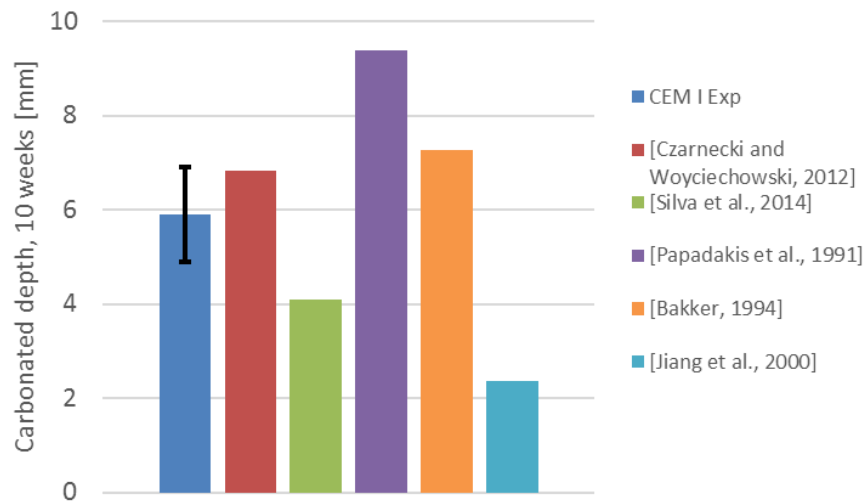

Figure 2: Experimental (included measured range) and estimated carbonated depths after 10 weeks of exposure: CEM I
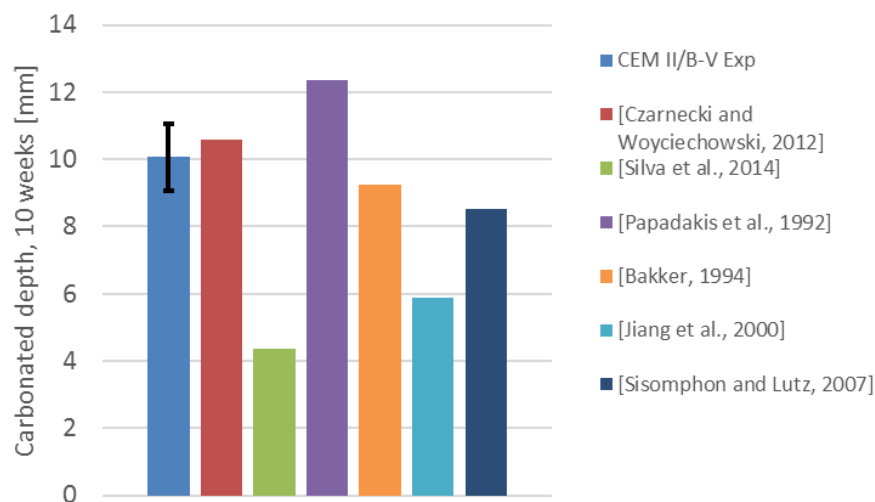

Figure 3: Experimental (included measured range) and estimated carbonated depths after 10 weeks of exposure: CEM II/B-V

The predicted carbonation depths show for both binders that the Czarnecki and Woyciechowski's model gives the closer approximation, even if it was developed on samples exposed to lower CO_2 concentration. Bakker's model predicted carbonation depths within the range of the experimentally determined values. Similar trends are observed comparing the prediction to the experimental values in both binders: Silva et al. and Jiang et al's models underestimate carbonation development while Papdakis et al's is a bit conservative.

Table 7 presents the numerical values applied to each model. The main difference is related to the carbonatable material, which can be depending on the author related to the CaO content, to the content of specific cement phases which carbonate or to the amount of CO_2 to complete carbonation. Note that the carbon dioxide diffusion coefficient in all cases is the one proposed by Papadakis et al's model because the other authors did not propose any alternative formulation.

Table 7: Summary of the numerical values used in each model

Model	CO2 [%]	CEM I RH 60% D_{CO_2} [m²/s]	CEM I RH 85% D_{CO_2} [m²/s]	CEM II/B-V RH 60% D_{CO_2} [m²/s]	CEM II/B-V RH 85% D_{CO_2} [m²/s]	Binder [kg/m³]	CEM I Carb. Material [mol/m³]	CEM I Carb. Material [Kg/m³]	CEM I kg [CO2/m³]	CEM II/B-V Carb. Material [mol/m³]	CEM II/B-V Carb. Material [Kg/m³]	CEM II/B-V kg [CO2/m³]	w/c [-]	Exposure EN-206	fc [MPa]
[Silva et al., 2014]	1.5	-	-	-	-	490	-	-	-	-	-	-	-	XC1	45
[Papadakis et al., 1991] [Papadakis et al., 1992]	1.5	5.1·10⁻⁸	5.9·10⁻⁹	6.0·10⁻⁸	6.9·10⁻⁹	-	4121	-	-	2799	-	-	0.55	-	-
[Bakker, 1994]	1.5	5.1·10⁻⁸	5.9·10⁻⁹	6.0·10⁻⁸	6.9·10⁻⁹	490	-	302	-	-	219	-	-	-	-
[Jiang et al., 2000]	1.5	-	-	-	-	490	-	362	-	-	231	-	0.55	-	-
[Sisomphon and Lutz, 2007]	1.5	-	-	6.0·10⁻⁸	6.9·10⁻⁹	490	-	-	-	-	-	163	-	-	-

1.1. Model proposed by Czarnecki and Woyciechowski

Czarnecki and Woyciechowski investigated accelerated carbonation of concrete containing fly ash [Czarnecki and Woyciechowski, 2012]. Concretes with different binder contents (CEM I 32,5 from 306 to 320 kg/m^3), fly ash contents (15% and 30 %) and water-binder ratios (0.45 and 0.55) were investigated. Two types of fly ash were used, the fly ash with a composition close to the one used in our investigation was chosen for comparison. Samples were water cured for 28 days and then preconditioned in laboratory conditions until constant mass was measured (at least for 14 days). Finally, samples were exposed to accelerated conditions: T 21°C, RH 60% and CO$_2$ 1%.

The proposed coefficients for water-to-binder ratio 0.55 for each mixture are presented in Table 8, following the hyperbolic model proposed by the authors.

Table 8: Coefficients for the Czarnecki's model (Czarnecki, 2009)

Binder	A [mm]	B [mm·day$^{0.5}$]
CEM I	12.99	51.61
CEM I + 30% FA	15.131	38.15

1.1.1. Prediction

Using the coefficients proposed for CEM I with w/b 0.55 and CEM I + 30% FA with w/b 0.55, the time dependent carbonation depths are predicted, see Figure 4.
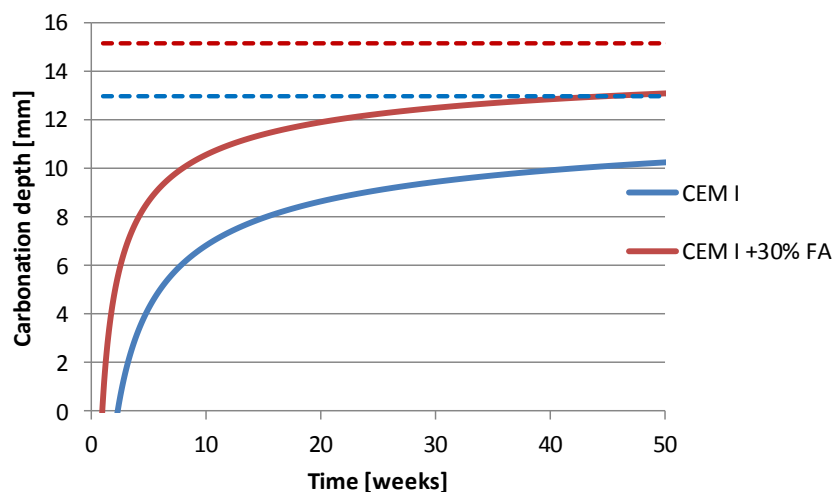
Figure 4: Predicted time dependent carbonation depth for the CEM I and the CEM I +30% FA binder as well as the upper bound of the carbonation depth using Czarnecki's model

The estimated carbonation depth for both investigated binders after 10 weeks of exposure is presented in Table 9. The model predicts that the carbonation depth reaches an upper bound over time, as indicated in Figure 4. The upper bound as well as the rate during the first 100 days is slightly higher for the binder which

contains fly ash. The difference between the upper bound for the carbonation depth of both binders seems negligible from a practical point of view (2.1 mm).

Table 9: Predicted carbonation depth after 10 weeks of exposure using Czarnecki's model

Time [weeks]	x_c [mm]	
	CEM I	CEM I + 30% FA
10	6.8	10.6

1.2. Model proposed by Silva et al.

Silva et al. proposed a model composed of two different equations depending on the RH [Silva et al., 2014].

The RH is related to the exposure class according to EN 1992 (2004) . A constant 60% RH is equivalent to exposure class XC1.

The input parameters used are given in Table 10.

Table 10: Input parameters for Silva's model

	RH 60 %		RH 85 %	
	CEM I	CEM II/B-V	CEM I	CEM II/B-V
CO_2 [%]	1.45	1.45	1.45	1.45
X (EN 1992)	1	1	-	-
f_c [MPa]	44	30	44	40
Cli [kg/m^3]	-	-	466	419

1.2.1. Prediction

The predicted carbonation depths after 10 weeks of accelerated exposure are given in Table 11.

Table 11: Predicted carbonation depth after 10 weeks of exposure using Silva's model

	RH 60 %		RH 85 %	
	CEM I	CEM II/B-V	CEM I	CEM II/B-V
x_c [mm]	4.1	4.4	2.2	3.5

1.3. Model proposed by Papadakis et al: PC

Papadakis et al. proposed a model for carbonation development, hydration and porosity evolution with time [Papadakis et al., 1991]. The degree of hydration of the main clinker phases, the porosity and the carbon dioxide diffusion coefficient (D_{CO_2}) can be obtained for Portland cement (PC) with different compositions.

The degree of hydration of the main clinker phases are estimated from [De Weerdt et al., 2011].

The porosity and D_{CO_2} are estimated from Papadakis' model. The latter is obtained as a function of the relative humidity and porosity.

The input parameters used are given in Table 12.

Table 12: Input parameters for Papadakis' model for CEM I

	RH 60 %	RH 85 %
D_{CO_2} [m²/s]	$5.1·10^{-8}$	$5.9·10^{-9}$
CO_2 [mol/m³]	0.6	0.6
$[CH]^0$ [mol/m³·10⁻³]	1.03	1.03
$[CSH]^0$ [mol/m³·10⁻³]	0.72	0.72
$[C_3S]^0$ [mol/m³·10⁻³]	0.15	0.15
$[C_2S]^0$ [mol/m³·10⁻³]	0.25	0.25

1.3.1. Prediction

The predicted carbonation depths after 10 weeks of accelerated exposure are given in Table 13.

Table 13: Predicted carbonation depth after 10 weeks of exposure using Papadakis' model for CEM I

RH [mm]	x_c [mm]
60	9.4
85	3.2

1.4. Model proposed by Papadakis et al: blended PC

Papadakis et al. proposed a carbonation model for blended PCs [Papadakis et al., 1992]. The carbonatable material in this case is the portlandite (CH) and calcium silicate hydrates (C-S-H). The model includes an additional porosity factor due to pozzolanic reaction.

Lavkarbsem (CEM II/B-V) contains a fly ash which is similar to the one they used. The molar concentrations of CH and CSH have been retrieved from Papadakis et al. [Papadakis et al., 1992].

The input parameters used are given in Table 14.

Table 14: Input parameters for Papadakis' model for blended cements: CEM II/B-V

	RH 60 %	RH 85 %
D_{CO_2} [m²/s]	$6.0 \cdot 10^{-8}$	$6.9 \cdot 10^{-9}$
CO_2 [mol/m³]	0.6	0.6
$[CH]^0$ [mol/m³·10⁻³]	0.2	0.2
$[CSH]^0$ [mol/m³·10⁻³]	0.75	0.75

1.4.1. Prediction

The predicted carbonation depths after 10 weeks of exposure are given in Table 15 .

Table 15: Predicted carbonation depth after 10 weeks of exposure using Papadakis' model for CEM II/B-V

RH [%]	x_c [mm]
60	12.4
85	4.2

The carbonation rates are slightly higher for CEM II/B-V compared to CEM I. CEM II/B-V presents a higher carbon dioxide diffusion coefficient as well as less carbonatable material.

1.5. Model proposed by Bakker

Bakker proposed a model which differed between dry and wet cycles [Bakker, 1994]. In this investigation, samples are exposed to constant RH and CO_2. Carbonation will then take place following the expression for dry concrete.

The input parameters used are given in Table 16.

Table 16: Input parameters for Bakker's model

	RH 60 %		*RH* 85 %	
	CEM I	CEM II/B-V	CEM I	CEM II/B-V
D_{CO_2} [m^2/s]	$5.1 \cdot 10^{-8}$	$6.0 \cdot 10^{-8}$	$5.9 \cdot 10^{-9}$	$6.9 \cdot 10^{-9}$
CO_2 [kg/m^3]	0.026	0.026	0.026	0.026
CaO [kg/m^3]	302.4	218.7	302.4	218.7

1.5.1. Prediction

The predicted carbonation depths after 10 weeks of exposure for the CEM I sample are given in Table 17.

Table 17: Predicted carbonation depth after 10 weeks of exposure using Bakker's model

	RH 60 %		*RH* 85 %	
	CEM I	CEMII/B-V	CEM I	CEMII/B-V
x_c (mm)	7.3	9.3	2.5	3.2

1.6. Model proposed by Jiang et al.

Jiang et al. proposed first a model for assessing the carbonation rate of Portland cement (PC), and a modified version for concrete containing a high volume of fly ash addition (>30%) [Jiang et al., 2000].

In the case of the PC model mortar, the degree of hydration is needed. This is retrieved from De Weerdt (2011).

The input parameters used are given in Table 18.

Table 18: Input parameters for Jiang's model

	RH 60 %		RH 85 %	
	CEM I	CEM II/B-V	CEM I	CEM II/B-V
W [Kg/m^3]	269.5	269.5	269.5	269.5
r_c [-]	1	-	1	-
c [kg/m^3]	470.4	318.5	470.4	318.5
DH [-]	0.77	0.95	0.77	0.95
CO_2 [%]	1.45	1.45	1.45	1.45
F' [kg/m^3]	-	20	-	20
k' [-]	-	0.94	-	0.94

1.6.1. Prediction

The predicted carbonation depths after 10 weeks of accelerated exposure for the CEM I sample are given in Table 19.

Table 19: Predicted carbonation depth after 10 weeks of exposure using Jiang's model for CEM I

RH %	x_c (mm)
60	2.4
80	0.8

The predicted carbonation depths after 10 weeks of exposure for the CEM II/B-V sample are given in Table 20. Note that the investigated fly ash blend in on the edge to be considered a high fly ash mortar.

Table 20: Predicted carbonation depth after 10 weeks of exposure using Jiang's model for CEM II/B-V

RH %	x_c (mm)
60	5.9
80	2.5

1.7. Model proposed by Sisomphon and Lutz

Sisomphon and Lutz proposed a model which requires the carbon dioxide diffusion coefficient (D_{CO_2}) and the amount of CO_2 for complete carbonation (a) [Sisomphon and Lutz, 2007]. In the case of D_{CO_2}, the value obtained by Papadakis' model is used. Parameter "a" is estimated from Lagerblad [Lagerblad, 2006].

The input parameters used are given in Table 21.

Table 21: Input parameters for Sisomphon's model for blended cements: CEM II/B-V

	RH 60 %	*RH* 85 %
D_{CO_2} [m^2/s]	$6.0 \cdot 10^{-8}$	$6.9 \cdot 10^{-9}$
CO_2 [mol/m^3]	26.1	26.1
a [kg/m^3]	163	163

1.7.1. Prediction

The predicted carbonation depths after 10 weeks of exposure for the CEM I sample are given in Table 22.

Table 22: Predicted carb. depths after 10 weeks of exposure using Sisomphon's model for CEM II/B-V

	RH 60 %	*RH* 85 %
x_c (mm)	8.5	2.9

1.8. Approach proposed by Leemann et al.

Leemann et al. proposed an approach where the reacted CaO governs the carbonation resistance [Leemann et al., 2015]. They did not propose a specific model, but found a good agreement between the carbonation rate and the reacted calcium oxide for both mortar exposed to accelerated conditions and natural sheltered conditions. However, the degree of hydration of the cement clinker particles was taken from the literature, which has an impact on the agreement they found between the two parameters.

Table 23 shows the data for the two investigated binders. If one compares the ratio between reacted CaO and carbonated depths after 10 weeks of exposure for both binders, both parameters do not seem to be related for the tested materials and exposure.

Table 23: Assessment Leemann's approach

	CaO [%]	DH [%]	$CaO_{reacted}$ [%]	X_c [mm]	$CaO_{reacted}/X_c$
CEM I	61.7	7	47.5	5.9	8.05
CEM II/B-V	44.6	5	42.4	10	4.24

3. References

Bakker, R. (1994). *Predictions of service life of reinforcement in concrete under different climatic conditions at given cover.* Paper presented at the International Conference on Corrosion and corrosion protection of steel in concrete, Sheffield, UK.

Belda Revert, A., De Weerdt, K., Hornbostel, K., & Geiker, M. (2016a). Carbonation Characterization of Mortar with Portland Cement and Fly Ash, Comparison of Techniques *Nordic Concrete Research*.

Belda Revert, A., De Weerdt, K., Hornbostel, K., & Geiker, M. (2016b). *Investigation of the effect of partial replacement of Portland cement by fly ash on carbonation using TGA and SEM-EDS*. Paper presented at the International RILEM Conference on Materials, Systems and Structures in Civil Engineering, Lyngby, Denmark.

Czarnecki, L., & Woyciechowski, P. (2012). Concrete carbonation as a limited process and its relevance to concrete cover thickness. *Materials Journal, 109*(3), 275-282.

De Weerdt, K., Haha, M. B., Le Saout, G., Kjellsen, K. O., Justnes, H., & Lothenbach, B. (2011). Hydration mechanisms of ternary Portland cements containing limestone powder and fly ash. *Cement and Concrete Research, 41*(3), 279-291. doi:10.1016/j.cemconres.2010.11.014

EN-196. (2005). EN 196-1:2005: Methods of testing cement – Part 1: Determination of strength.

EN-1992. (2004). EN 1992: Design of concrete structures.

Jiang, L., Lin, B., & Cai, Y. (2000). A model for predicting carbonation of high-volume fly ash concrete. *Cement and Concrete Research, 30*(5), 699-702. doi:10.1016/S0008-8846(00)00227-1

Lagerblad, B. (2006). *Carbon dioxide uptake during concrete life cycle – State of the art* (9197607002). Retrieved from Stockholm:

Leemann, A., Nygaard, P., Kaufmann, J., & Loser, R. (2015). Relation between carbonation resistance, mix design and exposure of mortar and concrete. *Cement and Concrete Composites, 62*, 33-43. doi:http://dx.doi.org/10.1016/j.cemconcomp.2015.04.020

Papadakis, V. G., Fardis, M. N., & Vayenas, C. G. (1991). Fundamental modelling and experimental investigation of concrete carbonation. *Materials Journal, 88*(4), 363-373.

Papadakis, V. G., Fardis, M. N., & Vayenas, C. G. (1992). Hydration and carbonation of pozzolanic cements. *ACI Materials Journal, 89*(89), 119-130.

Silva, a., Neves, R., & De Brito, J. (2014). Statistical modelling of carbonation in reinforced concrete. *Cement and Concrete Composites, 50*, 73-81. doi:10.1016/j.cemconcomp.2013.12.001

Sisomphon, K., & Lutz, F. (2007). Carbonation rates of concretes containing high volume of pozzolanic materials. *Cement and Concrete Research, 37*(12), 1647-1653. doi:10.1016/j.cemconres.2007.08.014

Appendix IV

Application of time dependent models for carbonation development to long-term Norwegian field data

Contents

1. Application of time dependent models for carbonation development to long-term Norwegian field data

Selected time dependent empirical models for carbonation are compared with long-term field data to illustrate their applicability. The following empirical models were selected:

- [Morinaga, 1990]
- [Silva et al., 2014]
- [Hills et al., 2015]

Mechanism based models are unfortunately not applied due to the lack of required input data.

2. Long-term Norwegian field data

Long-term Norwegian field data was provided by Steinar Helland [Helland, 2015] which also comprises the data from [Fossum, 2013]. The data consists of carbonation depth measurements from 15 different structures. The structures were made with concretes containing CEM II/A-V cement and w/b ratios ranging from 0.53 to 0.63. The concrete is exposed to conditions corresponding to environmental classes XC3 or XC4 according to EN-206 (2000), see Table 1. Cores were drilled from the structures and the carbonation depth was measured by spraying phenolphthalein indicator on the freshly split surfaces of the cores. The carbonation depth was determined by taking the average of a total of six points, three points on each of the two halves of the core. Helland has presented a discussion on service life modelling including this set of data [Helland, 2016].

Table 1 presents the summary of the provided data. Information about the name of the structure, location, orientation, concrete composition, exposure class, age, carbonation depth and concrete compressive strength is presented. The cells are shaded when the concrete or exposure conditions are the same.
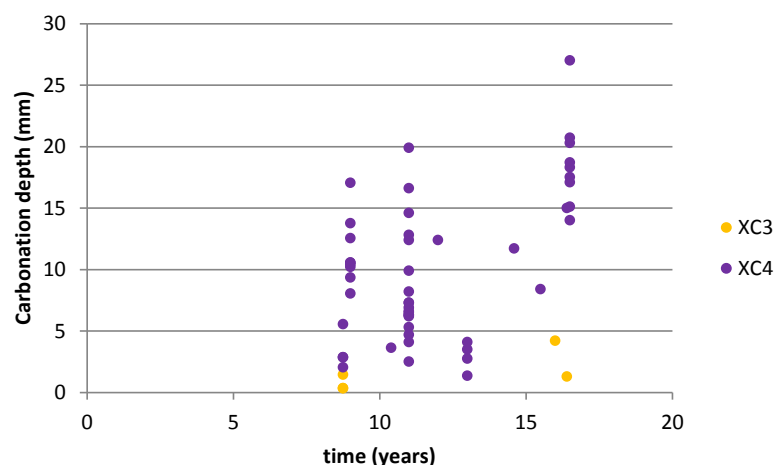

Figure 1: Field structures carbonation depths. Data provided by Helland (2015)

Table 1: Norwegian long-term carbonation field data for concrete structures in exposure classes XC3 and XC4 according to EN-206 (2000), after [Helland, 2015]

Structure	Location	Comments	Durability class	w/c	c (kg/m3)	w (kg/m3)	Cement type	Plast. (Kg/m3)	Exp. Class	Age (years)	xc (mm)	fc (Mpa)
Dokkgata 6	63°26'02.7"N 10°24'29.7"E	External wall.North-East	M 60	0.59	-	-	-	-	XC3	16	4.2	48.2
Fjord gata 16 A	63°26'06.2"N 10°24'12.5"E	External wall. East	M 60	0.59	-	-	-	-	XC4	16.5	17.1	45.1
Heggstadmoen 12	63°19'46.4"N 10°20'57.8"E	External wall	M 60	0.56	-	-	-	-	XC4	16.5		
1 A		South-West									18.3	29.58
1 B		South-West									17.5	40.02
1 C		South-West									15.1	
2 A		East									27.0	36.25
2 B		East									20.3	
2 C		East									20.7	
3 A		South									14.0	
3 B		South									18.7	34.3
Høvringen renseanlegg	63°26'47.7"N 10°20'12.0"E	External wall	M 60	0.59	-	-	-	-	XC4	11		
1 A		South-West									6.9	47.36
1 B		South-West									6.2	46.09
1 C		South-West									6.5	
2 A		North-East									6.6	40.59
2 B		North-East									5.3	39.22
2 C		North-East									4.7	
3		North-East									2.5	
Okstad skole	63°22'52.0"N 10°22'45.5"E	External wall. South-West	M 60	0.56	-	-	-	-	XC4	16.4	15.0	33.1
Sparkjøp	63°25'11.7"N 10°45'42.8"E	External wall	M 60	0.59	-	-	-	-	XC4	11		
1 A		North-East									12.4	36.21
1 B		North-East									12.8	
1 C		North-East									19.9	45.37
2 A		North									16.6	43.14
2 B		North									14.6	
2 C		North									8.2	
St. Olavs lab.	63°25'09.4"N 10°23'28.6"E	External wall	M 60	0.59	-	-	-	-	XC4	11		
1 A		East									6.3	36.61
1 B		East									7.3	
1 C		East									9.9	
2 A		West									7.3	36.56
2 B		West									6.3	
2 C		West									4.1	
Håarstad skole	63°21'03.1"N 10°22'59.0"E	External wall. South-East	M 60	0.59	-	-	-	-	XC3	16.4	1.3	31.8
Telenor	63°25'21.9"N 10°26'15.5"E	External wall. North-West	M 60	0.58	-	-	-	-	XC4	14.6	11.7	54
BI- Studentboliger	59°57'01.3"N 10°46'30.1"E	Foundation and reatiling walls	M 60	0.58	301	175	CEM II/A-V	2.4	XC3- XC4	8.75		
1		West							XC3		1.5	68.1
2		East							XC4		2.9	51.3
3		East							XC3		0.4	46.8
4		North-East							XC3		0.4	-
5		North-West							XC4		2.9	-
6		North-West							XC4		2.1	-
7		North-West							XC4		5.6	70.9
Ikea Storehouse	59°56'00.7"N 10°52'20.4"E	External walls. SCC	NA	0.53	329	183	CEM II/A-V	4.3	XC4	9		
1		South-East									17.1	32
2		South-East									12.6	
3		South-East									13.8	47.9
4		North-East									10.6	-
5		North-East									8.1	-
6		North-East									10.6	49.5
7		North-West									9.4	-
8		North-West									10.2	-
9		North-West									10.4	-
Lena terrasse	63°17'11.1"N 10°17'04.4"E	External wall	M 60	0.59	-	-	CEM II/A-V		XC4	12	12.4	45.1
Moholt Krematorie	63°24'52.6"N 10°26'39.4"E	External wall. North and South?	M 60	0.58	-	-	CEM II/A-V		XC4	15.5	8.4	46.5
Unicon Betongutstilling	-	Slabs on the ground	NA	0.57	307	176	CEM II/A-V	2.4	XC4	13	3.4	37.9
A		Horizontal elements									3.5	32.1
B		Horizontal elements									4.1	-
C		Horizontal elements									2.8	-
Unicon Betongutstilling	-	Slabs on the ground	LA	0.63	350	217	CEM II/A-V	3.4	XC4	13	1.4	20.4
Vålen borettslag	59°54'31.5"N 10°47'42.0"E	Retaining wall. East	NA	0.6	285	175	CEM II/A-V	2.3	XC4	10.4	3.6	45

It is interesting to see the high scatter observed in structures with the same age and included in the same exposure class, e.g. carbonated depths ranging from 27 to 14 mm in Heggstadmoen structure in Table 1. Figure 2 presents the various carbonation depths which were measured on the same structure depending on the orientation of the element, as illustrated for the IKEA storehouse in. This effect is incorporated in models using the "time of wetness"-concept described in *fib* (2006) which takes into account the duration of wet exposure and wind direction. However, other factors that can influence the length of the wet period as for example orientation of the elements or direct sun exposure are not include in the models.
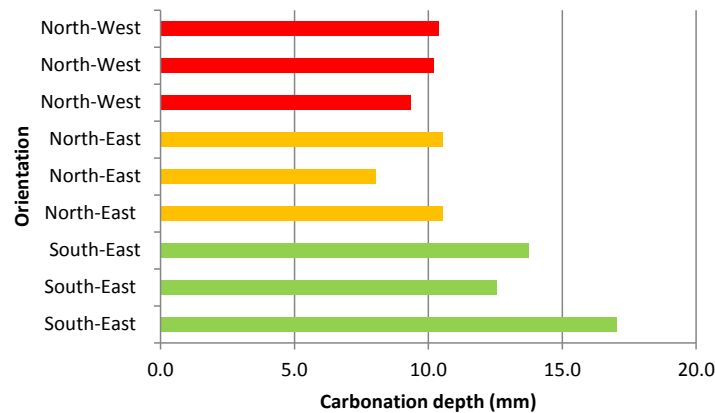

Figure 2: Impact of orientation (local exposure) on carbonation depth, for different cores (each bar represents one core) extracted from the IKEA storehouse

3. Predictions

Four models are applied to estimate carbonation depth based on the available data:

- Morinaga [Morinaga, 1990]: Assumptions: 70 to 80 % RH depending on the location of the structure, 7.5 to 8.5 °C, and 0.04 % CO_2
- Silva et al. [Silva et al., 2014]: Assumptions: RH higher than 70 % , 0.04 % CO_2 and in the cases that cement content is unknown 300 Kg/m^3 is assumed.
- Hills et al. [Hills et al., 2015] proposed two models, both models are applied: M 1 and M 2. No extra assumptions are necessary.

Figure 3 and Figure 4 present the field data (dots) together with the predicted values (crosses) for respectively XC3 and XC4 exposure. Figure 4 includes trend lines. It can be observed that Morinaga's model provides the most conservative prediction while Silva underestimates the carbonation depth in most cases, especially at later ages for XC4 exposure. The high scatter observed in the field measurements suggests the use of statistical approaches, otherwise it seems not possible to include such a high variation in a model.
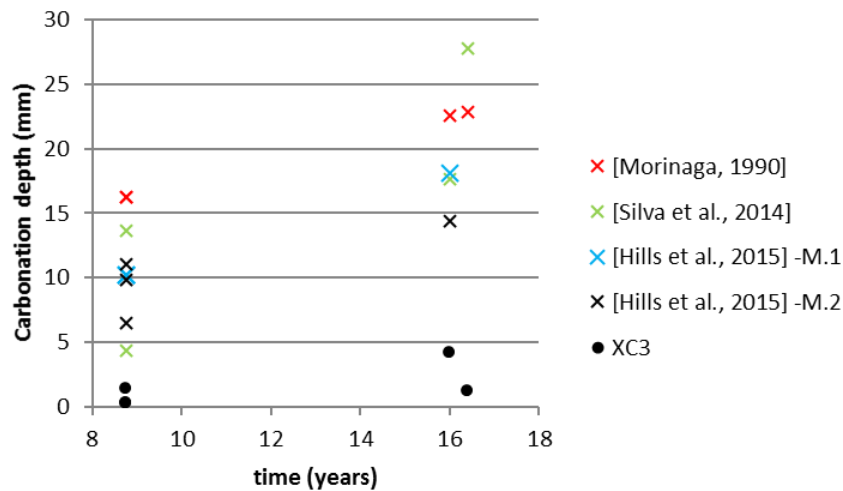
Figure 3: Measured (dots) and predicted carbonation depth (crosses); structures in exposure class XC 3 according to EN 1992 (2004). After [Helland, 2015]
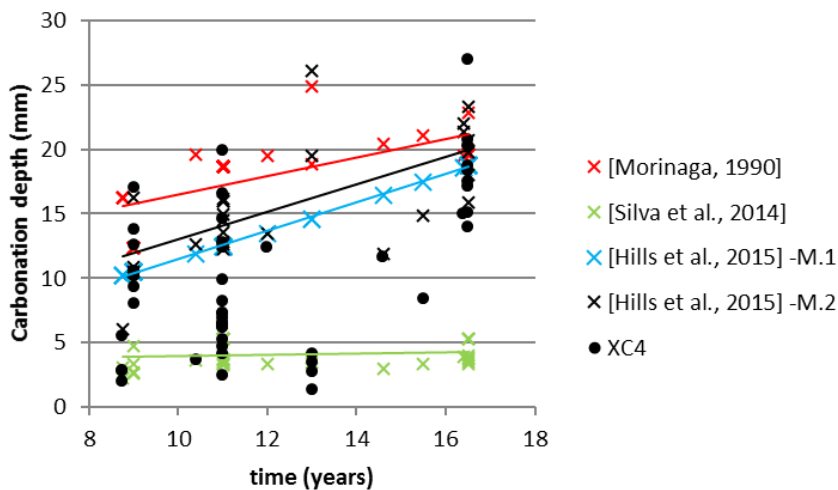

Figure 4: Measured (dots) and predicted carbonation depth (crosses); structures in exposure class XC 4 according to EN 1992 (2004). After [Helland, 2015]

4. Sensitivity analysis of the models

The sensitivity of the models is checked in order to study if the scatter observed in data can be covered by the parameters which are implemented in each model. Table 2 presents the evaluation of each model.

The input parameters of each model have been investigated in the range presented in the "Input parameter variation" column. This range tries to investigate if variation in concrete quality or exposure conditions within the same structure can explain the observed scatter in the field measurements. The lowest and highest

obtained *k* values are presented in the "*k* values" column. The column "Carbonation rate range" refers to the difference between the maximum and minimum carbonation rate obtained depending on the input parameter variation. Finally, the "Δx_c" column shows the difference in carbonation front development which would be measured after 10 years if the difference in the investigated parameters was kept.

Table 2: Sensitivity analysis of the models used for long-term field data validation

	Input parameter	Input parameter variation		*k* [mm/year^0.5]		Carbonation rate range [mm/year^0.5]	Δxc after 10 years [mm]
[Morinaga, 1990] (w/c<0.6)	RH [%]	60	100	5,5	5,3	0,2	1
	ΔT [C]	0	20	4,1	5,5	1,4	4
	CO2 [%]	0,05	0,1	6,2	8,7	2,6	8
	w/c [-]	0,45	0,55	2,2	5,5	3,3	10
[Silva et al., 2014] (RH<70)	Exposure	XC-3	XC-4	7,1	3,5	3,6	11
	fc [MPa]	30	40	10,7	9,2	1,5	5
	CO2 [%]	0,05	0,1	10,7	10,7	0,0	0
[Silva et al., 2014] (RH>70)	Clinker [Kg/m3]	300	350	4,0	3,1	0,9	3
	fc [MPa]	30	40	5,9	5,5	0,4	1
	CO2 [%]	0,05	0,1	6,8	6,9	0,2	1
[Hills et al., 2015] Model 1	Cement type	PC	FA	4,1	5,5	1,4	4
	Exposure	Sheltered	Exposed	5,5	3,1	2,4	8
	Origin	Field	Laboratory	5,5	3,5	1,9	6
	Time [years]	5	10	5,5	6,6	1,1	4
[Hills et al., 2015] Model 2	Cement type	PC	FA	6,1	9,0	2,9	9
	Exposure	Sheltered	Exposed	6,1	3,8	2,2	7
	fc [MPa]	30	40	6,1	4,6	1,5	5

Morinaga's model show how either differences in concrete properties, e.g. w/c, or exposure conditions, mainly CO_2, will influence carbonation. Silva et al's models give similar conclusion, but it seems that the model for RH<70% is more sensitive to the input data, once RH is higher than 70% less variation is observed on the output. Hills et al's models yielded to similar observations.

This variation in the carbonation depths due to either concrete properties or exposure conditions suggests a statistical approach for service life design. Additionally, as the influence of the exposure conditions is so relevant, it seems that the exposure class classification proposed at EN- 206 should include subclasses inside each current exposure class.

5. References

EN 206-1. (2000). EN 206-1 Concrete – Part 1: Specification, performance, production and conformity

EN 1992. (2004). EN 1992: Design of concrete structures.

fib (2006). International Federation for Structural Concrete, *fib*, Model Code for Service Life Design, Bulletin no 34. Lausanne, Switzerland Fossum, B. (2013). *Concrete with Carbonation of CEMII / A-V Cement.* (Master), Norwegian University of Science and Technology.

Helland, S. (2015). [Personal communication].

Helland, S. (2016). *Assessments of carbonation ingress in-field as a tool to calibrate code requirements*. Paper presented at the *fib* Symposium, Cape Town, South Africa.

Hills, T. P., Gordon, F., Florin, N. H., & Fennell, P. S. (2015). Statistical analysis of the carbonation rate of concrete. *Cement and Concrete Research, 72*, 98-107. doi:10.1016/j.cemconres.2015.02.007

Morinaga, S. (1990). *Prediction of service lives of reinforced concrete buildings based on the corrosion rate of reinforcing steel.* Paper presented at the Durability of building Materials and Component, London.

Silva, a., Neves, R., & De Brito, J. (2014). Statistical modelling of carbonation in reinforced concrete. *Cement and Concrete Composites, 50*, 73-81. doi:10.1016/j.cemconcomp.2013.12.001

Appendix V

Standards and Guidelines for service life design

Contents

1. ISO 16204: Durability- Service Life Design of Concrete Structures

The international standard ISO 16204 (2012) proposes two strategies for service life design. The first strategy is the design to resist the deterioration, which includes three levels of sophistication: full probabilistic, partial factor and deemed-to-satisfy approach. The second strategy is the avoidance of the deterioration. Both strategies are presented for carbonation-induced reinforcement corrosion.

ISO 16204 is based on *fib* (2006b), for further description of the carbonation model see Section 5.

1.1. Strategy I

1.1.1. Full probabilistic approach

The full probabilistic carbonation model is the one proposed at *fib* (2006). Other models may be used provided the following principles are fulfilled:

- The model is sufficiently validated to give realistic and representative data
- Parameters and their associated uncertainty are quantified
- Reproducible test methods are available to estimate action and material parameters

Two models were presented depending on the considered limit state:

- Depassivation (uncracked concrete).

$$p_{dep} = p\{co - x_{c(t_{SL})} < 0\} < p_0 \qquad \text{Eq. 1}$$

Where

p_{dep} Probability that depassivation occurs [-]
co Concrete cover [mm]
$x_{c(t_{SL})}$ Carbonation depth [mm] at t_{SL}
p_0 Target failure probability [-]

- Corrosion induced cracking

$$p_{crack} = p\{\Delta r_{(R)} - \Delta r_{(S)(t_{SL})} < 0\} < p_0 \qquad \text{Eq. 2}$$

Where

p_{crack} Probability that cracking occurs
$\Delta r_{(R)}$ Maximum allowed reinforcement radius increment [μm]
$\Delta r_{(S)(t_{SL})}$ Reinforcement radius increment at t_{SL} [μm]
p_0 Target failure probability

Alternatively another approach was proposed:

$$p_{crack} = p\{t_{SL} - t_{ini} - t_{prop} < 0\} < p_0 \qquad \text{Eq. 3}$$

Where

p_{crack} Probability that cracking occurs

t_{SL} Service life design [years]

t_i Duration of initiation period [years]

t_p Duration of propagation period [years]

p_0 Target failure probability

The variables $\Delta r_{(R)}$ and $\Delta r_{(S)(t_{SL})}$ or t_{ini} and t_{prop} have to be quantified in a full probabilistic approach. When this standard was published no models with international consensus were available for the propagation period. It is recommended to estimate t_{prop} from existing structures with similar materials and exposure.

Table 1 gives the recommended reliability index β and the associated probability of failure in the case of structures expose to carbonation *fib* (2006b). Note that this values are obtained assuming that the failure function (resistance of the structure minus the load, in this case concrete cover and carbonation front respectively) is normally distributed.

Table 1: Reliability index β for carbonation-induced corrosion service life design *fib* (2006b)

Reliability class	SLS		ULS	
	β	p_f	β	p_f
RC1	1.3	10^{-1}	3.7	10^{-4}
RC2	1.3	10^{-1}	4.2	10^{-5}
RC3	1.3	10^{-1}	4.4	10^{-6}

1.1.2. Partial factor method approach

Depassivation is the considered limit state. The service life ends when carbonation front reaches the reinforcement.

$$co_d - x_{c(t_{SL})} \geq 0$$ Eq. 4

Where

co_d Concrete cover, includes the nominal value and a safety margin [mm]

$x_{c(t_{SL})}$ Carbonation depth at t_{SL}. It is the characteristic carbonation depth value times the partial safety factor of the carbonation depth [mm]

Other models may be used provided that the partial factor method fulfills the target reliability of the limit state during the design service life. Partial factors include deviations of action and material values from the representative values, model uncertainties and dimensional variations.

1.1.3. Deemed-to-satisfy approach

This approach recommends geometrical, material and execution aspects to fulfill the design service life.

1.2. Strategy II

1.2.1. Avoidance of deterioration

Corrosion may be avoided if depassivation cannot take place or if the corrosion resistance is infinite. E.g. if stainless steel is used even if the carbonation front reaches the reinforcement corrosion will not propagate.

1.3. Comments

Additional information presented in the Annex B of the standard is presented:

- There are no models with international consensus to estimate the time from depassivation to carbonation induced cracking or spalling.
- Splitting stresses in the concrete cover due to actions, loads and bond stresses from the reinforcement are recommended to be included in the model.
- In case the target reliability level for failing the depassivation limit state is bigger than 10^{-1}, special attention should be given to the limit state of cracking, which can be passed at the same time.
- Further information about parameters controlling carbonation is available in *fib* (2006b), see Section 5. When deriving these values from real structures, the older the structure the lower the uncertainty. An overview of the models in use is given at Concrete Society Technical Report 61 [Bamforth, 2004].

2. Eurocode 2: EN-1992

The standard Eurocode 2 (2004) provides a deemed-to-satisfy approach for durability service life design. Environmental exposure class, structural classification and concrete composition recommendations are mandatory to implement on a national level, and given by the national standardization bodies. The environment is classified into different exposure classes. Carbonation-induced corrosion is classified in four exposure classes depending on the water availability:

- XC 1: Dry or permanently wet (concrete inside buildings with low air humidity or concrete permanently submerged in water)
- XC 2: Wet, rarely dry (concrete surfaces subject to long-term water contact. Many foundations
- XC 3: Moderate humidity (concrete inside buildings with moderate or high air humidity. External concrete sheltered from rain)
- XC 4: Cyclic wet and dry (concrete surfaces subject to water contact, not within exposure class XC2)

Recommended values for concrete composition and strength depend on the exposure class, see Table 2.

Table 2: Recommended limiting values for composition and properties of concrete (EN 206, Table F 1)

	X 0	XC 1	XC 2	XC 3	XC 4
Maximum w/c ratio	-	0.65	0.6	0.55	0.5
Minimum strength class	C12/15	C20/25	C25/30	C30/37	C30/37
Minimum cement content (Kg/m^3)	-	260	280	280	300

Structures are classified into structural classes according to EN-1990 (2002), see Table 3. The higher the structural class, the more demanding the requirements. With the cover proposed in Table 4 the structures will have at least the design working life specified depending on the structural class.

Table 3: Design working life depending on the structural class (EN 1990:2002, Table 2.1)

Structural class	Design working life (years)	Example
1	10	Temporary structures
2	10 to 25	Replaceable structural parts
3	15 to 30	Agricultural and similar buildings
4	50	Building structures and other common structures
5	100	Monumental building structures, bridges and other civil Engineering structures

*Structures or part of structures that can be dismantled with a view to being re-used should not be considered as temporary

The recommended minimum concrete cover depends on the exposure and structural class, see (Table 4).

Table 4: Values of minimum cover [mm] (EN 1992, Table 4.4)

Structural Class	X 0	XC 1	XC 2-XC 3	XC 4
S1	10	10	10	15
S2	10	10	15	20
S3	10	10	20	25
S4	10	15	25	30
S5	15	20	30	35
S6	20	25	35	40

2.1. Comments

If the considered limit state is the depassivation of the reinforcement, there are some inconsistencies comparing XC 3 and XC 4 exposure classes. A structure sheltered from the rain or inside a building with moderate humidity (XC 3) will carbonate much faster compared to a structure exposed to rain (XC 4). However, according to the standard lower maximum w/b and thicker concrete covers are recommended for XC 4 class. It is true that once depassivation occurs, the corrosion rate will be higher on the structure exposed to XC 4 class.

Carbonation does not seem a treat for exposure classes XC 1 and XC 2, even if the depassivation of the reinforcement occurs, the corrosion rate will be very low.

3. Spanish Concrete Structural Code (EHE-08)

The Spanish Concrete Structural Code (2008) provides a deemed-to-satisfy approach for durability service life design. However, a model for service life prediction is included in Annex 9: "Additional considerations about durability in EHE-08".

The initiation period model follows the square root law. The carbonation coefficient (k) depends on the exposure as well as concrete composition. The considered limit state is the depassivation of the reinforcement.

$$x_c = k \cdot \sqrt{t} = \left(c_{env} \cdot c_{air} \cdot a \cdot f_c^b \right) \cdot \sqrt{t} \qquad \text{Eq. 5}$$

Where

x_c	Carbonation depth [mm]
c_{env}	Environmental coefficient [-]
c_{air}	Entrained air coefficient [-]
a, b	Aggregate coefficients [-]
f_c	Compressive strength [MPa]
t	Exposure time [years]

As an example, the carbonation coefficient for a concrete structure containing CEM II/B-V, sheltered from rain with entrained air < 4.5% and compressive strength 30 MPa is given:

$$x_c = 6.08 \cdot \sqrt{t} \qquad \text{Eq. 6}$$

For the propagation period, an equation which includes the concrete cover, reinforcement diameter and corrosion rate was proposed. The limit state considered was the appearance of cracks.

$$t_p = \frac{80}{\phi} \frac{Co}{i_{corr}} \qquad \text{Eq. 7}$$

Where

ϕ	Reinforcement diameter (mm)
Co	Concrete cover (mm)
i_{corr}	Corrosion rate (μm/year)

Two corrosion rate values were given depending on the relative humidity:
- High RH: 3 µm/year
- Low RH: 2 µm/year.

3.1. Comments

The model proposed for the propagation period includes corrosion rates depending on the RH. However, the data is limited and ill-defined.

4. DuraCrete- Propabilistic performance based durability design of concrete structures

In Duracrete (2000) , a full probabilistic method was presented for the initiation period. As it is the predecessor of the *fib* (2006b) model, presented in Section 5, it is not included in this report.

For the propagation period a probabilistic model was proposed. The model covers the period from steel depassivation, which is assumed to take place when carbonation front reaches rebars, to unacceptable structure deterioration, which is defined by the corrosion allowance.

An attack penetration function ($P_f(t)$) was proposed to represent the loss of section due to corrosion:

$$P_f(t) = \int_{t_i}^{t} i_{corr}(\tau)d\tau \qquad \text{Eq. 8}$$

Three possibilities were presented to estimate corrosion rate.

4.1. Corrosion rate as function of exposure

The corrosion rate depends on the exposure.

$$i_{corr} = i_{corr,a} \cdot w_t \qquad \text{Eq. 9}$$

Where

$i_{corr,a}$ Mean corrosion rate during corrosion propagation

w_t Wet periods on which corrosion is active [-]

4.2. Corrosion rate estimated by direct measurements

The corrosion rate is measured directly from the structure.

$$i_{corr} = i_{corr}' \cdot k_t \qquad \text{Eq. 10}$$

Where

i_{corr}' Experimentally measured using a given technique

k_t Influence of the given technique [-]

4.3. Empirical expressions, based on concrete resistivity control:

The corrosion rate is estimated assuming that concrete resistivity governs corrosion rate. Two alternatives were presented.

- Andrade and Arteaga:

$$i_{corr} = \frac{m_0}{\rho_{es} \cdot k_t \cdot k_{env} \cdot k_e} F_{Cl} \cdot F_{Galv} \cdot F_{O_2} \cdot F_{oxi}$$

Eq. 11

Where

m_0 Corrosion rate

k_t Influence of aging [-]

k_{env} Influence of environment [-]

k_e Influence of laboratory testing [-]

F Factors refers to chloride, galvanic and oxygen affecting the corrosion rate [-]

- Gehlen and Nilsson:

$$V_{corr} = \frac{m_0}{\rho_{es} \cdot \left(\frac{t_{Hydr}}{t_0}\right)^n \cdot k_t \cdot k_c \cdot k_{R,T} \cdot k_{R,RH} \cdot k_{R,Cl}} F_{Cl} \cdot F_{Galv} \cdot F_{O_2}$$

Eq. 12

Where

k Factors refer to concrete resistivity: test method, age, curing and environmental conditions [-]

F Factors refers to corrosion rate: chloride, galvanic and oxygen [-]

5. *fib* Model Code for Service Life Design

The *fib* Model Code for service life design (2006b) describes the strategies for service life design, which are given in ISO 16204 (2012), described in Section **Error! Reference source not found.**. Similar strategies a re also presented in the revised version of the Model Code for concrete structures (2012) .

This section presents the description of the carbonation model for the full probabilistic design method for the initiation period included in the strategy design to resist deterioration. The limit state considered is the depassivation of the steel. Depassivation occurs when carbonation front reaches rebars.

The depassivation equation is the following:

$$g(co, x_c(t)) = co - x_c(t) = co - \sqrt{2k_e k_c (k_t R_{ACC,0}^{-1} + \varepsilon_t) C_S} \cdot \sqrt{t} \cdot W(t) \qquad \text{Eq. 13}$$

Where

co Concrete cover. It is considered as a stochastic variable [mm]

k_e Environmental function: Influence of the RH on the CO_2 diffusion

$$k_e = \left(\frac{1 - \left(\frac{RH_{real}}{100}\right)^5}{1 - \left(\frac{65}{100}\right)^5} \right)^{2.5} \qquad \text{Eq. 14}$$

RH_{real} Relatively humidity on the air (Stochastic) [%]

The environmental function (k_e) takes into account the influence of RH on carbonation. Even if the maximum carbonation rates are observed at RH 60 %, the proposed equation is on the safe side, giving higher values for RH < 60 %. Reference RH is taken 65 % based on the proposed accelerated tests (Chapter B 1.2.5.2 *fib* Bulletin 34).

Figure 1 gives the obtained values for k_e depending on RH: for 65 % the coefficient equals to 1; lower RH is on the safe side and gives higher k_e values (up to 1.85) while higher RH gives lower values (for higher than 90% RH no carbonation occurs).
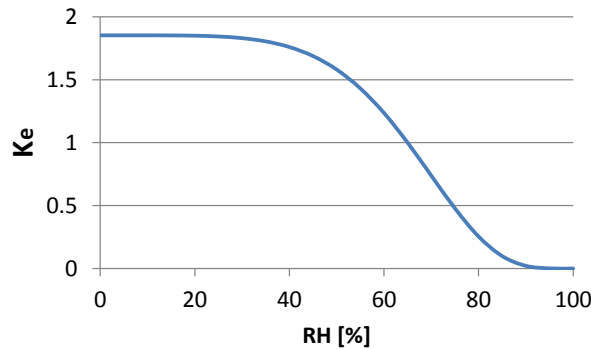
Figure 1: Influence of RH on carbonation

k_c Execution transfer parameter: Influence of curing

$$k_c = \left(\frac{t_c}{7}\right)^{-0.567}$$
Eq. 15

t_c Curing time (Stochastic) [days]

The execution transfer parameter (k_c) takes into account the effect of curing. All the activities related to preventing fresh concrete from premature desiccation are considered curing. Time reference is 7 days: if curing time is lower carbonation will be bigger (k_c equals to 3 for one curing day) while if longer curing time is applied carbonation will develop gradually, see Figure 2.
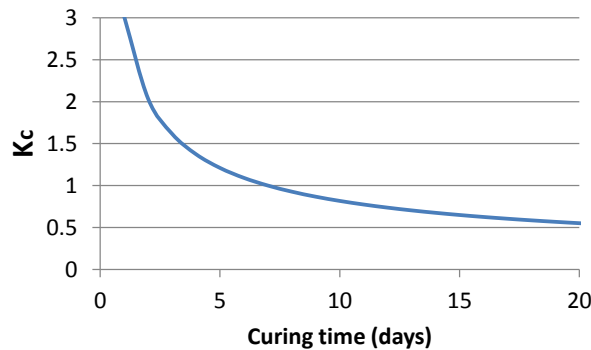

Figure 2: Effect of curing time on carbonation

$R_{ACC,0}^{-1}$ Inverse effective carbonation resistance of concrete (Stochastic) [(m²/s)/(Kg/m³)] It is estimated using as reference carbonation accelerated testing described at "*fib Bulletin 34. Annex B: B1.2.5.2*"

$$R_{ACC,0}^{-1} = \left(\frac{x_c}{420}\right)^2$$
Eq. 16

x_c Carbonation depth [m]

This is the mean value of the accelerated carbonation test. In order to transform it into an inverse carbonation resistance under "natural carbonation" the following equation applies. Note that $R_{ACC,0}^{-1}$ shall be express in the same units as $R_{NAC,0}^{-1}$

$$R_{NAC,0}^{-1} = k_t R_{ACC,0}^{-1} + \varepsilon_t \qquad \text{Eq. 17}$$

$R_{NAC,0}^{-1}$ Inverse effective carbonation resistance under "natural carbonation" [(mm²/year)/(Kg/m³)]
k_t Regression parameter which considers the influence of ACC test.
Assuming normal distribution: m=1.25, s=0.35
ε_t Error term which considers the influence of ACC test.
Assuming normal distribution: m=315.5, s =48

Figure 3 presents the relation between carbonation depth measured in the proposed accelerated conditions (T 20°C, RH 65 %, CO₂ 2 %) and the inverse effective carbonation resistance under natural exposure.
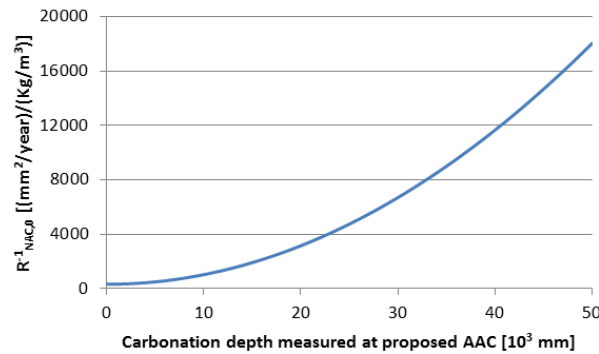

Figure 3: Relation between natural and accelerated carbonation

C_S Environment impact: The CO_2 concentration of the ambient air (Stochastic) [Kg/m³]

$$C_S = C_{S,atm} + C_{S,emi} \qquad \text{Eq. 18}$$

$C_{S,atm}$ CO₂ concentration of the atmosphere [Kg/m³]
$C_{S,emi}$ CO₂ due to emission sources [Kg/m³]

$W(t)$ Weather function: Takes into account mesoclimate conditions due to wetting events of the concrete surface:

$$W(t) = \left(\frac{0.0767}{t}\right)^{\frac{\left(p_{SR}\frac{days\ with\ rain\ fall \geq 2.5\ mm}{365}\right)^{0.446}}{2}} \qquad \text{Eq. 19}$$

t Time (years)

p_{SR} Probability of driving rain: Average distribution of the wind direction during rain events. For horizontal elements is 1 and for sheltered elements 0. In the case of unsheltered vertical elements should be estimated based on weather station data

6. References

Bamforth, P. (2004). *Enhancing reinforced concrete durability: Guidance on selecting measures for minimising the risk of corrosion of reinforcement in concrete.* (T. C. Society Ed. Vol. 61). Camberley, United Kingdom.

Duracrete. (2000). *Duracrete The European Union – Brite EuRam III, DuraCrete – Probabilistic Performance Based Durability Design of Concrete Structures. Final Technical Report of Duracrete project, Document BE95-1347/R17. CUR*. Retrieved from Gouda, the Netherlands.:

EHE-08;. (2008). Spanish Structural Concrete Code.

EN-1990. (2002). EN 1990: Basis of structural design.

EN-1992. (2004). EN 1992: Design of concrete structures.

fib. (2006b). International Federation for Structural Concrete, *fib*, Model Code for Service Life Design, Bulletin no 34. Lausanne, Switzerland.

fib. (2010). International Federation for Structural Concrete, fib, Model Code for Service Life Design-bulletin no 55,56.

ISO-16204. (2012). ISO 16204: Durability- Service Life Design of Concrete Structures.